Critical dynamics of magnets

By E. FREY and F. SCHWABL

Technische Universität München, Institut für Theoretische Physik,
D-85747 Garching, Germany

Abstract
We review our current understanding of the critical dynamics of magnets above and below the transition temperature with focus on the effects due to the dipole–dipole interaction present in all real magnets. Significant progress in our understanding of real ferromagnets in the vicinity of the critical point has been made in the last decade through improved experimental techniques and theoretical advances in taking into account realistic spin–spin interactions. We start our review with a discussion of the theoretical results for the critical dynamics based on recent renormalization group, mode coupling and spin-wave theories. A detailed comparison is made of the theory with experimental results obtained by different measuring techniques, such as neutron scattering, hyperfine interaction, muon spin resonance, electron spin resonance, and magnetic relaxation, in various materials. Furthermore we discuss the effects of dipolar interaction on the critical dynamics of three-dimensional isotropic antiferromagnets and uniaxial ferromagnets. Special attention is also paid to a discussion of the consequences of dipolar anisotropies on the existence of magnetic order and the spin-wave spectrum in two-dimensional ferromagnets and antiferromagnets. We close our review with a formulation of critical dynamics in terms of nonlinear Langevin equations.

Contents

1. Introduction

Remarkable progress has been achieved in our qualitative and quantitative understanding of the critical dynamics of magnetic materials. This is partly due to the advances and new developments in experimental techniques such as neutron scattering, electron spin resonance and hyperfine interaction probes. Simultaneously, on the theoretical side, important developments were provided by dynamical scaling theory, mode-coupling theory and the renormalization group theory. The theoretical progress has been mainly promoted by including effects of magnetic interactions, such as dipole–dipole and spin–orbit interaction, on top of the exchange interaction. These interactions, which are present in all real magnetic materials, were found to change the critical dynamics quite drastically. Around 1986 the experimental situation was quite puzzling, showing both quite excellent agreement but also large discrepancies with the theories existing at that time. Motivated by this seemingly contradictory situation, renewed theoretical interest on the subject of critical dynamics was promoted.

In this review we shall mostly be interested in the effects of the dipole–dipole interaction on the critical dynamics of isotropic ferromagnetic materials in three dimensions. The static properties are reviewed only inasmuch as they are needed for the dynamics or if they emerge naturally together with the dynamical results. We shall also discuss other dipolar systems, such as dipolar antiferromagnets and uniaxial ferromagnets in three dimensions as well as the consequence of dipolar interactions in two-dimensional (2D) magnets. We do not consider pure dipolar systems such as the nuclear magnets Cu, Ag and Au. We aim at giving an up-to-date account of the situation in the field, where we try to give attention to the theoretical as well as the experimental

progress. In order to make the discussion as self-contained as possible we give brief discussions of the various theoretical concepts where needed.

Ferromagnets have always played a special role in the field of critical phenomena. Several simplified models, such as the Ising (1926), Heisenberg (1928) and Hubbard (1979a, b) models, have been developed in order to understand the fundamental questions of the statistical behaviour of magnetically ordered systems. The attraction of these models resides in the simplicity of their form and complexity of behaviour that they are capable to describe. Over the last two decades, various approaches to study the above models have been intensively developed, which led to a profound understanding of the statistical mechanics of magnetic systems on the basis of the above simplified models. However, one has to keep in mind that for a more realistic description of magnetic materials it is not sufficient to consider solely the electrostatic interaction between the electrons in the partly filled shells leading in conjunction with the Pauli principle to the exchange interaction. There are magnetic interactions, such as the mutual interaction of the electron spins (dipole–dipole interaction) and the interaction of the spin and orbital moments of electrons (spin–orbit interaction) which may lead to magnetocrystalline anisotropies.

The exchange interaction is responsible for the phenomenon of magnetic ordering itself (at least above two dimensions). The characteristic feature of the exchange forces is their isotropic and short-range nature. They do not impose any definite orientation of the magnetic moments with respect to the crystallographic axis. Magnetocrystalline anisotropies are due to relativistic or magnetic forces (spin–spin dipole, quadrupole, etc.; spin–orbital; orbital–orbital). Microscopic models of various magnetic interactions have shown that, in the majority of cases, the spin–orbital interaction is the basic interaction responsible for the magnetocrystalline anisotropy (for example Morrish (1965) and Turov (1965)). It relates the directions of the spin magnetic moments of atoms through their orbital states to the crystallographic axes. Irrespective of the microscopic nature of the magnetic anisotropy forces, their macroscopic manifestation in a crystal seems to be determined mainly by the type of symmetry of the lattice. A special role among the magnetic forces is played by the dipole–dipole interaction between the magnetic moments of the electrons, because it is of long-range nature and in cubic crystals leads to an anisotropy with respect to the wave-vector but to leading order not to the crystallographic axes.

A Hamiltonian which takes into account exchange interaction as well as dipole–dipole interaction between the magnetic moments of the electrons has first been given and studied by Holstein and Primakoff (1940). The dipolar interaction is usually two to three orders of magnitude weaker than the exchange interaction, and it can therefore (in many cases) be considered to be a small perturbation. However, because of its long-range nature, the effects of the dipole–dipole interaction become significant at least very close to the Curie temperature T_C and for small wave-vectors $\mathbf{q}$, as will become clear in this review. Note that in particular it leads to the appearance of the demagnetization factors. Using renormalization group theory it has been shown (Aharony 1973a, b, Aharony and Fisher 1973, Fisher and Aharony 1973) that the dipolar interaction is a relevant perturbation with respect to the Heisenberg model. It was found that the short-range Heisenberg fixed point of the renormalization group is unstable against perturbations resulting from the dipolar interaction, and the asymptotic critical behaviour is characterized by a new dipolar critical fixed point. Furthermore, the long-range nature of the dipolar interaction reflects itself in the Fourier transform containing a contribution of the singular direction-dependent form $q^\alpha q^\beta / q^2$.

An immediate consequence is the fact that longitudinal fluctuations are reduced in comparison with the two transverse fluctuations and do not have a divergent susceptibility any longer at T_C. Here, by longitudinal and transverse we refer to the direction of the wave-vector $\mathbf{q}$. A consequence of this reduction of the number of effective order parameter components is a change in the static critical indices. Hence in a system with dominating exchange interaction there is a crossover from Heisenberg critical behaviour to dipolar critical behaviour. For instance the effective temperature-dependent critical exponent of the static susceptibility γ approaches the Heisenberg value, then goes through a minimum until finally it ends up at the dipolar limiting value.

In general the long-range dipolar interaction is of importance whenever fluctuations become large. This is the case in the vicinity of critical points and in systems of reduced dimensionality. In the vicinity of critical points, longitudinal fluctuations are suppressed and rotational invariance is destroyed. This leads to modified static critical behaviour and to drastic changes in the dynamics. In systems of reduced dimensionality, which on the basis of short-range interactions would not have a phase transition at a finite temperature owing to the large fluctuations destroying the order parameter, the dipole interaction suppresses these fluctuations and thereby allows a finite order parameter. With the detection of high-T_C superconductors and their fascinating magnetic properties, the study of mechanisms which lead to phase transitions in such quasi-2D systems (interplane interaction, anisotropy, dipolar interaction, etc.) is of prime importance.

In this paper we review the critical dynamics of magnetic systems. As a reference and a simpler situation to start with, we treat in section 2 first isotropic ferromagnets without dipolar interaction. This allows us to introduce the main theoretical concepts such as dynamic scaling, mode coupling and dynamic renormalization group theory in a quite elementary and hopefully pedagogical way.

In section 3 we describe the theoretical results on the dynamics of dipolar ferromagnets with an emphasis on the mode-coupling theory for the paramagnetic phase. A detailed analysis of the consequences of the dipolar interaction on the functional form of the dynamic scaling laws, the critical exponents and the line-shape and linewidth cross-overs will be given. For the ferromagnetic phase we give some results based on spin wave theory and we also comment on some recent theoretical approaches, which go beyond the linearized spin-wave theory.

In section 4 the theoretical results are then compared with the findings from a variety of experimental techniques. They include neutron scattering, electron spin resonance, magnetic relaxation, hyperfine techniques and muon spin resonance experiments.

Whereas the main part of the review concentrates on dipolar effects in isotropic ferromagnets, section 5 concerns dipolar effects in other magnetic systems. These include three-dimensional (3D) isotropic antiferromagnets, bulk uniaxial ferromagnets and 2D systems. In the latter case the dipolar interaction leads to long range order, which would not be possible for the isotropic Heisenberg model in two dimensions.

Finally, in section 6, we discuss alternative derivations of the mode-coupling theory via the generalized Langevin equations of Zwanzig and Mori. These methods allow systematic derivation of the mode-coupling theory in the framework of a diagrammatic analysis. Also, some systematic improvements are possible. We conclude with a summary and an outlook in section 7. Some technical details and important conceptual background material is collected in the appendices.

2. Isotropic ferromagnets

Our main concern in this review is the immediate vicinity of the critical point and the influence of the dipolar interaction on the critical dynamics. As a reference and a simpler situation to start with we treat first isotropic ferromagnets without dipolar interaction. This allows us to introduce the basic concepts and results of the different theoretical approaches and compare them with the experimental situation.

2.1. *Dynamical scaling and hydrodynamics*

In systems where a continuous symmetry is broken, hydrodynamics together with dynamical scaling allows one to obtain definite conclusions about the dynamic critical behaviour.

To start with, we remind the reader of the structure of the hydrodynamic modes in isotropic ferromagnets. In an isotropic ferromagnet, magnetization is conserved, giving rise to three hydrodynamic equations for the magnetization vector $\mathbf{M}(\mathbf{x})$. In the paramagnetic phase, that is for temperatures above the Curie Temperature T_C and in zero magnetic field $\mathbf{H}$ ($T > T_C$; $\mathbf{H} = 0$) the magnetization obeys a diffusion equation

$$\frac{\partial \mathbf{M}}{\partial t} = D \nabla^2 \mathbf{M}, \tag{2.1}$$

with a diffusion constant D. Hence the long-wavelength excitations are diffusive

$$\omega(q) = iDq^2. \tag{2.2}$$

In the ferromagnetic phase the magnetization $\mathbf{M}$ is finite and the spin fluctuations which are perpendicular to the mean magnetization obey spin-wave equations of motion. The spin-wave frequency is according to hydrodynamics given by

$$\omega(q) = \frac{M}{\chi^{T}(q)} - iq^4 \Lambda. \tag{2.3}$$

Here $\chi^{T}(q)$ is the transverse susceptibility, M the magnetization and Λ a damping constant. The real part of the frequency is related to static critical quantities. For the imaginary part, the damping, hydrodynamics predict a decay rate proportional to the fourth power of the wavenumber[†].

Dynamical scaling states that the critical frequency is of the homogeneous form

$$\omega(q, \xi) = q^z \Omega(q\xi), \tag{2.4}$$

where z is the dynamic critical exponent and $\xi \propto |T - T_C|^{-\nu}$ the correlation length with the static critical exponent ν. Using the scaling behaviour of the static quantities (see for example the excellent book by Ma (1976)) in the hydrodynamic region ($M \sim \xi^{-\beta/\nu}$ and $\chi^{T}(q) \sim q^{-2}\xi^{-\eta}$) and the scaling relations between the static exponents ($\gamma = \nu(2 - \eta)$; $2\beta = (d - 2 + \eta)\nu$), one finds for the spin-wave frequency in the hydrodynamic region

$$\text{Re}\,\{\omega(q, \xi)\} = \frac{M}{\chi^{T}(q)} \propto q^2 \xi^{(2 - d + \eta)/2} = q^{(d + 2 - \eta)/2}(q\xi)^{(2 - d + \eta)/2}. \tag{2.5}$$

Here d is the spatial dimension of the system. One thus finds as a result of the dynamic

---

† Indeed the microscopic theory of the Heisenberg model predicts a spin-wave decay rate of the form $q^4 [c_2(\ln q)^2 + c_1 \ln q + c_0]$ (Dyson 1965a, b, Kashcheev and Kvivoglaz 1961, Vaks *et al.* 1967a, b, Harris 1968).
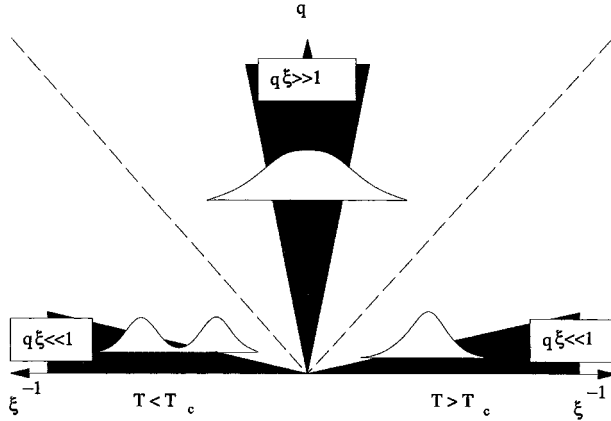
E. Frey and F. Schwabl

q

Figure 2.1. The macroscopic domain of wave-vector q and correlation length ξ. In the three shaded regions the correlation functions have different characteristic behaviours: hydrodynamic regions, $q\xi \ll 1$, $T > T_C$ and $T < T_C$; critical region, $q\xi \gg 1$, $T \approx T_C$. There is a change-over from underdamped spin waves to spin diffusion when the temperature is raised from below T_C to above T_C, as schematically indicated in the diagram.

scaling law, equation (2.4) and the hydrodynamic behaviour of the static quantities an exact relation for the dynamic exponent:

$$z = \frac{d + 2 - \eta}{2}. \tag{2.6}$$

Using again equations (2.5) and (2.6) the damping coefficient $\varLambda$ of the spin waves and the spin diffusion coefficient D in the paramagnetic phase are

$$\varLambda \sim \xi^{(6 - d + \eta)/2}, \quad D \sim \xi^{(2 - d + \eta)/2}. \tag{2.7}$$

The spin diffusion coefficient D goes to zero at the critical temperature, a phenomenon known as *critical slowing down*. Thus hydrodynamics and dynamical scaling allow one to determine the main critical dependences of the transport coefficients. The picture emerging from equations (2.2)–(2.7) is summarized in figure 2.1.

   The critical frequency is a function of the wavenumber and the inverse correlation length. The hydrodynamic region is given by $q \ll \xi^{-1}$, and the non-hydrodynamic critical region by $q \gg \xi^{-1}$. Of course the critical region is limited to $q \ll a^{-1}$ and $\xi \gg a$, where a is a microscopic length scale (e.g. the lattice spacing).

   We close this section by giving the hydrodynamic equations of the low-temperature phase (Schwabl and Michel 1970, Hohenberg and Halperin 1977):

$$\frac{\mathrm{d}}{\mathrm{d}t} M_{\mathbf{q}}^x = \frac{M}{\chi^{\mathrm{T}}(q)} M_{\mathbf{q}}^y - \varLambda q^4 M_{\mathbf{q}}^x,$$

$$\frac{\mathrm{d}}{\mathrm{d}t} M_{\mathbf{q}}^y = \frac{M}{\chi^{\mathrm{T}}(q)} M_{\mathbf{q}}^x - \varLambda q^4 M_{\mathbf{q}}^y,$$

$$\frac{\mathrm{d}}{\mathrm{d}t} M_{\mathbf{q}}^z = - \varGamma(q) M_{\mathbf{q}}^z,$$

the excitations of which were the basis of our discussion. Here we assumed that the magnetization is oriented along the z direction. In addition to the transverse equation

the magnetization component along the order parameter obeys a diffusion equation in three dimensions: $\Gamma(q) = D_M q^2$.

2.2. *Mode-coupling theory*

Some of the most successful theoretical approaches in critical dynamics are mode-coupling theories. The first such theory was proposed by Fixman (1960, 1962) and then placed on a more rigorous basis by Kandanoff and Swift (1968), and especially Kawasaki (1967, 1970, 1976). In this section we exemplify the mode-coupling theory for the critical dynamics of an isotropic ferromagnet, where the spins are coupled only by short-range isotropic exchange interaction. The Hamiltonian for such a spin system is given by

$$H = \int_{\mathbf{q}} J(\mathbf{q}) \mathbf{S_q} \cdot \mathbf{S}_{-\mathbf{q}}. \tag{2.8}$$

Here we have introduced the notation $\int_{\mathbf{q}} = v_a \int d^3 q/(2\pi)^3$, where v_a is the volume of the primitive cell of the Bravais lattice. Upon introducing the cube edge length a of the corresponding cubic cell, the dimensionless quantity $b = (a^3/v_a)^{1/2}$ characterizes the lattice structure. The Fourier transforms of the Cartesian components $S^i(\mathbf{x})$ of the spin operator are defined by

$$S_{\mathbf{q}}^i = \int d^3 x \exp(i\mathbf{q} \cdot \mathbf{x}) S^i(\mathbf{x}), \tag{2.9}$$

and $J(\mathbf{q}) = -J_0 + Jq^2 a^2$ characterizes the exchange interaction. We are retaining only terms up to second order in the wave-vector $\mathbf{q}$ and have supposed that the exchange interaction extends up to the second-nearest neighbours. For b.c.c. and f.c.c. lattices we have $J = J_1 + J_2$, where J_1 and J_2 are the values of the exchange parameters between the nearest and between the next-nearest neighbours respectively. For a s.c. crystal the relation is $J = J_1 + 4J_2$. The parameter J_0 does not enter the equations of motion. It is convenient to introduce the ladder operators

$$S_{\mathbf{q}}^{\pm} = S_{\mathbf{q}}^x \pm iS_{\mathbf{q}}^y, \tag{2.10}$$

and $S_{\mathbf{q}}^z$ instead of the Cartesian components of the spin operator. Then, using the commutation relation for spin operators, one finds for the Hamiltonian (2.8) the following set of equations of motion (we take $\hbar = 1$):

$$\frac{d}{dt} S_{\mathbf{q}}^z = -i \int_{\mathbf{k}} [J(\mathbf{k}) - J(\mathbf{q} - \mathbf{k})] S_{\mathbf{q}-\mathbf{k}}^+ S_{\mathbf{k}}^-, \tag{2.11}$$

$$\frac{d}{dt} S_{\mathbf{q}}^{\pm} = \pm 2i \int_{\mathbf{k}} [J(\mathbf{k}) - J(\mathbf{q} - \mathbf{k})] S_{\mathbf{q}-\mathbf{k}}^{\pm} S_{\mathbf{k}}^z. \tag{2.12}$$

The equations of motion (2.11) and (2.12) exhibit explicitly the vanishing of $dS_{\mathbf{q}}^i/dt$ at $\mathbf{q} = 0$, that is the order parameter itself is a constant of motion. Starting from these microscopic equations of motion there are a variety of different schemes for deriving the mode-coupling equations for the spin correlation functions (Bennett and Martin 1965, Kawasaki 1967, Résibois and De Leener 1967, 1969, Wegner 1968, Hubbard 1971a, b).

The quantity of interest is the Kubo relaxation matrix for a set of dynamical variables denoted $\{X^\alpha(\mathbf{x})\}$, which is defined by

$$\Phi^{\alpha\beta}(\mathbf{q}, t) = \mathrm{i} \lim_{\varepsilon \to 0} \left(\int_t^\infty \mathrm{d}\tau \exp(-\varepsilon\tau) \langle [X^\alpha(\mathbf{q}, \tau), X^\beta(\mathbf{q}, 0)^\dagger] \rangle \right), \qquad (2.13)$$

where $\langle \dots \rangle$ denotes the thermal average. The dynamical variables are normalized such that

$$(X^\alpha, X^\beta) := \Phi^{\alpha\beta}(\mathbf{q}, t = 0) = \delta^{\alpha\beta}, \qquad (2.14)$$

that is we use normalized spin variables $X_\mathbf{q}^\alpha(t) = S_\mathbf{q}^\alpha(t)/[\chi^\alpha(\mathbf{q})]^{1/2}$, where $\chi^\alpha(\mathbf{q})$ are the static susceptibilities.

One of the most concise ways of deducing mode-coupling equations utilizes the projection operator technique, originally introduced by Mori (1965) and Zwanzig (1961). The main idea is that one can separate the set of dynamical variables into two classes: one slowly and one rapidly varying class. With the aid of this projection operator method the fast variables are eliminated and one can derive generalized Langevin equations for the dynamic variables or equivalently for the correlation functions (Kawasaki 1973, Mori and Fujisaka 1973, Mori *et al.* 1974) (see also section 6 and appendix 2). The corresponding equation for the Kubo relaxation function is

$$\frac{\partial \Phi^{\alpha\beta}(\mathbf{q}, t)}{\partial t} = \mathrm{i}\omega^{\alpha\gamma}(\mathbf{q})\Phi^{\gamma\beta}(\mathbf{q}, t) - \int_0^t \mathrm{d}\tau\, \Gamma^{\alpha\gamma}(\mathbf{q}, t - \tau)\Phi^{\gamma\beta}(\mathbf{q}, \tau), \qquad (2.15)$$

and for its half-sided Fourier transform

$$\Phi^{\alpha\beta}(\mathbf{q}, \omega) = \int_0^\infty \mathrm{d}t\, \Phi^{\alpha\beta}(\mathbf{q}, t) \exp(\mathrm{i}\omega t), \qquad (2.16)$$

one obtains

$$\Phi(\mathbf{q}, \omega) = \mathrm{i}[\omega\mathbf{1} + \omega(\mathbf{q}) + \mathrm{i}\Gamma(\mathbf{q}, \omega)]^{-1}. \qquad (2.17)$$

The frequency matrix $\omega^{\alpha\beta}(\mathbf{q})$ is given by

$$\mathrm{i}\omega^{\alpha\beta}(\mathbf{q}) = (\dot{X}_\mathbf{q}^\alpha, X_\mathbf{q}^\beta) = -\mathrm{i}\langle X_\mathbf{q}^\alpha, X_{-\mathbf{q}}^\beta] \rangle, \qquad (2.18)$$

where we have used the Kubo (1957) identity $(\dot{A}, B) = \mathrm{i}\langle [A, B^\dagger] \rangle$. The nonlinear aspects of the spin dynamics are contained in the matrix Γ of the transport coefficients (memory matrix). As a result of the projection operator technique these can be written in terms of the Kubo relaxation matrix (Kawasaki 1970, 1976)

$$\Gamma^{\alpha\beta}(\mathbf{q}, t) = (\delta\dot{X}_\mathbf{q}^\alpha(t), \delta\dot{X}_\mathbf{q}^\beta(t)) \qquad (2.19)$$

of the non-conserved parts of the currents†

$$\delta\dot{X}_\mathbf{q}^\alpha = \dot{X}_\mathbf{q}^\alpha - \mathrm{i}\omega^{\alpha\beta}(\mathbf{q})X_\mathbf{q}^\beta. \qquad (2.20)$$

The simplest approximation which can be made at this stage is to consider only two-mode decay processes, which in technical terms amounts to a factorization of the Kubo formulae (2.19) after insertion of the equations of motions. Frequently one makes additionally an approximation for the line shape (i.e. frequency dependence) of the relaxation matrix, for example a Lorentzian approximation. In principle, however, one can solve directly the set of self-consistent equations for the shape functions resulting

---

† Here we have chosen a linear projection operator $\mathscr{P}X = (X, X^\alpha)X^\alpha$. Then the random forces can be written in terms of the projection operator as $\delta\dot{X}_\mathbf{q} = \exp[\mathrm{i}(1 - \mathscr{P})\mathscr{L}t](1 - \mathscr{P})\dot{X}_\mathbf{q}$, where $\mathscr{L}$ is the Liouville operator. Neglecting the projection operator in the time development, one obtains equation (2.20); see also appendix 2.

from the decoupling approximation only. For the isotropic ferromagnet this was first achieved by Wegner (1968) and Hubbard (1971a) in the paramagnetic phase. For most practical purposes an excellent approximation for the linewidth can be obtained from the mode-coupling equations simplified by the Lorentzian approximation.

2.2.1. *Paramagnetic phase*

In the paramagnetic phase the order parameter is zero, $\langle \mathbf{S_q} \rangle|_{\mathbf{q}=0} = 0$, implying that the frequency matrix $\omega^{\alpha\beta}$ vanishes. Upon using the above decoupling procedure, one obtains the following set of coupled integrodifferential equations for the Kubo relaxation function:

$$\frac{\partial \Phi(\mathbf{q}, t)}{\partial t} = \int_0^t d\tau\, \Gamma(\mathbf{q}, t - \tau) \Phi(\mathbf{q}, \tau), \tag{2.21}$$

and the transport coefficients

$$\Phi(\mathbf{q}, t) = 4k_B T \int_{\mathbf{k}} v(\mathbf{k}, \mathbf{q}) \frac{\chi(\mathbf{q} - \mathbf{k})\chi(\mathbf{k})}{\chi(\mathbf{q})} \Phi(\mathbf{k}, t) \Phi(\mathbf{q} - \mathbf{k}, t), \tag{2.22}$$

with the vertex function ($\hbar = 1$)

$$v(\mathbf{k}, \mathbf{q}) = [J(\mathbf{k}) - J(\mathbf{q} - \mathbf{k})]^2 = \left[2Jq^2a^2 \left(\frac{\mathbf{q} \cdot \mathbf{k}}{q^2} - \frac{1}{2} \right) \right]^2. \tag{2.23}$$

Essentially the same equations have been derived by numerous workers (Bennett and Martin 1965, Kawasaki 1967, 1976, Résibois and De Leener 1967, 1969, Wegner 1968, Hubbard 1971a, b) using different approaches. The temperature dependence enters the equations only implicitly via the correlation length

$$\xi = \xi_0 \left(\frac{T - T_C}{T_C} \right)^{-\nu}. \tag{2.24}$$

The equations for the Kubo relaxation function must in general be solved numerically. However, in the critical region, one can deduce certain important properties of the solution analytically. Upon inserting the static scaling law (Wilson and Kogut 1974)

$$\chi(q, \xi) = \frac{1}{2Ja^2} q^{-2+\eta} \hat{\chi}(x), \tag{2.25}$$

with the scaling variable $x = 1/q\xi$, one can show by inspection that the solution of equations (2.21) and (2.22) fulfils dynamic scaling

$$\Phi(q, \xi, \omega) = (\Lambda q^z)^{-1} \phi(x, v), \tag{2.26}$$

$$\Gamma(q, \xi, \omega) = \Lambda q^z \gamma(x, v), \tag{2.27}$$

with the scaling variable $v = \omega / \Lambda q^z$ and the non-universal constant

$$\Lambda = \frac{a^{5/2}}{b} \left(\frac{2Jk_B T_C}{4\pi^4} \right)^{1/2}, \tag{2.28}$$

where *b* is a dimensionless parameter which depends on the crystal structure (table 1). Note that in equations (2.25)–(2.27) we have explicitly incorporated the correlation length ξ into the list of arguments of the correlation functions in order to indicate the reduction in arguments accomplished by the dynamic scaling form. In order to simplify

Table 1. Crystal structure dependent parameters of cubic Bravais lattices. c is the number of
next-nearest neighbours to a given lattice site. The parameter b is defined as $b = (a^3/v_a)^{1/2}$
and characterizes the lattice structure. δ is the distance between nearest-neighbour ions
and v_a the volume of the Bravais lattice primitive cell. a is the cube edge.

Lattice	c	b	δ (units of a)	v_a (units of a^3)
S.c.	6	1	1	1
B.c.c.	8	$2^{1/2}$	$3^{1/2}/2$	$\frac{1}{2}$
F.c.c.	12	2	$2^{1/2}/2$	$\frac{1}{4}$

notation this temperature dependence is in most of the remaining text not written out
explicitly.

The above mode-coupling equations give a dynamic critical exponent $z = (5 + \eta)/2$
instead of the correct expression $z = (5 - \eta)/2$ (Halperin and Hohenberg 1967, 1969,
Ma and Mazenko 1975, Bausch $et\ al.$ 1976, Janssen 1976). This inconsistency of the
conventional derivation of the mode-coupling equations is fortunately not a very serious
problem since η is very small in the case of 3D ferromagnets: $\eta \approx 0.05$ (Mezei 1984).
In order to be consistent, one has to take for the scaling functions on Ornstein–Zernike
form

$$\hat{\chi}(x) = \frac{1}{1 + x^2}, \tag{2.29}$$

neglecting the exponent η. In section 6 we shall give a derivation of modified
mode-coupling equations based on a path integral formulation of the stochastic
equations of motion. There we shall show how the above inconsistency can be resolved
by taking into account certain kinds of vertex correction which are neglected in the
conventional derivation of mode-coupling equations.

The scaling relations (2.26) and (2.27) for the Fourier-transformed quantities imply
for their time-dependent counterparts

$$\Phi(q, \xi, t) = \phi(x, \tau), \tag{2.30}$$

$$\Gamma(q, \xi, t) = (\Lambda q^z)^2 \gamma(x, \tau), \tag{2.31}$$

with the scaled time variable

$$\tau = \Lambda q^z t. \tag{2.32}$$

The mode-coupling equations for the corresponding scaling functions are

$$\frac{\partial \phi(x, \tau)}{\partial \tau} = - \int_0^\tau d\tau' \gamma(x, \tau - \tau') \phi(x, \tau') \tag{2.33}$$

and

$$\gamma(x, \tau) = 2\pi^2 \int_{-1}^{+1} d\eta \int_0^\infty d\rho\, \rho_-^2\, \hat{v}(\rho, \eta) \frac{\hat{\chi}(x/\rho)\hat{\chi}(x/\rho_-)}{\hat{\chi}(x)} \phi\left(\frac{x}{\rho}, \tau\rho^z\right) \phi\left(\frac{x}{\rho_-}, \tau\rho_-^z\right). \tag{2.34}$$

The scaled vertex function reads

$$\hat{v}(\rho, \eta) = 2(\rho\eta - \tfrac{1}{2})^2, \tag{2.35}$$

where we have defined $\rho = k/q$, $\rho_- = |\mathbf{k} - \mathbf{q}|/q$ and $\eta = \cos(\mathbf{k}, \mathbf{q})$.

Before turning to the numerical solution of the mode-coupling equations, let us quote some results which can be obtained analytically. For temperatures not to close to T_C one can infer from equations (2.22) and (2.23) that in the limit $q \to 0$ (hydrodynamic limit) the vertex factor $v(\mathbf{k}, \mathbf{q})$ and hence the memory kernel $\Gamma(q, t)$ becomes small. Hence one could argue that the relaxation function $\Phi(q, t)$ varies very slowly and the solution of equation (2.21) becomes an exponential (Hubbard 1971a)

$$\Phi(q, t) = \exp(-Dq^2 t), \tag{2.36}$$

where the diffusion constant is given by

$$D = \lim_{q \to 0} \left(\frac{1}{q^2} \int_0^\infty \Gamma(q, t) \, \mathrm{d}t \right) = \lim_{q \to 0} \left(\frac{1}{q^2} \Gamma(q, \omega = 0) \right). \tag{2.37}$$

A scaling analysis of the right-hand side gives for the temperature dependence of the diffusion coefficient $D \sim \xi^{-1/2}$ in agreement with the scaling result by Halperin and Hohenberg (1967, 1969).

The above argument leading to the spin diffusion behaviour has been questioned by Månson (1974). Starting from a relaxation function which is of spin diffusion type (see equation (2.36)), Månson (1974) showed that the memory kernel becomes of the form

$$\Gamma(q, t) \propto t^{-5/2} \exp\left(-\frac{Dq^2 t}{2} \right) \tag{2.38}$$

for asymptotic times and small q. From this, Månson (1974) concludes that the spin diffusion type of behaviour cannot be the correct form of the relaxation function as asymptotic times, which would raise some questions on the validity of the mode-coupling theory (since it invalidates the results obtained from a hydrodynamic theory based on the conservation of the magnetization). The above argument leading to an exponentially decaying relaxation function becomes invalid also close to T_C because the static susceptibilities in the expression for the memory matrix diverge and therefore the relaxation function no longer varies slowly. A shape crossover from a Lorentzian to a different critical shape takes place by approaching the critical temperature (Hubbard 1971a). Nevertheless, a Lorentzian approximation for the line shape still gives reasonable an approximation for the linewidth, since the latter is not so sensitive to the precise form of the line shape.

In the Lorentzian approximation the mode-coupling equations reduce to a single integral equation for the linewidth $\Gamma_{\mathrm{Lor}}(q) = Aq^z \gamma_{\mathrm{Lor}}(x)$:

$$\gamma_{\mathrm{Lor}}(x) = \frac{2\pi^2}{\hat{\chi}(x)} \int_{-1}^{+1} \mathrm{d}\eta \int_0^\infty \mathrm{d}\rho \, \rho_-^2 \, \hat{v}(\rho, \eta) \, \frac{\hat{\chi}(x/\rho) \hat{\chi}(x/\rho_-)}{\rho^{5/2} \gamma_{\mathrm{Lor}}(x/\rho) + \rho_-^{5/2} \gamma_{\mathrm{Lor}}(x/\rho_-)}. \tag{2.39}$$

Therefrom one can deduce the asymptotic behaviour of the typical linewidth analytically:

$$\gamma_{\mathrm{Lor}}(x) \sim \begin{cases} 1, \\ x^{1/2}, \end{cases} \quad \text{for} \begin{cases} x \ll 1, \\ x \gg 1, \end{cases} \tag{2.40}$$

implying that $\Gamma(q) \sim q^{5/2}$ right at $T = T_C$ and $\Gamma(q) \sim q^2 \xi^{-1/2}$ in the hydrodynamic limit $q\xi \ll 1$, that is the temperature dependence of the diffusion constant is given by $D \sim \xi^{-1/2}$ (Kawasaki 1967) as we have already deduced from scaling arguments. The full scaling function resulting from equation (2.39) is shown in figure 2.2 It is usually called the Résibois–Piette (1970) scaling function since Résibois and Piette did
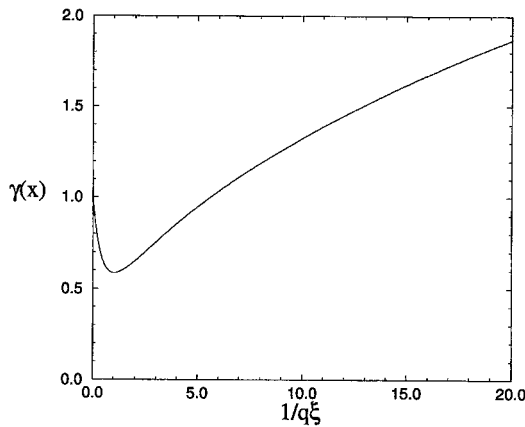
Figure 2.2.   The Résibois–Piette (1970) scaling function against $x = 1/q\xi$, resulting from the numerical solution of the mode-coupling equations in the Lorentzian approximation for a Heisenberg ferromagnet in the paramagnetic phase.
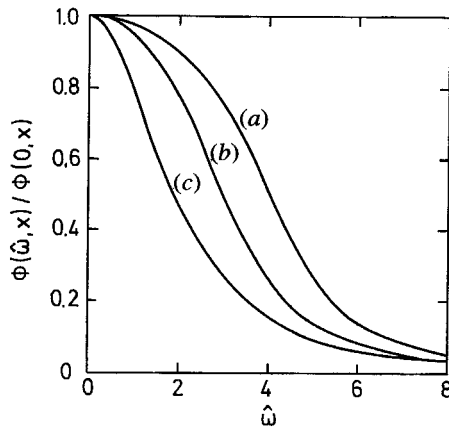

Figure 2.3.   The universal function $\phi(\omega/\sigma q^{5/2}, 1/q\xi)$ for several values of $1/q\xi$: (a) $1/q\xi = 0$; (b) $1/q\xi = 0\cdot2$; (c) $1/q\xi = 1\cdot04$. (From Hubbard (1971a) where the scale σ is defined.)

the first numerical solution of the mode-coupling equations in the Lorentzian approximation.

In order to find the complete behaviour of the relaxation function $\Phi(q, t)$, one has to solve equations (2.33) and (2.34) numerically. This was done by Wegner (1968) at T_C and extended to temperatures above T_C by Hubbard (1971a, b). The results are shown in figure 2.3. It is found that for small wave-vectors (not too close to the zone boundary) there is a shape crossover from a Lorentzian (see equation (2.36)) to a more Gaussian-like shape by approaching the critical temperature. The critical shape at T_C is essentially the same as obtained from renormalization group (RG) theory (de Dominicis 1976, Bhattacharjee and Ferrell 1981) (see also section 2.3.1).

Recently, this shape crossover has been re-examined by Aberger and Folk (1988) and Frey et al. (1989) in detail with emphasis on constant-energy scans. Their results, shown in figures 2.4 (a) and (b) for the scaling function of the spin relaxation function
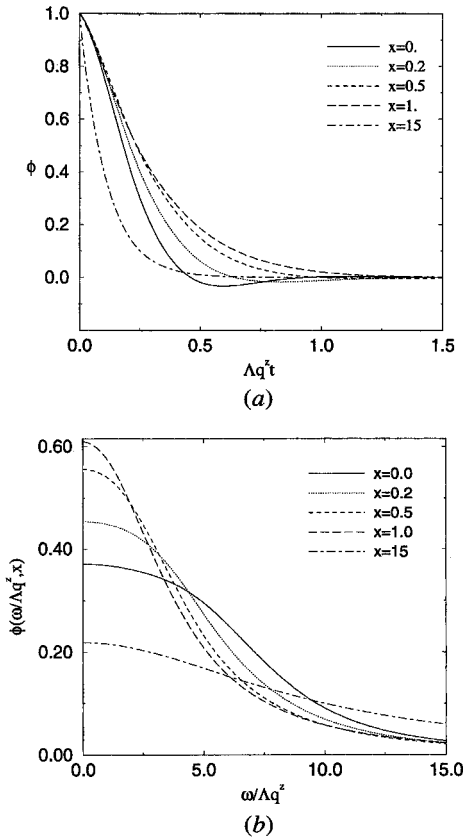
Figure 2.4.   (*a*) The spin relaxation $\phi(Aq^{5/2}t, 1/q\xi)$ for several values of $1/q\xi$ indicated in the graph. (*b*) The scaling function $2\mathrm{Re}[\phi(\omega/Aq^{5/2}, 1/q\xi)]$ for the spin relaxation function $\Phi(q, \omega) = \phi(\omega/Aq^{5/2}, 1/q\xi)/Aq^{5/2}$ for several values of $1/q\xi$ indicated in the graph, showing the shape crossover to a Lorentzian shape for $1/q\xi \geqslant 1$.

against time and frequency respectively confirm the shape crossover from a Lorentzian to a critical shape first found by Hubbard (1971a, b). In addition, strongly overdamped oscillations in the time-dependent spin relaxation function at T_C are found. These oscillations, however, do not lead to an observable structure in the Fourier transform apart from a flatter decrease at small frequencies. With increasing temperature these oscillations almost disappear. At present, it is not clear whether these oscillations are an artefact of the mode-coupling approximation and go away when higher-order terms are included. A RG analysis does not show these oscillations (de Dominicis 1976, Bhattacharjee and Ferrell 1981, Iro 1987).

Hubbard (1971a) also discusses the shape function for cubic ferromagnets with nearest-neighbour interaction for wave-vectors close to the Brillouin zone boundary: $J(\mathbf{q}) \propto J[\cos(q_x a) + \cos(q_y a) + \cos(q_z a)]$. He finds that there is a tendency of the shapes to become squarer than a Lorentzian and, as the wave-vectors come close to the zone boundary one observes the formation of small shoulders. Recently Cuccoli *et al.* (1989) have studied the shape of the correlation function at the zone boundary for EuO and EuS with a f.c.c. lattice taking into account nearest- and next-nearest-neighbour exchange interactions. The numerical solutions of the mode-coupling equations give,

as in the s.c. case with nearest-neighbour interaction considered by Hubbard (1971a), inelastic shoulders at the zone boundary, but less intense than seen in the experiment (Bohn *et al.* 1984, Böni *et al.* 1987a).

2.2.2. *Ferromagnetic phase*

In this section we review the mode-coupling equations for isotropic ferromagnets below the Curie point (Schwabl 1971, Frey and Schwabl 1988a, 1989a). On the assumption that the spontaneous magnetization points are along the z axis the frequency matrix is given by

$$\omega^{\alpha\beta}(q) = \omega(q) \begin{bmatrix} 0 & 0 & 0 \\ 0 & -1 & 0 \\ 0 & 0 & +1 \end{bmatrix}, \qquad (2.41)$$

where $\alpha, \beta = z, +, -$. The frequency of the transverse modes is

$$\omega(q) = \frac{M}{\chi^T(q)}, \qquad (2.42)$$

where $M = \langle S^z_{q=0} \rangle$ denotes the magnetization and $\chi^T(q)$ the static transverse susceptibility. Owing to the rotational symmetry of the Hamiltonian the Kubo relaxation matrix $\Phi^{\alpha\beta}(q, \omega)$ is diagonal:

$$\Phi^{zz}(q, \omega) = \frac{i}{\omega + i\Gamma^{zz}(q, \omega)}, \qquad (2.43)$$

$$\Phi^{\pm\pm}(q, \omega) = \frac{2i}{\omega \mp \omega(q) + i\Gamma^{\pm\pm}(q, \omega)}. \qquad (2.44)$$

The mode-coupling approximation for the transport coefficients

$$\Gamma^{zz}(q, t) = \frac{(\dot{S}^z_q(t), \dot{S}^z_q(0))}{\chi^L(q)} \equiv \Gamma(q, t), \qquad (2.45)$$

$$\Gamma^{\pm\pm}(q, t) = \frac{(\dot{S}^\pm_q(t) \pm i\omega(q)S^\pm_q(t), \dot{S}^\pm_q(0) \pm i\omega(q)S^\pm_q(0))}{2\chi^T(q)} \equiv \Lambda^\pm(q, t), \qquad (2.46)$$

where $\chi^L(q)$ is the longitudinal susceptibility, results in the following set of integral equations (Schwabl 1971):

$$\Gamma(\mathbf{q}, \omega) = k_B T \int_\nu \int_\mathbf{k} v(\mathbf{k}, \mathbf{q}) \frac{\chi^T(\mathbf{q} - \mathbf{k})\chi^T(\mathbf{k})}{\chi^L(\mathbf{q})} \Phi^{++}(\mathbf{q} - \mathbf{k}, \omega - \nu)\Phi^{--}(\mathbf{k}, \nu), \qquad (2.47)$$

$$\Lambda^\pm(\mathbf{q}, \omega) = 2k_B T \int_\nu \int_\mathbf{k} v(\mathbf{k}, \mathbf{q}) \frac{\chi^T(\mathbf{q} - \mathbf{k})\chi^L(\mathbf{k})}{\chi^T(\mathbf{q})} \Phi^{\pm\pm}(\mathbf{q} - \mathbf{k}, \omega - \nu)\Phi^{zz}(\mathbf{k}, \nu). \qquad (2.48)$$

Here we have used the notation $\int_\nu = \int d\nu/2\pi$. Equations (2.43) and (2.44) together with equations (2.47) and (2.48) constitute a complete set of self-consistent integral equations for the Kubo relaxation functions $\Phi^{\alpha\alpha}(q, \omega)$, which in principle could be solved numerically. For $M = 0$ and $\chi^L = \chi^T$, equations (2.47) and (2.48) reduce to the mode-coupling equations for the paramagnetic phase, equation (2.22).

The above mode-coupling equations have been analysed in the Lorentzian approximation for the relaxation functions

$$\Phi^{zz}(q,\omega) = \frac{\mathrm{i}}{\omega + \mathrm{i}\Gamma(q)}, \quad \Phi^{\pm\,\pm}(q,\omega) = \frac{2\mathrm{i}}{\omega \mp \omega(q) + \mathrm{i}\Lambda^{\pm}(q)}, \tag{2.49}$$

with

$$\Gamma(q) = \Gamma(q, \omega = 0), \quad \Lambda(q) \equiv \Lambda^{+}(q) = \Lambda^{-}(q)^{*} = \Lambda^{+}(q, \omega(q)). \tag{2.50}$$

The frequency integrals can now be carried out readily and one finds the following set of coupled integral equations for the linewidths:

$$\Gamma(\mathbf{q}) = \frac{4\mathrm{i}k_{B}T}{\chi^{L}(\mathbf{q})} \int_{\mathbf{k}} v(\mathbf{k},\mathbf{q}) \frac{\chi^{T}(\mathbf{q}-\mathbf{k})\chi^{T}(\mathbf{k})}{\omega(\mathbf{k}) - \omega(\mathbf{q}-\mathbf{k}) + \mathrm{i}\Lambda(\mathbf{q}-\mathbf{k}) + \mathrm{i}\Lambda^{*}(\mathbf{k})}, \tag{2.51}$$

$$\Lambda(\mathbf{q}) = \frac{4\mathrm{i}k_{B}T}{\chi^{T}(\mathbf{q})} \int_{\mathbf{k}} v(\mathbf{k},\mathbf{q}) \frac{\chi^{T}(\mathbf{q}-\mathbf{k})\chi^{L}(\mathbf{k})}{\omega(\mathbf{q}) - \omega(\mathbf{q}-\mathbf{k}) + \mathrm{i}\Lambda(\mathbf{q}-\mathbf{k}) + \mathrm{i}\Gamma(\mathbf{k})}. \tag{2.52}$$

As is easily seen, $\Gamma(q)$ is real, but $\Lambda(q)$ in general is complex. The imaginary part of the transverse damping function $\Lambda(q)$ leads to a shift in the frequency of the transverse spin waves which, however, is a negligible correction in comparison with the frequency matrix (2.41), as will be seen later.

In the hydrodynamic regime, equations (2.51) and (2.52) can be solved analytically with the result

$$\Gamma(q) \propto \frac{q}{\chi^{L}(q)}, \quad \Lambda(q) \propto q^{4} \left[c_{1} \ln\left(\frac{1}{q\xi}\right) + c_{0} \right], \tag{2.53}$$

where c_{0} and c_{1} are constants[†]. With the well known scaling properties of the static susceptibilities (neglecting the Fisher exponent η) given by

$$\chi^{L,T}(q) = \frac{1}{2Jq^{2}a^{2}} \hat{\chi}^{L,T}(x), \tag{2.54}$$

equation (2.41) gives

$$\omega(q) = \Lambda q^{z} \hat{\omega}(x), \tag{2.55}$$

where the dynamical critical exponent $z = \frac{5}{2}$ as in the paramagnetic phase.

The scaling function for the bare frequency of the transverse modes following from equation (2.42) can be written as

$$\hat{\omega}(x) \sim \begin{cases} f x^{1/2}, \\ 0, \end{cases} \quad \text{for} \begin{cases} T \leqslant T_{C}, \\ T \geqslant T_{C}. \end{cases} \tag{2.56}$$

Analysing the scaling properties of the mode-coupling equations and combining this with the static and dynamic scaling law, it was shown (Schinz 1994a, Schinz and Schwabl 1994) that the amplitude f for the scaling function of the spin-wave frequency is a universal quantity and determined by other universal amplitude ratios:

$$f = \left(\frac{\hat{c}}{2}\right)^{1/2} \left(\frac{R_{c}}{(R_{\xi}^{+})^{d}}\right)^{1/2} \left(\frac{\xi_{0}}{\xi_{0}^{T}}\right)^{d-2} \left(\frac{\xi_{-}}{\xi_{+}}\right)^{z-2}. \tag{2.57}$$

Here $\hat{c}$ is an arbitrary normalization constant for the scaling functions. If one chooses

---

[†] The low-temperature spin-wave theory of Dyson (1965a, b) gives in addition a term $q^{4}[\ln(1/q\xi)]^{2}$ (Kascheev and Krivoglaz 1961, Vaks *et al.* 1967a, b, Harris 1968). This will probably come out from a mode-coupling theory where decays of the transverse mode into three transverse modes are included.

Table 2.   Experimental values for the spin-wave amplitude $\hat{b} = f/5\cdot1326$. Data are collected from Bohn *et al.* (1984), Böni *et al.* (1987a, b, 1991b) and Pieper *et al.* (1993).

	$\hat{b}$	
Fe	1·5 (1)	1·8 (1)
Ni	1·5 (1)	2·1 (1)
Co	1·6 (2)	
EuO	1·3 (2)	
EuS	1·4 (2)	1·9 (3)

the value of the scaling functions at criticality to be $\gamma(0) = 5\cdot1326$, $\hat{c}$ becomes $\hat{c} = 8\pi^4$ (Schinz 1994a). The quantities R_c and R_ξ^+ are universal amplitude ratios as defined in the review article by Privman *et al.* (1991), ξ_0^T is a transverse correlation length below T_C (Privman *et al.* 1991), and ξ_+ and ξ_- are longitudinal correlation lengths above and below T_C respectively.

The amplitude f for the spin-wave frequency can be determined from random-phase approximation (RPA) arguments (for example Schwabl (1971)), which gives $f = \pi^{3/2}$. This value has been used in consecutive applications of mode-coupling theory on magnets (Frey and Schwabl 1988a, 1989a) below T_C. Upon using the known values for the static amplitude ratios (Privman *et al.* 1991) it is found that (Schinz 1994a, Schinz and Schwabl 1994)

$$f = 9\cdot5 \pm 1\cdot8. \tag{2.58}$$

This amplitude can also be determined from the available experimental data obtained by Böni *et al.* (1984), Böni *et al.* (1987a, b, 1991b) and Pieper *et al.* (1993) and references cited therein. The results are summarized in table 2 (Schinz 1994a, Schinz and Schwabl 1994) where, depending on which experiment (Bohn *et al.* 1984, Böni *et al.* 1987a, b, 1991b, Pieper *et al.* 1993) one analyses, one obtains slightly different values for f.

Hence equations (2.51) and (2.52) can be solved by using a dynamic scaling *ansatz*

$$\Gamma(q) = \Lambda q^z \gamma(x), \quad \Lambda(q) = \Lambda q^z \lambda(x), \tag{2.59}$$

where the dynamical scaling functions $\gamma(x)$ and $\lambda(x)$ obey the following set of coupled integral equations:

$$\gamma(x) = 2\pi^2 i \int_{-1}^{+1} d\eta \int_0^\infty d\rho \, \rho_-^{-2} \hat{\upsilon}(\rho, \eta) \frac{\hat{\chi}^T(x/\rho_-)\hat{\chi}^T(x/\rho)}{\hat{\chi}^L(x)}$$

$$\times \frac{1}{-\rho^z \hat{\omega}(x/\rho) + \rho_-^z \hat{\omega}(x/\rho_-) + i\rho^z \lambda(x/\rho) + i\rho_-^z \lambda^*(x/\rho_-)}, \tag{2.60}$$

$$\lambda(x) = 2\pi^2 i \int_{-1}^{+1} d\eta \int_0^\infty d\rho \, \rho_-^{-2} \hat{\upsilon}(\rho, \eta) \frac{\hat{\chi}^L(x/\rho_-)\hat{\chi}^T(x/\rho)}{\hat{\chi}^T(x)}$$

$$\times \frac{1}{\hat{\omega}(x) - \rho^z \hat{\omega}(x/\rho) + i\rho^z \lambda(x/\rho) + i\rho_-^z \gamma(x/\rho_-)}. \tag{2.61}$$

Here we have used the same notation as in section 2.2.1.

In order to solve those mode-coupling equations, one has to know the static susceptibilities. In the ferromagnetic phase the global continuous rotation symmetry is spontaneously broken. Although one of the equivalent directions of the order parameter is selected, no free energy is required for an infinitesimal quasistatic rotation of the
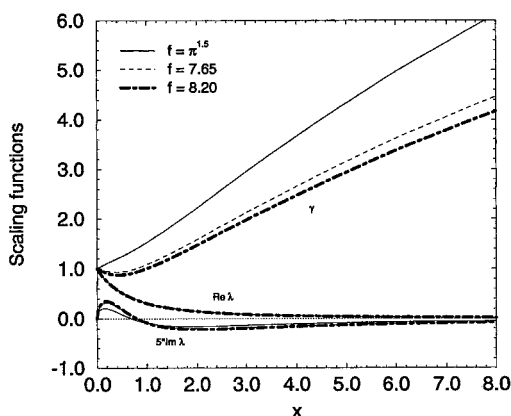
Figure 2.5. Dynamic scaling function for ferromagnets with short-range exchange interaction only against $1/q\xi$ below T_C for three different amplitudes of the spin-wave frequency: (————),$f = \pi^{3/2}$; (------),$f = 7.65$; (—·—),$f = 8.20$. (From Schinz (1994a) and Schinz and Schwabl (1994).)

magnetization vector, which in turn leads to a diverging transverse correlation length. This physical effect is mathematically expressed by the Goldstone (1961) theorem, stating that there is exactly one massless mode for each generator of the broken-symmetry group. In the context of a ferromagnet below T_C this implies that the transverse susceptibility is given by

$$\chi^T(q) = \frac{1}{2Jq^2a^2}.$$ (2.62)

The longitudinal correlation functions entering these integral equations has been computed by Mazenko (1976) to first order in $\varepsilon = 4 - d$ using Wilson's matching technique:

$$\frac{1}{\chi^L(q)} = 2Jq^2a^2\left[1 - \frac{9\varepsilon}{n+8}x^2\left(1 + (1 + 4x^2)^{1/2}\ln\left(\frac{(1 + 4x^2)^{1/2} - 1}{2x}\right)\right)\right.$$
$$\left. + x^2\left(\frac{n + 8 + (5 - n/2)\varepsilon}{9 + (n - 1)x^\varepsilon}\right)\right],$$ (2.63)

where n is the number of spin components. The last term in $\chi^L(q)$ results from the presence of Goldstone modes below T_C, and it implies that also the longitudinal susceptibility diverges in the limit $q \to 0$ for any temperature below T_C.

The resulting numerical solution of the mode-coupling equations (2.60) and (2.61) have been achieved by Frey and Schwabl (1988a, 1989a), Schinz (1994a) and Schinz and Schwabl (1994). The results are shown in figure 2.5 for three different values of the frequency amplitude f.

One recognizes that the scaling function Im $[\lambda(x)]$ for the frequency shift of the transverse modes is very small compared with $\hat{\omega}(x)$. In the critical region Im $[\lambda(x)]$ starts at the critical point with infinite slope and is negative in the hydrodynamical region. The scaling functions for the longitudinal and transverse linewidths split off linearly at the critical temperature and differ by orders of magnitude in the hydrodynamic region. This linear split-off of the longitudinal and transverse widths and the infinite slope of the frequency shift at the critical temperature below T_C is an immediate consequence

Table 3. Asymptotic behaviour of the scaling functions below the critical temperature in units of the value at criticality $\gamma(0)$.

	$\gamma(x)/\gamma(0)$	$\Gamma(q)$	$\{\mathrm{Re}\,[\lambda(x)]\}/\gamma(0)$	$\{\mathrm{Im}\,\{\lambda(x)\}\}/\gamma(0)$	$\mathrm{Im}\,[\Lambda(q)]; \mathrm{Re}[\Lambda(q)]$
$x \gg 1$	$1{\cdot}37 + 0{\cdot}37x^{-1/2}/\chi^L(x)$	$q^2\xi^{-1/2}$	$0{\cdot}16x^{-3/2}\ln x$	$-0{\cdot}07x^{-3/2}\ln x$	$q^4\xi^{3/2}\ln(1/q\xi)$
$x \ll 1$	$1{\cdot}0 + 0{\cdot}55x$	$q^{5/2}$	$1{\cdot}0 - 1{\cdot}34x$	$0{\cdot}77x^{1/2}$	$q^2\xi^{-1/2}; q^{5/2}$

of the presence of Goldstone modes below T_C. This feature can be derived analytically from equations (2.51) and (2.52). The sign of the slope of the longitudinal linewidth depends on the magnitude of the amplitude f for the frequency of the spin waves. For values of f close to the RPA value the slope is positive. If this value is increased towards the universal value determined by Schinz (1994a) and Schinz and Schwabl (1994) the slope becomes negative and one obtains a minimum in the longitudinal scaling function γ. The minimum has been observed in a recent experiment by Böni *et al.* (1991b) (see below). Above T_C the scaling function for the linewidth starts quadratically in agreement with a renormalization group calculation by Iro (1987), but in contrast with the numerically found infinite slope of Hubbard (1971a). It disagrees also with a computation of Bhattacharjee and Ferrell (1985), who predict, using Ward identities, a linear dependence on $1/q\xi$.

The numerical data can be fitted in the limits $x \gg 1$ (hydrodynamical region) and $x \ll 1$ (critical region) by simple approximants as summarized in table 3 (note that all functions are given in units of the value at criticality $\gamma(0) = \mathrm{Re}\,[\lambda(0)] \approx 5{\cdot}1326$).

In unpolarized neutron scattering experiments on Fe (Collins *et al.* 1969), Ni (Minkiewicz *et al.* 1969) and EuO (Passell *et al.* 1976) no quasi-elastic peak from spin diffusion, as predicted by the mode-coupling theory (Frey and Schwabl 1988a, 1989a), was discernible. Only the side peaks originating from the transverse spin waves were observed. This is plausible in the light of the mode-coupling results (Frey and Schwabl 1988a, 1989a). In the hydrodynamic region ($x = 1/q\xi \gg 1$) the width of the longitudinal peak is much wider than the separation of the transverse peaks (Schwabl 1971). Moreover, its intensity is smaller than that of the transverse magnons, which altogether implies that it may be very difficult to distinguish the longitudinal peak from the background. In the critical region the linewidths are of the same order of magnitude. In this limit, however, the frequency of the transverse modes tends to zero. Using unpolarized neutrons, one can observe a superposition of the peaks. Lacking a theory for the linewidth in the critical region below T_C it was impossible up to recently to resolve the longitudinal and transverse peaks.

The first observation of the longitudinal peak was reported by Mitchell *et al.* (1984) using polarized neutrons. This study shows in agreement with the theory that the width of the quasi-elastic longitudinal peak becomes comparable with the spin-wave energy explaining why this peak was not observed by neutron scattering experiments with unpolarized neutrons. However, there are not sufficient data yet to permit a quantitative comparison with the theoretical predictions. Furthermore, the material is disordered (Pd with 10% Fe) which makes it not an ideal system (Böni *et al.* 1991b). Very recently, Böni *et al.* (1991b) have investigated the spin dynamics of a Ni single crystal by means of polarized neutron scattering. They observe that the longitudinal fluctuations are quasi-elastic in agreement with our theoretical predictions (Schwabl 1971, Frey and Schwabl 1988a, 1989a) and renormalization group calculations (Ma and Mazenko 1975). In figure 2.6 we show a quantitative comparison of the longitudinal linewidth,
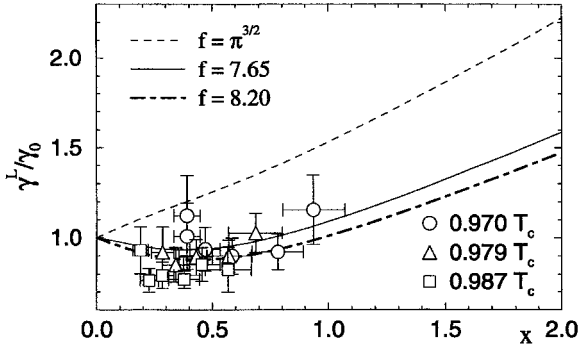
Figure 2.6. Comparison of the longitudinal linewidth with the polarized neutron scattering
experiments on Ni (Böni *et al.* 1991b). All line-widths are normalized to unity at criticality.
The result of mode-coupling theory is shown for three different values of the spin-value
frequency amplitude: (———), $f = \pi^{3/2}$; (------), $f = 7\cdot65$; (—·—), $f = 8\cdot20$. (From
Schinz (1994a) and Schinz and Schwabl (1994).)

obtained from solving the mode-coupling equations in the Lorentzian approximation
(Zobel 1991, Schinz 1994a, Schinz and Schwabl 1994), with the experiment (Böni *et
al.* 1991b). The light broken line represents the result of the mode-coupling equations
with an amplitude $f = \pi^{3/2}$, taken from random-phase approximation arguments. The
solid curve and the chain curve represent the results of solving the mode-coupling
equations with an amplitude of $f = 5\cdot1326 \times 1\cdot49$ and $f = 5\cdot1326 \times 1\cdot60$ respectively.
The agreement between theory and experiment is quite well for an appropriate choice
of the universal amplitude. One should especially note that the scaling function of the
longitudinal linewidth shows a minimum in accord with the experimental data.

Finally we note that the above analysis does not take into account effects from the
dipole–dipole interaction. Those effects have up to now not been studied quantitatively
in the ferromagnetic phase, but one may expect similar effects as above T_C, which we
are going to describe in the next section.

2.3. Renormalization group theory

2.3.1. Paramagnetic phase

Renormalization group calculations of the critical dynamics of ferromagnets start
from a stochastic equation of motion for the spin density $\mathbf{S}(\mathbf{x}, t)$:

$$\frac{\partial \mathbf{S}(\mathbf{x}, t)}{\partial t} = \lambda f \mathbf{S} \times \frac{\delta \mathscr{H}}{\delta \mathbf{S}} + \lambda \nabla^2 \frac{\delta \mathscr{H}}{\delta \mathbf{S}} + \zeta, \tag{2.64}$$

where $\zeta(\mathbf{x}, t)$ is a random force with a Gaussian probability distribution with zero mean
and variance

$$\langle \zeta^i(\mathbf{x}, t)\zeta^j(\mathbf{x}', t') \rangle = 2\Gamma k_B T \delta^{(3)}(\mathbf{x} - \mathbf{x}')\delta(t - t')\delta^{ij}. \tag{2.65}$$

The effective Landau–Ginzburg–Wilson free energy functional is given by

$$\mathscr{H} = \int d^d x \left[\tfrac{1}{2}(r|\mathbf{S}|^2 + |\nabla \mathbf{S}|^2) + \frac{u}{4!}(|\mathbf{S}|^2)^2 \right]. \tag{2.66}$$

These equations can be derived (Kawasaki 1973, Mori and Fujisaka 1973, Mori *et al.*
1974) using a Mori–Zwanzig projection operator formalism (Zwanzig 1961,
Mori 1965) (see also section 6). An exhaustive discussion of these semiphenomenolog-
ical equation of motion can be found in the article by Ma and Mazenko (1975).
The first term in equation (2.64) describes the Larmor precession of the spins in the local
magnetic field, $\delta\mathcal{H}/\delta\mathbf{S}$, and the second term characterizes the damping of the conserved
order parameter. The precession term of the spins in the local magnetic field plays a
major role in the dynamics. From the RG analysis by Ma and Mazenko (1975) and
Bausch *et al.* (1976), one can infer that its effect can be ignored above the upper critical
dimension $d_c = 6$ and can be treated by perturbation theory in $\varepsilon = 6 - d$.†

The RG theory proves (Ma and Mazenko 1975, Bausch *et al.* 1976) the dynamical
scaling hypothesis (Ferrell *et al.* 1967a, b, 1968, Halperin and Hohenberg 1967, 1969)
and shows that the spin correlation function fulfils the dynamical scaling form near the
fixed point given by

$$C(q, \xi, \omega) = \chi(q, \xi)\,\frac{1}{\omega_c(q, \xi)}\,\phi(x, v), \tag{2.67}$$

with the scaling variables $x = 1/q\xi$ and

$$v = \frac{\omega}{\omega_c(q, \xi)}, \tag{2.68}$$

where the characteristic frequency has itself the scaling form

$$\omega_c(q, \xi) = \Lambda q^z \Omega(x). \tag{2.69}$$

The dynamic critical exponent z is known exactly from RG theory (Ma and Mazenko
1975, Bausch *et al.* 1976, Janssen 1976):

$$z = \frac{d + 2 - \eta}{2}, \tag{2.70}$$

in accord with the general dynamic scaling considerations of section 2.1. Here η is the
Fisher exponent from the static scaling law

$$\chi(q, \xi) = q^{-2+\eta}\hat{\chi}(x). \tag{2.71}$$

The Fourier transform of the spin correlation function can be written in the form

$$C(q, \xi, \omega) = \chi(q, \xi)\,\frac{1}{\lambda q^z}\,\mathrm{Re}\left(\frac{2}{-i\hat{\omega} + [\hat{\chi}(x)\Pi(x, \hat{\omega})]^{-1}}\right), \tag{2.72}$$

where $\Pi(x, \hat{\omega})$ is the self-energy of the dynamic susceptibility and we have defined
$\hat{\omega} = \omega/\lambda q^z$. The asymptotic behaviour of the self-energy is known exactly from a RG
analysis (Bausch *et al.* 1976, Dohm 1976):

$$\Pi(x, \hat{\omega}) \sim \begin{cases} \hat{\omega}^{(4-z)/z}, \\ x^{4-z}, \end{cases} \quad \text{for} \quad \begin{cases} \hat{\omega} \to \infty, \\ x \to \infty. \end{cases} \tag{2.73}$$

One-loop RG calculations give to order $O(\varepsilon)$

$$\Pi(x, \hat{\omega}) = 1 - \varepsilon[F(x, i\hat{\omega}) + \tfrac{1}{2}\ln 2] + O(\varepsilon^2), \tag{2.74}$$

---

† The upper critical dimension for the corresponding static problem (see Hamiltonian in
equation (2.65)) is $d_c = 4$. Since the precessional term is of second order in the equations of
motion corresponding to third order in the Lagrangian the upper critical dimension is shifted to
$d_c = 6$.

with (Dohm 1976, Iro 1987)

$$F(0, i\hat\omega) = \begin{cases} -\frac{1}{8}\ln(-i\hat\omega) - \frac{3}{8}\ln 2 + O(\hat\omega^{-1/2}), & \hat\omega \gg 1, \\ -\frac{(\pi + \frac{1}{3})}{8} + \frac{3(2 + 2\ln 2 - \pi)i\hat\omega}{8}, & \text{for} \quad \hat\omega \ll 1, \end{cases} \quad (2.75)$$

and (Ma and Mazenko 1975, Iro 1987)

$$F(x, 0) = \begin{cases} -\frac{1}{2}\ln x - \frac{(\ln 2 + \frac{3}{4})}{2} - \frac{13}{128}x^{-2}, & x \gg 1, \\ -\frac{(\pi + \frac{1}{3})}{8} + \frac{(3\pi - \frac{25}{8} - 3\ln 4)x^2}{4}, & \text{for} \quad x \ll 1. \end{cases} \quad (2.76)$$

In an ε expansion with respect to the upper critical dimension $d_c = 6$ the ϕ^4 term is irrelevant for $4 < d$; hence the static critical behaviour is classical. This is no longer the case for $d < 4$, a fact which has to be kept in mind if one extends the results of the renormalization group ε expansion to $\varepsilon = 3$. The explicit form of $F(x, i\hat\omega)$ to order $O(\varepsilon)$ can be found in the paper by Iro (1987). The logarithms in the limits $(x \to 0, v \to \infty)$ and $(x \to \infty, v \to 0)$ are the $O(\varepsilon)$ contributions of the power-law behaviour in equations (2.73) which are known exactly for any dimension d. Exponentiating these logarithms in such a way that the exactly known asymptotic behaviour in equations (2.73) is matched, one obtains (Bhattacharjee and Ferrell 1981, Iro 1988, 1989) the two-parameter interpolation formula

$$\Pi(x, \hat\omega) = [(1 + bx^2)^{2 - \varepsilon/4} - ai\hat\omega]^{\varepsilon/(8 - \varepsilon)}, \quad (2.77)$$

with $a = 0.46$ ($a = z(6 + 6\ln 2 - 3\pi)/4$) and $b = 3.16$ for $\varepsilon = 3$. This reasoning for exponentiating the leading logarithms of a first-order ε expansion to match the exactly known asymptotic results is due to Bhattacharjee and Ferrell (1981). One should note, however, that this exponentiation procedure is not unique. To test the validity of the exponentiated expression, one would have to calculate contributions to order $O(\varepsilon^2)$ which would be quite cumbersome a task.

The shape function

$$\phi(x, \hat\omega) = 2\,\text{Re}\left(\frac{1}{-i\hat\omega + [\hat\chi(x)\Pi(x, \hat\omega)]^{-1}}\right) \quad (2.78)$$

shows the crossover form the critical shape at $x = 0$ to a Lorentzian at $x = \infty$ in agreement with the mode-coupling results by Hubbard (1971a) and a more recent reanalysis by Aberger and Folk (1988a). From equation (2.72), one can also determine the half-width at half-maximum ω_c defined by

$$C(q, \xi, \omega_c) = \frac{1}{2}C(q, \xi, 0). \quad (2.79)$$

In figure 2.7 the scaling function $\omega_c(x)$ resulting from equations (2.72) and (2.79) is compared with mode-coupling (MC) results (Résibois and Piette 1970, Aberger and Folk 1988a). Whereas the MC result in the Lorentzian approximation (Résibois and Piette 1970) shows large deviations from the RG-result in the hydrodynamic limit, the complete MC result abandoning the Lorentzian approximation (Aberger and Folk 1988) follows closely the RG scaling function. One should note, however, that if all scaling functions are rescaled in such a way that they coincide in the hydrodynamic limit, the differences between the scaling functions appear much less pronounced.

Let us now compare the theoretical predictions with the experiment. In early neutron scattering experiments almost all data have been fitted by a Lorentzian shape function.
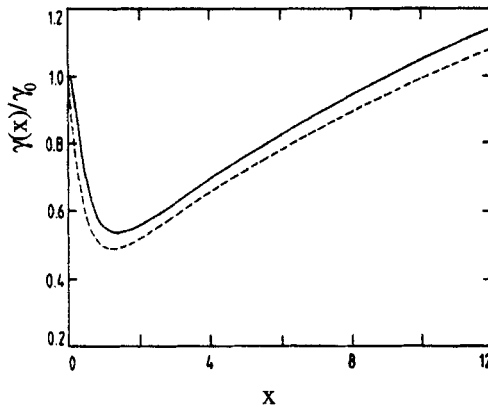
Figure 2.7.   Comparison of the linewidth obtained from mode-coupling and renormalization group analysis. (From Iro (1989).)

Recently, however, with the advances in neutron scattering techniques leading to higher intensities and better resolution, deviations of the measured spectra from a Lorentzian have been observed. By comparing the RG result at T_C (Dohm 1976, Bhattacharjee and Ferrell 1985) with constant energy scans on Fe (Wicksted *et al.* 1984, Lynn 1975, 1983) it has been shown (Folk and Iro 1985) that theory was in accord with the data in the observed experimental wave-vector and frequency window. As has been demonstrated by Böni *et al.* (1987a) the peak positions as well as the peak profile in constant-energy scans of EuO could be explained on the basis of RG theory, taking into account short-range exchange interaction only, for wave-vectors in the range $0.15\,\text{Å} \leqslant q \leqslant 0.3\,\text{Å}$ and energies $0.2\,\text{meV} \leqslant 0.4\,\text{meV}$.

If a model based on the exchange coupling between neighbouring spins is the correct description of the critical behaviour of real ferromagnets, one would have expected that the results from RG and MC theories would become even closer to the experimental data as one comes close to the critical temperature or/and for very large wavelengths. It came as a completely unexpected surprise, when Mezei (1986) found in spin echo experiments on EuO that the observed shape at even smaller wave-vectors $q = 0.024\,\text{Å}^{-1}$ clearly resembled a Lorentzian shape in disagreement with the predictions of RG theory for the dynamics of an isotropic Heisenberg ferromagnet, which would give a bell-shaped decay.

As we shall explain in section 3 this ultimate crossover to a Lorentzian can be explained by taking into account the long-range dipolar interaction. Further evidence of dipolar effects have been found in EuS, where it was observed that the peak positions (in constant-E scans) do not scale (Böni *et al.* 1988).

Concerning the linewidth the experimental situation is as follows. Right at the critical temperature there is almost perfect agreement of the wavevector dependence of the linewidth with $\Gamma \sim q^{5/2}$ in EuS (Böni *et al.* 1987b), EuO (Dietrich *et al.* 1976, Mezei 1984, Böni and Shirane 1986), Fe (Collins *et al.* 1969, Mezei 1982a, b, Wicksted *et al.* 1984) and Ni (Minkiewicz *et al.* 1969, Böni *et al.* 1991b). In early experimental studies on Fe it seemed that the experimental data (Parette and Kahn 1971, Parette 1972) are in reasonable agreement with the theoretically predicted scaling function of Résibois and Piette (1971). Recent neutron scattering experiments, however, showed large deviations from the Résibois–Piette scaling function in Fe (Mezei 1982a, b, 1984), EuO (Mezei 1988, Mezei *et al.* 1989) and EuS (Böni *et al.* 1991a). This puzzling situation

can only be resolved by additionally taking into account the dipolar interaction, which is the subject of sections 3 and 4.

2.3.2. *Ferromagnetic phase*

The critical dynamics below the transition temperature have also been studied by renormalization group methods. Ma and Mazenko (1975) calculated the transport coefficient for the longitudinal magnetization for small wave-vectors in an ε expansion ($\varepsilon = 6 - d$). Their result was

$$\Gamma(q) = \frac{\hat{\Gamma}(q)}{\chi^L(q)} q^2, \tag{2.80}$$

with

$$\hat{\Gamma} \propto q^{(d-6)/6}. \tag{2.81}$$

With $\chi^L(q) \propto 1/q$ in $d = 3$ dimensions this would give $\Gamma(q) \propto q^{5/2}$ in contradiction to the mode coupling result for small q (i.e. in the hydrodynamic limit (Résibois and Piette 1970)). However, Sasvári's (1977) reanalysis of Ma and Mazenko's (1975) exponentiation method showed that taking into account the regular parts of $\hat{\Gamma}(q)$ results in

$$\hat{\Gamma}(q) \propto q^{(d-6)/3}. \tag{2.82}$$

This leads to $\Gamma(q) \propto q^2$ for $d = 3$ dimensions, in agreement with the mode-coupling result in table 3. The q^4 dependence of the transverse transport coefficient in the hydrodynamic limit is also confirmed by the renormalization group calculations (Ma and Mazenko 1975).

A thorough renormalization group study of the critical dynamics of a Heisenberg ferromagnet below T_C is still lacking. Such a study would have to take into account all the peculiarities resulting from the presence of the Goldstone modes below T_C. As a first step towards this end, there is a recent study (Täuber and Schwabl 1992) of the critical dynamics of the $O(n)$-symmetric relaxational models with either non-conserved (model A) or conserved order parameters (model B) below the transition temperature (see also section 5).

3. Dipolar ferromagnets

In this section we review the static and dynamic critical behaviour of dipolar ferromagnets, that is spin systems with both short-range exchange and long-range dipole–dipole interactions. Special emphasis is put on the discussion of the mode-coupling theory in the paramagnetic phase.

However, before turning to the detailed analysis we would like to emphasize the following characteristic features of the dipole–dipole interaction, which have important implications on the critical dynamics.

(1) In contrast with the short-range exchange interaction the dipolar interaction is long ranged and thus dominates the asymptotic critical behaviour of ferromagnets.

(2) It introduces an anisotropy of the spin fluctuations longitudinal and transverse to the wave-vector $\mathbf{q}$. This implies that the longitudinal static susceptibility remains finite for $\mathbf{q} \to 0$ and $T \to T_C$ (Aharony 1973a, Aharony and Fisher 1973).

Table 4.   Coefficients in the Taylor expansion of $A_q^{\alpha\beta}$ for three-dimensional cubic lattices. (From Aharony (1973b, c).) c denotes the coordination number, v_a the volume of the primitive unit cell and α_i are lengths characterizing the dipolar interaction.

Lattice	c	v_a (units of a^3)	α_1 (units of a)	α_2 (units of a)	a_3 (units of a)
S.c.	6	1	1·2755	0·1649	1·7700
B.c.c.	8	$4/3^{3/2}$	1·7420	− 0·321	0·8210
F.c.c.	12	$1/2^{1/2}$	2·8313	− 0·355	1·823

(3) The order parameter is no longer conserved as can be inferred from the equations of motion.

(4) The strength of the dipolar interaction introduces, besides the correlation length ξ, a second length scale q_D^{-1}, where q_D is the so-called dipolar wave-vector defined below. This leads to generalized scaling laws for the relaxation functions and the line widths.

3.1. The model Hamiltonian

Our starting point is a Hamiltonian for a spin system including both isotropic short-range exchange and long-range dipolar interactions:

$$H = - \sum_{l \neq l'} (J_{ll'}\delta^{\alpha\beta} + A_{ll'}^{\alpha\beta})S_l^\alpha S_{l'}^\beta, \tag{3.1}$$

where $J_{ll'}$ denotes the short-range exchange interaction, usually restricted to nearest or next-nearest neighbours, and $A_{ll'}^{\alpha\beta}$ is the dipolar interaction tensor given by

$$A_{ll'}^{\alpha\beta} = - \tfrac{1}{2}(g_L\mu_B)^2 \left(\frac{\delta^{\alpha\beta}}{|\mathbf{x}_l - \mathbf{x}_{l'}|^3} - \frac{3(x_l - x_{l'})^\alpha(x_l - x_{l'})^\beta}{|\mathbf{x}_l - \mathbf{x}_{l'}|^5} \right). \tag{3.2}$$

Here g_L is the Landé factor, and μ_B the Bohr magneton. As shown by Cohen and Keffer (1955), the lattice sums

$$A_q^{\alpha\beta} = \sum_{l \neq 0} A_{l0}^{\alpha\beta} \exp{(i\mathbf{q} \cdot \mathbf{x}_l)} \tag{3.3}$$

can be evaluated using Ewald's (1917a, b, 1921) method, and one finds for infinite 3D cubic lattices (Cohen and Keffer 1955, Aharony 1973a, b, Aharony and Fisher 1973)

$$A_q^{\alpha\beta}v_a = \tfrac{1}{2}(g_L\mu_B)^2 \left[\frac{4\pi}{3} \left(\delta^{\alpha\beta} - \frac{3q^\alpha q^\beta}{q^2} \right) \right.$$

$$\left. + \alpha_1 q^\alpha q^\beta + [\alpha_2 q^2 - \alpha_3(q^\alpha)^2]\delta^{\alpha\beta} + O(q^4, (q^\alpha)^4, (q^\alpha)^2(q^\beta)^2) \right], \tag{3.4}$$

where v_a is the volume of the primitive unit cell with lattice constant a, and α_i are constants, which depend on the lattice structure (table 4). Upon expanding the exchange interaction

$$J_q = \sum_l{'} J_{l0} \exp{(i\mathbf{q} \cdot \mathbf{x}_l)} = J_0 - Jq^2a^2 + O(q^4), \tag{3.5}$$

and keeping only those terms which are relevant in the sense of renormalization group theory, this results in the following effective Hamiltonian for dipolar ferromagnets:

$$H = \sum_{\mathbf{q}} \left(-J_0 + Jq^2a^2 + Jg\frac{q^\alpha q^\beta}{q^2} \right) S^\alpha_{-\mathbf{q}} S^\beta_{\mathbf{q}}, \tag{3.6}$$

where the Fourier transform of the spin variables is defined by

$$S^\alpha_{\mathbf{q}} = \frac{1}{\sqrt{N}} \sum_l S^\alpha_l \exp(i\mathbf{q}\cdot\mathbf{x}_l). \tag{3.7}$$

Here we have defined a dimensionless quantity g as the ratio of the dipolar energy $(g_L\mu_B)^2/a^3$ and exchange energy $2J$, multiplied by a factor of $4\pi a^3/v_a$, which depends on the lattice structure:

$$g = \frac{4\pi a^3}{v_a}\frac{(g_L\mu_B)^2/a^3}{2J} \propto \frac{\text{dipolar energy}}{\text{exchange energy}}. \tag{3.8}$$

Strictly speaking there are dipolar corrections $O(q^2)$ to the exchange coupling. However, those can be neglected, since the strength of the dipolar interaction is small compared with the exchange interaction.

The dipolar interaction induces an anisotropy of the static as well as the dynamic spin–spin correlation function with respect to the wave-vector $\mathbf{q}$. It was shown by Aharony and Fisher (1973) that the static transverse susceptibility diverges with the dipolar critical exponent γ as the critical temperature is approached, whereas the longitudinal susceptibility remains finite. The finite value is inversely proportional to the strength of the dipolar interaction g. The dipolar anisotropy becomes substantial when $q^2 + \xi^{-2} \lesssim q_D^2$, where the dipolar wave-vector is defined as $g = (q_D a)^2$. The strong suppression of the longitudinal fluctuations has been observed in EuS and EuO by polarized neutron scattering experiments (Kötzler *et al.* 1986).

The matrix of the static susceptibility is given by

$$\chi^{\alpha\beta}(g,\mathbf{q}) = \chi^T(g,q)\left(\delta^{\alpha\beta} - \frac{q^\alpha q^\beta}{q^2}\right) + \chi^L(g,q)\frac{q^\alpha q^\beta}{q^2}, \tag{3.9}$$

where one often uses the Ornstein–Zernike forms for the longitudinal and transverse susceptibilities given by

$$\chi^T(g,q) = \frac{\Upsilon}{q^2 + \xi^{-2}}, \tag{3.10}$$

$$\chi^L(g,q) = \frac{\Upsilon}{q^2 + q_D^2 + \xi^{-2}}, \tag{3.11}$$

with the non-universal static amplitude

$$\Upsilon = \frac{(g_L\mu_B)^2}{2Ja^2}. \tag{3.12}$$

Conventional mode-coupling theory does not account for effects of the critical exponent η, which will be neglected in the following†. Here $\xi = \xi_0[(T-T_C)/T_C]^{-\nu}$ is the correlation length. The static crossover from Heisenberg to dipolar critical behaviour is partly contained in ξ through the effective temperature-dependent exponent (Bruce *et al.* 1976, Frey and Schwabl 1988b, 1991) $\nu \approx \gamma_{\text{eff}}/2$. The full dipolar crossover

---

† For a refined version of mode-coupling theory with allows for a consistent treatment of the Fisher exponent η see section 6.

in the static critical behaviour has previously been studied (Bruce *et al.* 1976, Nattermann and Trimper 1976, Bruce 1977, Frey and Schwabl 1988b, 1991).

The tensorial structure of the static susceptibility suggests a decomposition of the spin operator $\mathbf{S_q}$ into one longitudinal and two transverse components with respect to the wave-vector $\mathbf{q}$, that is

$$\mathbf{S_q} = S_{\mathbf{q}}^{L}\hat{\mathbf{q}} + S_{\mathbf{q}}^{T_1}\hat{\mathbf{t}}^1(\hat{\mathbf{q}}) + S_{\mathbf{q}}^{T_2}\hat{\mathbf{t}}^2(\hat{\mathbf{q}}), \tag{3.13}$$

where the orthonormal set of unit vectors is defined by

$$\hat{\mathbf{q}} = \frac{\mathbf{q}}{q}, \quad \hat{\mathbf{t}}^1(\hat{\mathbf{q}}) = \frac{\mathbf{q} \times \mathbf{e}_3}{(q_1^2 + q_2^2)^{1/2}}, \quad \hat{\mathbf{t}}^2(\hat{\mathbf{q}}) = \hat{\mathbf{q}} \times \hat{\mathbf{t}}^1(\hat{\mathbf{q}}). \tag{3.14}$$

For vanishing components of $\mathbf{q}$ the limits are taken in the order of increasing Cartesian components.

From the Hamiltonian (equation (3.16)), one deduces the following microscopic Heisenberg equations of motion (Frey 1986, Frey and Schwabl 1987)

$$\frac{d}{dt} S_{\mathbf{q}}^{L} = Ja^2 \int \frac{v_a d^3k}{(2\pi)^3} \frac{1}{k} \left[\mathbf{q} \cdot (2\mathbf{k} - \mathbf{q})[(k_1^2 + k_2^2)^{1/2}\{S_{\mathbf{q}-\mathbf{k}}^{T_1}, S_{\mathbf{k}}^{L}\} + k_3\{S_{\mathbf{q}-\mathbf{k}}^{T_1}, S_{\mathbf{k}}^{T_2}\}] \right.$$

$$\left. + g(k_1^2 + k_2^2)^{1/2}\{S_{\mathbf{q}-\mathbf{k}}^{T_1}, S_{\mathbf{k}}^{L}\} \right], \tag{3.15}$$

$$\frac{d}{dt} S_{\mathbf{q}}^{T} = -Ja^2 \int \frac{v_a d^3k}{(2\pi)^3} \frac{1}{k} \left[\mathbf{q} \cdot (2\mathbf{k} - \mathbf{q}) \left(\frac{-k_1 k_3}{(k_1^2 + k_2^2)^{1/2}} \{S_{\mathbf{q}-\mathbf{k}}^{T_1}, S_{\mathbf{k}}^{L}\} + k_1\{S_{\mathbf{q}-\mathbf{k}}^{T_1}, S_{\mathbf{k}}^{T_2}\} \right. \right.$$

$$\left. + \frac{k_2(k_3 q - k^2)}{|\mathbf{q} - \mathbf{k}|(k_1^2 + k_2^2)^{1/2}} \{S_{\mathbf{q}-\mathbf{k}}^{T_2}, S_{\mathbf{k}}^{L}\} + \frac{1}{2}\frac{k_2 q}{|\mathbf{q} - \mathbf{k}|}(\{S_{\mathbf{q}-\mathbf{k}}^{L}, S_{\mathbf{k}}^{L}\} - \{S_{\mathbf{q}-\mathbf{k}}^{T_2}, S_{\mathbf{k}}^{T_2}\}) \right)$$

$$\left. + g\left(\frac{-k_1 k_3}{(k_1^2 + k_2^2)^{1/2}} \{S_{\mathbf{q}-\mathbf{k}}^{T_1}, S_{\mathbf{k}}^{L}\} + \frac{k_2(k_3 q - k^2)}{|\mathbf{q} - \mathbf{k}|(k_1^2 + k_2^2)^{1/2}} \{S_{\mathbf{q}-\mathbf{k}}^{T_2}, S_{\mathbf{k}}^{L}\} \right) \right], \tag{3.16}$$

and for $S_{\mathbf{q}}^{T_2}$ correspondingly, where $\{,\}$ denotes the anticommmutator. The terms proportional to g, resulting from the dipolar term in the Hamiltonian remain finite as the wave-vector $\mathbf{q}$ tends to zero, whereas all the other terms vanish in this limit. This is responsible for the fact that the dipolar forces lead to relaxational dynamics in the limit of long wavelengths, that is the order parameter is no longer a conserved quantity.

3.2. *Mode-coupling theory for the paramagnetic phase*

3.2.1. *General mode-coupling equations*

As we have explained in section 2, mode-coupling theory amounts to a factorization approximation for the transport coefficients

$$\Gamma^{L}(q, g, t) = \frac{(g_L \mu_B)^2}{\chi^{L}(q, g)} (\dot{S}^{L}(\mathbf{q}, t), \dot{S}^{L}(\mathbf{q}, 0)), \tag{3.17}$$

$$\Gamma^{T}(q, g, t) = \frac{(g_L \mu_B)^2}{\chi^{T}(q, g)} (\dot{S}^{T_1}(\mathbf{q}, t), \dot{S}^{T_1}(\mathbf{q}, 0))$$

$$= \frac{(g_L \mu_B)^2}{\chi^{T}(q, g)} (\dot{S}^{T_2}(\mathbf{q}, t), \dot{S}^{T_2}(\mathbf{q}, 0)). \tag{3.18}$$

The mode-coupling equations resulting from considering two-mode decay processes have been derived by Frey (1986) and Frey and Schwabl (1987) ($\alpha = $ L, T) and are

given by

$$\Gamma^\alpha(q,g,t) = 2(2Ja^2)^2 \frac{k_\mathrm{B}T}{(g_\mathrm{L}\mu_\mathrm{B})^2} \int \frac{v_a\,\mathrm{d}^3k}{(2\pi)^3} \sum_{\beta,\sigma} v^\alpha_{\beta\sigma}(k,q,g,\theta)(\delta^{\sigma,\mathrm{T}} + \delta^{\alpha,\mathrm{T}}\delta^{\beta,\mathrm{L}}\delta^{\sigma,\mathrm{L}})$$

$$\times \frac{\chi^\beta(\mathbf{k},g)\chi^\sigma(\mathbf{q}-\mathbf{k},g)}{\chi^\alpha(\mathbf{q},g)}\; \Phi^\beta(\mathbf{k},g,t)\Phi^\sigma(\mathbf{q}-\mathbf{k},g,t). \tag{3.19}$$

Here the k integration runs over the first Brillouin zone. The vertex functions $v^\alpha_{\beta\sigma}$ for the decay of the mode α into the modes β and σ are given by (Frey and Schwabl 1987)

$$v^\mathrm{L}_\mathrm{TT}(k,q,g,\eta) = 2q^4\cos^2\theta \left(\frac{k\cos\theta}{q} - \frac{1}{2}\right)^2, \tag{3.20}$$

$$v^\mathrm{L}_\mathrm{LT}(k,q,g,\eta) = 2q^4\sin^2\theta \left(\frac{k\cos\theta}{q} - \frac{1}{2} + \frac{g}{2q^2}\right)^2, \tag{3.21}$$

$$v^\mathrm{T}_\mathrm{TT}(k,q,g,\eta) = q^4\sin^2\theta \left(\frac{k\cos\theta}{q} - \frac{1}{2}\right)^2 \left(1 + \frac{q^2}{2|\mathbf{q}-\mathbf{k}|^2}\right), \tag{3.22}$$

$$v^\mathrm{T}_\mathrm{LT}(k,q,g,\eta) = q^4 \left(\frac{k\cos\theta}{q} - \frac{1}{2} + \frac{g}{2q^2}\right)^2 \left[2 - \left(1 + \frac{q^2}{|\mathbf{q}-\mathbf{k}|^2}\right)\sin^2\theta\right], \tag{3.23}$$

$$v^\mathrm{T}_\mathrm{LL}(k,q,g,\eta) = q^4\sin^2\theta \left(\frac{k\cos\theta}{q} - \frac{1}{2}\right)^2 \frac{q^2}{2|\mathbf{q}-\mathbf{k}|^2}, \tag{3.24}$$

with $\eta = \cos\theta$. In passing we note that there were certain attempts to develop a mode-coupling theory already 20 years ago, although nobody succeeded in deriving the appropriate mode-coupling equations. A type of mode-coupling calculation was used by Huber (1971) to determine the uniform spin relaxation for temperatures larger than the dipolar crossover temperature. This analysis was extended by Finger (1977b), who put forward certain scaling estimates and computed the uniform spin relaxation in the strong dipolar region. An attempt to construct a mode-coupling theory was launched by Borckmans *et al.* (1977), using an incomplete basis and ending up with equations containing undetermined vertices. The theoretical and experimental situation was rather controversial and no explanation was available for the apparent contradictions (Kötzler 1986, Mezei 1987). Only in 1986 was a complete self-consistent mode coupling theory developed by Frey (1986) and Frey and Schwabl (1987) and its various properties and consequences were studied in detail (Frey and Schwabl 1988a, b, 1989a, Frey *et al.* 1988, 1989). Some of the results were confirmed numerically by Aberger and Folk (1988b, 1989) and by Kalashnikov and Tret'jakov (1990a, b, 1991) using analytical approximants.

The mode coupling result for the transport coefficients (equation (3.19)), together with the relation

$$\frac{\partial}{\partial t}\,\Phi^\alpha(q,g,t) = -\int_0^t \mathrm{d}\tau\,\Gamma^\alpha(q,g,t-\tau)\Phi^\alpha(q,g,\tau) \tag{3.25}$$

for the Kubo relaxation functions constitute, as in section 2, a complete set of self-consistent equations.

As emphasized before, the dipolar interaction introduces a second length scale q_D^{-1} besides the correlation length ξ. This entails the following extension of the static scaling law for the spin susceptibilities:

$$\chi^\alpha(q,\xi,g) = \Upsilon q^{-2}\hat\chi^\alpha(x,y), \tag{3.26}$$

with the scaling variables

$$x = \frac{1}{q\xi} \quad \text{and} \quad y = \frac{q_D}{q}. \tag{3.27}$$

Note that here and in the remainder of this section we have explicitly indicated the dependence of the susceptibility on the correlation length. In all other parts of this review we suppress this dependence for notational convenience. Since the vertex functions $v_{\beta\sigma}^\alpha$ are proportional to the fourth power of the wavenumber, that is $v_{\beta\sigma}^\alpha \propto q^4$, and because of the homogeneity of equation (3.26), the relaxation functions and linewidths derived from equations (3.19)–(3.25) obey the dynamical scaling laws

$$\Phi^\alpha(ql, gl^2, \omega l^z) = l^{-z}\Phi^\alpha(q, \xi, g, \omega) \tag{3.28}$$

and

$$\Gamma^\alpha(ql, gl^2, \omega l^z) = l^z\Gamma^\alpha(q, \xi, g, \omega), \tag{3.29}$$

with $z = \frac{5}{2}$ and a scaling parameter l. We emphasize that, despite z assuming the isotropic value $\frac{5}{2}$, there is a crossover to dipolar critical behaviour contained in the functional form of the correlation functions, as will become clear below.

An immediate consequence of equation (3.29) is the following scaling property of the characteristic longitudinal and transverse frequencies $\omega_c^\alpha(q, \xi, g)$:

$$\omega_c^\alpha(q, \xi, g) = Aq^z\Omega^\alpha(x, y), \tag{3.30}$$

where A is a non-universal coefficient.

Now there are various ways to rewrite the scaling laws equations (3.28) and (3.29) by appropriate choices of the scaling parameter l. If one sets $l = q^{-1}$, one finds that

$$\Phi^\alpha(q, \xi, g, \omega) = q^{-z}\hat{\Phi}^\alpha\left(\frac{1}{q\xi}, \frac{g}{q^2}, \frac{\omega}{q^z}\right) \tag{3.31}$$

and

$$\Gamma^\alpha(q, \xi, g, \omega) = q^z\hat{\Gamma}^\alpha\left(\frac{1}{q\xi}, \frac{g}{q^2}, \frac{\omega}{q^z}\right). \tag{3.32}$$

A disadvantage of the representation given in equations (3.31) and (3.32) is that the crossovers both of the time scales and of the shapes of the correlation functions are intermixed in $\hat{\Phi}^\alpha$. Since the time scales for the isotropic and dipolar critical and hydrodynamic behaviours differ quite drastically, it is more natural to measure frequencies in units of the characteristic frequencies. Hence we fix the scaling parameter by the condition

$$l^z = \frac{1}{Aq^z\Omega^\alpha(x, y)}, \tag{3.33}$$

and find from equations (3.31) and (3.32) the scaling forms

$$\Phi^\alpha(q, \xi, g, \omega) = \frac{1}{Aq^z\Omega^\alpha(x, y)}\phi^\alpha(x, y, v_\alpha) \tag{3.34}$$

and

$$\Gamma^\alpha(q, \xi, g, \omega) = Aq^z\Omega^\alpha(x, y)\gamma^\alpha(x, y, v_\alpha), \tag{3.35}$$

with the scaling variable for the frequency

$$v_\alpha = \frac{\omega}{Aq^z\Omega^\alpha(x, y)}. \tag{3.36}$$

With equation (3.33), one has separated the crossover of the frequency scales and the

crossover of the shapes of the correlation functions. The former mainly is contained in $\Omega^\alpha(x, y)$, and the latter in $\phi^\alpha(x, y, v_\alpha)$.

There is still some freedom in the choice of the characteristic frequencies ω_c^α in equation (3.33); for instance, one could take the half-width at half-maximum (HWHM) of the frequency-dependent Kubo functions. This, however, would require to solve equations (3.19) and (3.25) simultaneously for the time scales and the shapes of the correlation functions. Therefore, in the following, we shall use as characteristic frequencies the half-widths resulting from the Lorentzian approximation for the line shape (see section 3.3). The Lorentzian linewidths qualitatively obey the same scaling laws as the HWHM and have the same asymptotic (hydrodynamic, dipolar and isotropic) properties. Thus this choice for the characteristic frequencies solely is a matter of numerical convenience and does not introduce any approximations in the final result. From the final result, one can obtain the HWHM and rewrite the scaling functions in terms of these new variables.

Equations (3.34)–(3.36) imply for the Laplace transformed quantities the scaling laws

$$\Phi^\alpha(q, \xi, g, t) = \phi^\alpha(x, y, \tau_\alpha) \tag{3.37}$$

and

$$\Gamma^\alpha(q, \xi, g, t) = [Aq^z\Omega^\alpha(x, y)]^2\gamma^\alpha(x, y, \tau_\alpha), \tag{3.38}$$

where the scaled time variables τ_α are given by

$$\tau_\alpha = Aq^z\Omega^\alpha(x, y)t. \tag{3.39}$$

One should note that the characteristic time scales $1/Aq^z\Omega^\alpha(x, y)$ are different for the longitudinal and transverse modes. This is mainly due to the non-critical longitudinal static susceptibility, implying that the longitudinal characteristic frequency $Aq^z\Omega^L(x, y)$ shows no critical slowing down asymptotically. In other words for $T = T_C$ and $q \to 0$ the longitudinal characteristic frequency does not tend to zero, which implies an effective longitudinal dynamical critical exponent $z_{\text{eff}}^L = 0$ for the wave-vector dependence in the limit $q \to 0$. In comparison, the effective exponent for the transverse characteristic frequency at T_C shows a crossover from $z_{\text{eff}}^T = \frac{5}{2}$ to $z_{\text{eff}}^T = 2$ (see also the following section). This mode-coupling result disagrees with a calculation based on nonlinear spin-wave theory, where $z_{\text{eff}}^T = 1$ is found in the dipolar region (Maleev 1974).

Inserting equations (3.37)–(3.38) together with the static scaling law (3.26) into equations (3.19) and (3.25) we find the following coupled integrodifferential equations:

$$\gamma^\alpha(x, y, \tau_\alpha) = 2\left(\frac{\pi}{\Omega^\alpha(x, y)}\right)^2 \int_{-1}^{+1} \mathrm{d}\eta \int_0^{\rho_{\text{cut}}} \mathrm{d}\rho\, \rho_-^{-2} \sum_{\beta, \sigma} \vartheta_{\beta\sigma}^\alpha(y, \rho, \eta)(\delta^{\sigma, \text{T}} + \delta^{\alpha, \text{T}}\delta^{\beta, \text{L}}\delta^{\sigma, \text{L}})$$

$$\times \frac{\hat{\chi}^\beta(x/\rho, y/\rho)\hat{\chi}^\sigma(x/\rho_-, y/\rho_-)}{\hat{\chi}^\alpha(x, y)}\, \phi^\beta\left(\frac{x}{\rho}, \frac{y}{\rho}, \tau_{\alpha\beta}(x, y, \rho)\right)$$

$$\times \phi^\sigma\left(\frac{x}{\rho_-}, \frac{y}{\rho_-}, \tau_{\alpha\sigma}(x, y, \rho_-)\right) \tag{3.40}$$

and

$$\frac{\partial}{\partial\tau_\alpha}\phi^\alpha(x, y, \tau_\alpha) = -\int_0^{\tau_\alpha} \mathrm{d}\tau\, \gamma^\alpha(x, y, \tau_\alpha - \tau)\phi^\alpha(x, y, \tau), \tag{3.41}$$

connecting the scaling functions for the transport coefficients with the scaling functions for the Kubo relaxation functions. In equation (3.40) we introduced the notations $\rho = k/q$, $\rho_- = |\mathbf{q} - \mathbf{k}|/q$, $\eta = \cos(\mathbf{q}, \mathbf{k})$ and $\tau_{\alpha\beta}(x, y, \mu) = \tau_\alpha\mu^z\Omega^\beta(x/\mu, y/\mu)/\Omega^\alpha(x, y)$.

The non-universal frequency scale resulting from the transformation of equation (3.19) in equation (3.40) is

$$A = \frac{a^{5/2}}{b} \left(\frac{2Jk_B T}{4\pi^4} \right)^{1/2}. \tag{3.42}$$

The apparent critical dynamic exponent contained in equation (3.40) equals $z = \frac{5}{2}$. However, as noted before, the crossover to dipolar behaviour is contained in the scaling functions for the transport coefficients $\gamma^\alpha(x, y \tau_\alpha)$, the scaling functions for the Kubo relaxation functions $\phi^\alpha(x, y, \tau_\alpha)$ and the scaling functions of the characteristic frequencies $\Omega^\alpha(x, y)$.

The scaled vertex functions appearing in equation (3.40) are (Frey and Schwabl 1987)

$$\hat{v}^\alpha_{\beta\beta} = \left[2\eta^2 \delta^{\alpha,L} + (1 - \eta^2) \left(\delta^{\beta,T} + \frac{1}{2\rho_-^2} \right) \delta^{\alpha,T} \right] (\rho\eta - \tfrac{1}{2})^2, \tag{3.43}$$

$$\hat{v}^\alpha_{LT} = \left[2(1 - \eta^2 \delta^{\alpha,L}) - (1 - \eta^2) \left(1 + \frac{1}{\rho_-^2} \right) \delta^{\alpha,T} \right] \left(\rho\eta - \frac{1}{2} + \frac{y^2}{2} \right)^2, \tag{3.44}$$

which are related to the vertex functions $v^\alpha_{\beta\sigma}$ of equations (3.20)–(3.24) by $v^\alpha_{\beta\sigma} = q^4 \hat{v}^\alpha_{\beta\sigma}$. For both longitudinal and transverse modes, the dipolar interaction enters only in vertices involving decays into a longitudinal and a transverse mode, since the dipolar interaction enters the Hamiltonian only through the longitudinal modes.

Because the k integration is restricted to the Brillouin zone the ρ integration of equation (3.40) contains the cut-off

$$\rho_{cut} = \frac{q_{BZ}}{q} = \frac{q_{BZ}}{q_D} y, \tag{3.45}$$

where q_{BZ} denotes the boundary of the first Brillouin zone. All other material-dependent parameters are contained in the frequency scale A. The cut-off is important for small times, because the integrand of equation (3.40) is of the order of unity for $t = 0$ and $\rho \gg 1$. Hence, for small times, wave-vectors near the zone boundary also contribute to the relaxation mechanism.

As explained before, in the numerical solution of the MC equations one has taken (Frey *et al.* 1988, 1989) for the characteristic frequencies the linewidths resulting from the Lorentzian approximation of the MC equations, that is

$$\Omega^\alpha(x, y) = \gamma^\alpha_{Lor}(x, y). \tag{3.46}$$

Using as input the solution of the mode-coupling equations in the Lorentzian approximation one can solve the complete set of MC equations for different values of q_{BZ}. Because there are three scaling variables (x, y and v_α) it is impossible to present here all the numerical results. Instead, in section 4, we shall concentrate on a limited number of temperatures and wave-vectors motivated by the available experiments on the substrate of primary interest, namely EuS, EuO and Fe.

3.2.2. *The Lorentzian approximation*

For later reference we want to close this section by quoting the results from the so-called Lorentzian approximation (Frey and Schwabl 1987, 1988a, 1989a). The results of the numerical solution of the full mode-coupling equations will be discussed in section 4 in conjunction with the experimental data.

Table 5. Asymptotic behaviour of the scaling functions for the longitudinal and transverse Lorentzian linewidths in the paramagnetic phase. The different regions, namely dipolar critical, isotropic critical, dipolar hydrodynamic and isotropic hydrodynamic are defined as follows: dipolar critical, $y \gg 1$, $x \ll 1$; isotropic critical, $y \ll 1$, $x \ll 1$; dipolar hydrodynamic, $y \gg x, x \gg 1$; isotropic hydrodynamic, $y \ll x, x \gg 1$.

Region	γ^T	γ^L
Dipolar critical	$y^{1/2}$	$y^{5/2}$
Isotropic critical	1	1
Dipolar hydrodynamic	$y^{1/2}x^2$	$y^{5/2}$
Isotropic hydrodynamic	$x^{1/2}$	$x^{1/2}$

If the transport coefficients vary only slowly with ω, we may approximate the relaxation functions by Lorentzians, that is we replace the transport coefficients by their values at $\omega = 0$:

$$\Gamma^L_{\text{Lor}}(q, \xi, g) = \Gamma^L(q, \xi, g, \omega = 0), \quad \Gamma^T_{\text{Lor}}(q, \xi, g) = \Gamma^T(q, \xi, g, \omega = 0). \quad (3.47)$$

Despite a Lorentzian being not the correct shape of the correlation function for all values of the scaling variables, the resulting linewidths obtained in the Lorentzian approximation already capture most of the crossover in the time scale.

The Lorentzian linewidths obey the scaling law

$$\Gamma^\alpha_{\text{Lor}}(q, \xi, g) = \Lambda q^z \gamma^\alpha_{\text{Lor}}(x, y). \quad (3.48)$$

From equation (3.20) it is then easily inferred that the scaling functions of the Lorentzian linewidths $\gamma^\alpha_{\text{Lor}}(x, y)$ are determined by the coupled integral equations

$$\gamma^\alpha_{\text{Lor}}(x, y) = \frac{2\pi^2}{\hat{\chi}^\alpha(x, y)} \int_{-1}^{+1} d\eta \int_0^\infty d\rho\, \rho_-^{-2} \sum_\beta \sum_\sigma \hat{v}^\alpha_{\beta\sigma}(y, \rho, \eta)$$

$$\times (\delta^{\sigma, T} + \delta^{\alpha, T}\delta^{\beta, L}\delta^{\sigma, L}) \frac{\hat{\chi}^\beta(x/\rho, y/\rho)\hat{\chi}^\sigma(x/\rho_-, y/\rho_-)}{\rho^{5/2}\gamma^\beta_{\text{Lor}}(x/\rho, y/\rho) + \rho_-^{5/2}\gamma^\sigma_{\text{Lor}}(x/\rho_-, y/\rho_-)}. \quad (3.49)$$

As summarized in table 5 the mode-coupling equations (3.49) can be solved analytically in the dipolar (D) and isotropic (I) critical (C) and hydrodynamic (H) limiting regions. These regions are defined as follows: DC, $y \gg 1, x \ll 1$; IC, $y \ll 1, x \ll 1$; DH, $y \gg x, x \gg 1$; IH, $y \ll x, x \gg 1$.

Concerning the critical dynamic exponent, one finds for the longitudinal linewidth a crossover from $z = \frac{5}{2}$ in the isotropic critical region to $z = 0$ in the dipolar critical region, whereas for the transverse linewidth the crossover is from $z = \frac{5}{2}$ to $z = 2$. The precise position of the crossover can only be determined numerically.

The numerical solution (Frey 1986, Frey and Schwabl 1987) of equation (3.49) shows that the dynamic crossover for the transverse width is shifted to smaller wave-vectors by almost one order of magnitude with respect to the static crossover, whereas the crossover for the longitudinal width occurs at the static crossover. For the numerical solution of the mode-coupling equations it is convenient to introduce polar coordinates

$$r = (x^2 + y^2)^{1/2} \quad \text{and} \quad \varphi = \tan^{-1}\left(\frac{y}{x}\right).$$

The transverse and longitudinal scaling functions $\gamma^T(r, \varphi)$ and $\gamma^L(r, \varphi)$ are shown in figures 3.1 and 3.2 as functions of the radical scaling variables r and φ. A different

E. Frey and F. Schwabl

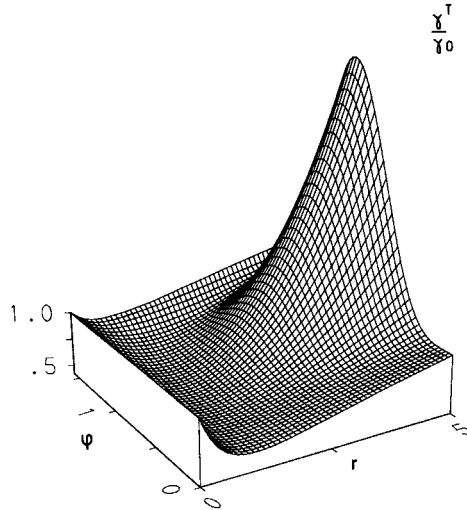$$\frac{\gamma^{T}}{\gamma_0}$$

Figure 3.1.   Scaling function γ^T for the transverse width in the Lorentzian approximation against $r = 1/q\xi[1 + (q_D\xi)^2]^{1/2}$ and $\varphi = \tan^{-1}(q_D\xi)$.
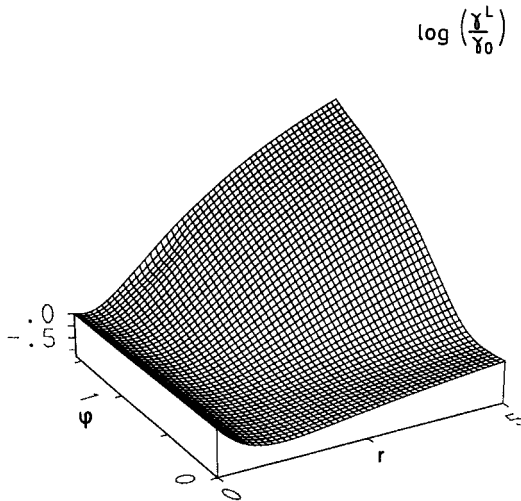
$$\log\left(\frac{\gamma^L}{\gamma_0}\right)$$

Figure 3.2.   Scaling function γ^L for the transverse width in the Lorentzian approximation against $r = 1/q\xi[1 + (q_D\xi)^2]^{1/2}$ and $\varphi = \tan^{-1}(q_D\xi)$.

representation of the results can be given by plotting the linewidth against the single scaling variable x for several values of φ. This is shown in figures 3.3–3.5 where we have drawn the two-parameter scaling functions $\gamma_{\text{Lor}}^{L,T}(x,y)$ in units of the value at criticality, $\gamma_0 = \gamma_{\text{Lor}}^{L(T)}(0,0) \approx 5\cdot1326$. The physical content of the two-parameter scaling surfaces is illustrated best by considering cuts for fixed q_D and various temperatures. In figures 3.3 and 3.4 the scaling functions against $x = 1/q\xi$ are displayed for different values of $\varphi = \tan^{-1}(q_D\xi) = N\pi/20$ with $N = 0, 1, \dots, 9$. For $\varphi = 0$, corresponding to vanishing dipolar coupling g, the scaling functions coincide with the Résibois–Piette scaling function. If the strength q_D of the dipolar interaction is finite, the curves approach the Résibois–Piette scaling function for small values of the scaling variable x and deviate therefrom with increasing x. For a given material, q_D is fixed and the
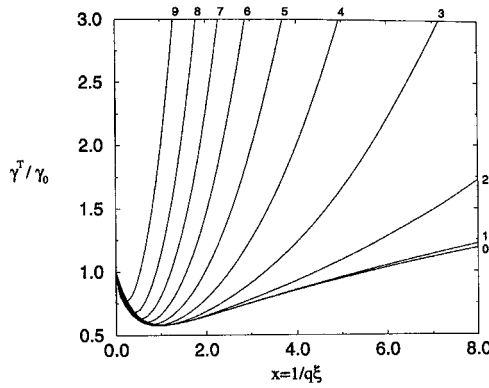
Figure 3.3. Scaling function γ^T for the transverse width in the Lorentzian approximation against $1/q\xi$ for values of $\varphi = N\pi/20$ with N indicated on the graph.

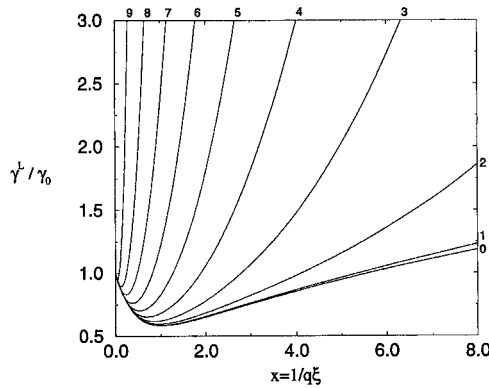Figure 3.4. Scaling function γ^L for the longitudinal width in the Lorentzian approximation against $1/q\xi$ for values of $\varphi = N\pi/20$ with N indicated on the graph.

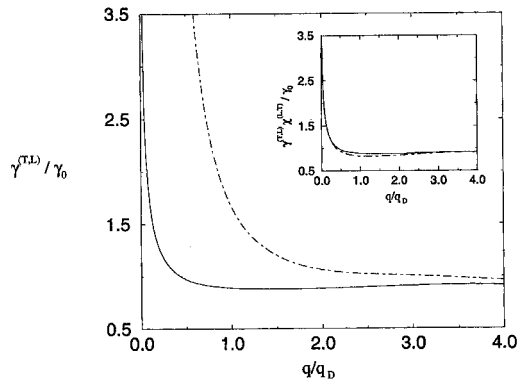Figure 3.5. Scaling functions for the transverse (——) and the longitudinal (—·—) widths against q/q_D in the Lorentzian approximation at the critical temperature. The inset shows the scaling functions for the transverse (——) and the longitudinal (—·—) Onsager coefficients against q/q_D at the critical temperature.

parametrization by φ corresponds to a parametrization in terms of the reduced temperature $(T - T_C)/T_C$.

To examine the dipolar crossover precisely at the Curie point, figure 3.5 displays the scaling function for the transverse and longitudinal width at $T = T_C$ against the wavenumber, that is $y^{-1} = q/q_D$. This graph shows that the crossover from the isotropic Heisenberg to dipolar critical dynamics in the transverse linewidth occurs at a wavenumber which is almost one order of magnitude smaller than the static crossover wave-vector q_D. The crossover of the longitudinal width, from $z = 2.5$ to $z = 0$, is more pronounced and occurs in the intermediate vicinity of q_D. The reason for the different location of the dynamic crossover is mainly that it is primarily the longitudinal static susceptibility which shows a crossover due to the dipolar interaction. Since the changes in the static critical exponents is numerically small, the transverse static susceptibility is nearly the same as for the ferromagnets without dipolar interaction (Aharony 1973a, Aharony and Fisher 1973). Hence the crossover in the transverse width is purely a dynamical crossover, whereas the crossover of the longitudinal width which is proportional to the inverse static longitudinal susceptibility is enhanced by the static crossover. In order to substantiate these arguments we have plotted in the inset of figure 3.5 the scaling functions of the Onsager coefficients $\hat{\chi}^{\alpha}\gamma^{\alpha}$ at the critical temperature against q/q_D, showing only the dynamical crossover.

3.2.3. *Selected results of the complete mode-coupling equations*

All the scaling functions for the dipolar ferromagnet depend on the three scaling variables $x = 1/q\xi$, $y = q_D/q$ and $v_{\alpha} = \omega/Aq^z\Omega^{\alpha}(x, y)$. Therefore it is impossible to present all the results obtained from the numerical solution of the complete mode-coupling equations. In this section we intend to review the most important features of the shape and linewidth crossover reported by Frey *et al.* (1988, 1989). Further results and discussion will be presented in the next section in conjunction with a comparison with experimental data.

The results from the Lorentzian approximation show that the dipolar linewidth crossover in the transverse linewidth sets in at a wave-vector almost one order of magnitude smaller than the dipolar wave-vector q_D. In order to obtain information about the line shape, one has to dismiss this approximation and to solve the complete set of mode-coupling equations, equations (3.40) and (3.41). This has been achieved by Frey *et al.* (1988, 1989), and one finds the following crossover scenario. First of all, the crossover in the line shape sets in at wave-vectors of the order of the dipolar wave-vector.

Let us first consider the case of temperatures very close to $T = T_C$. Figures 3.6 and 3.7 show the transverse and longitudinal scaling functions $\phi^{\alpha}(r, \varphi, \tau_{\alpha})$ against the scaling variables r and τ_{α} for $\varphi = 1.49$. Referring to EuO, characterized by the (non-universal) parameters $q_D = 0.147\,\text{Å}^{-1}$, $T_C = 69.1\,\text{K}$ and $\xi_0 = 1.57\,\text{Å}$, this corresponds to a temperature $T \approx (1 + 0.003)T_C$. The line shapes of the longitudinal and transverse relaxation function agree in the isotropic Heisenberg limit, that is for $r \rightarrow 0$ corresponding to large values of the wave-vector q ($\geqslant q_D$). In this limit the dipolar interaction becomes negligible and the shape is of the Hubbard–Wegner type as discussed in section 2. Upon increasing the value of the scaling variable r the line shapes of the transverse and longitudinal relaxation functions become drastically different. Whereas the transverse relaxation function shows a nearly exponential decay, pronounced overdamped oscillations show up for the transverse relaxation function. The shape crossover is also shown in figure 3.8, where the transverse and longitudinal
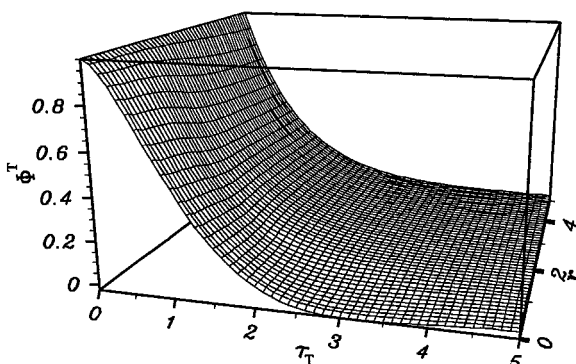
Figure 3.6.   Scaling function of the transverse Kubo relaxation function $\phi^T(r, \varphi, \tau_T)$ at $\varphi = 1\cdot49$ (close to the critical temperature) against τ_T and $r = [(q_D/q)^2 + (1/q\xi)^2]^{1/2}$.
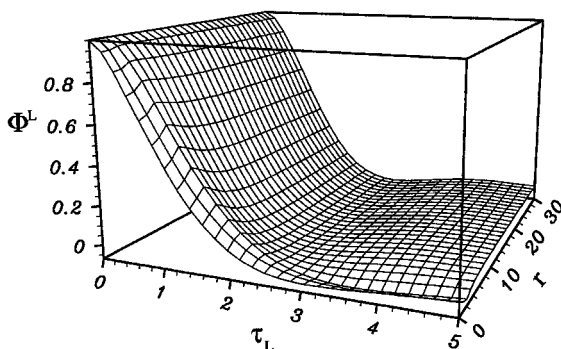

Figure 3.7.   Scaling function of the longitudinal Kubo relaxation function $\phi^L(r, \varphi, \tau_L)$ at $\varphi = 1\cdot49$ (close to the critical temperature) against τ_L and $r = [(q_D/q)^2 + (1/q\xi)^2]^{1/2}$.

relaxation functions are plotted against the scaling variable τ_α for three different values of the scaling variable $r = (x^2 + y^2)^{1/2}$ ($r = 0$, $r = 1$ and $r = 10$).

For temperatures well separated from T_C, that is $q_D\xi \ll 1$, the dipolar interaction become negligible. Hence, the difference between the shape crossovers of the longitudinal and transverse relaxation functions diminishes with decreasing $q_D\xi$. For $q_D\xi \ll 1$ the shape crossover as a function of r corresponds to the crossover from the critical (Hubbard–Wegner) shape to the hydrodynamic shape as discussed in section 2. (Note that, for $q_D\xi \ll 1$, the scaling variable r reduces to $x = 1/q\xi$.) Figures 3.9 and 3.10 show the shape crossover for $q_D\xi = 3\cdot52$ ($\varphi = 1\cdot294$) for the transverse and longitudinal relaxation functions respectively. Figures 3.11 and 3.12 display the corresponding crossovers for $q_D\xi = 1\cdot46$ ($\varphi = 0\cdot97$). In the latter case the shape crossover of the transverse and longitudinal relaxation functions are already quite similar and almost identical with the shape crossover found for the isotropic Heisenberg ferromagnet without dipolar interaction. The various crossover scenarios can also be read off figure 3.8.

Finally let us add a comment on how the line-shape crossover affects the linewidth crossover. It has been shown (Frey *et al.* 1988, 1989) (see section 4) that there are only slight changes in the linewidth crossover, when the linewidth is determined from the full solution of the mode-coupling equations, compared with the widths obtained from
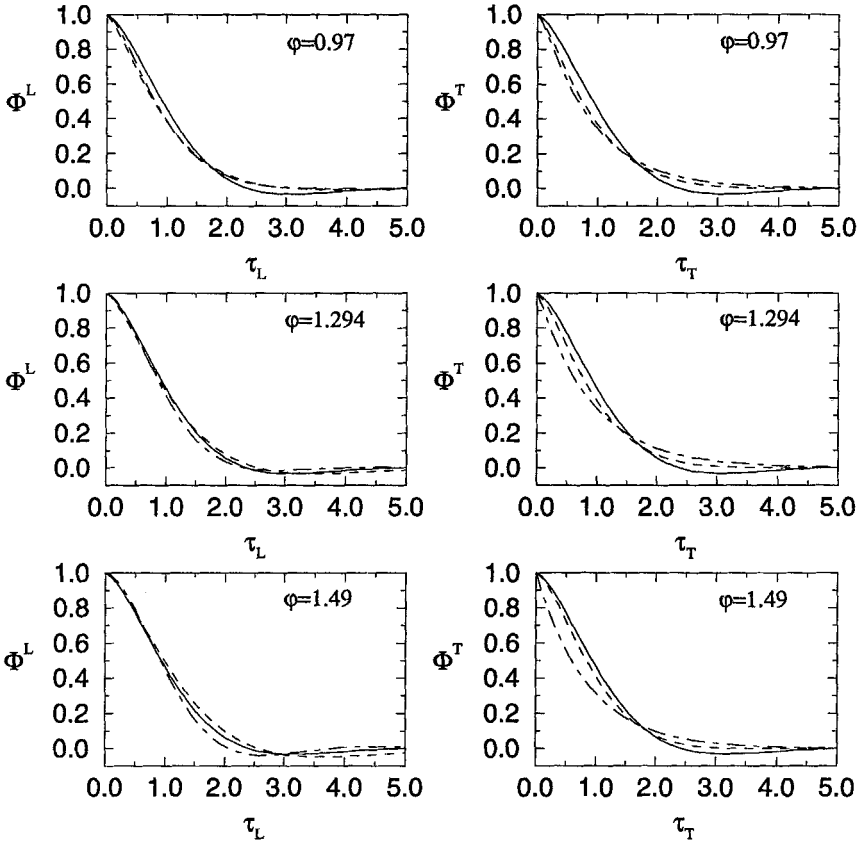
Figure 3.8.   Scaling function of the longitudinal and transverse Kubo relaxation function
$\phi^\alpha(r, \varphi, \tau_T)$ against τ_α for three different values of φ ($\varphi = 1{\cdot}49$, $1{\cdot}294$ and $0{\cdot}97$). In each
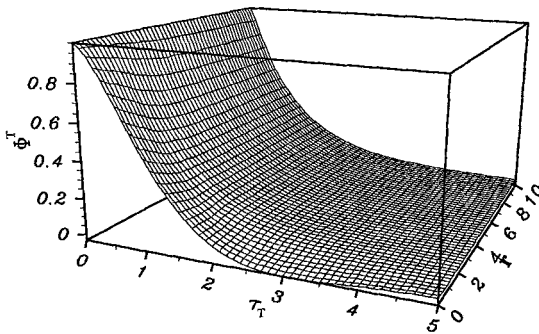graph the scaling function is shown for $r = 0$ (———), $r = 1$ (------) and $r = 10$ (—·—).

Figure 3.9.   Scaling function of the transverse Kubo relaxation function $\phi^T(r, \varphi, \tau_T)$ at
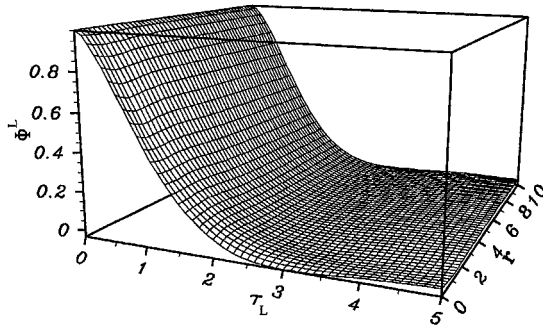$\varphi = 1{\cdot}294$ against τ_T and $r = [(q_D/q)^2 + (1/q\xi)^2]^{1/2}$.

Figure 3.10.   Scaling function of the longitudinal Kubo relaxation function $\phi^L(r, \varphi, \tau_L)$ at $\varphi = 1 \cdot 294$ against τ_L and $r = [(q_D/q)^2 + (1/q\xi)^2]^{1/2}$.
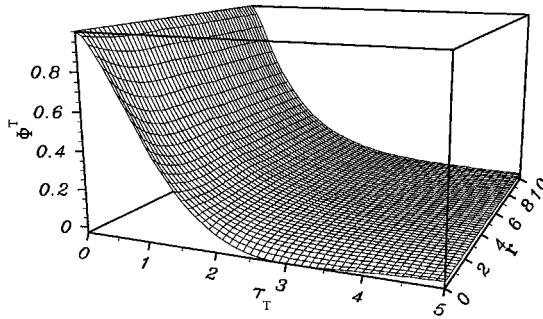

Figure 3.11.   Scaling function of the transverse Kubo relaxation function $\phi^T(r, \varphi, \tau_T)$ at $\varphi = 0 \cdot 97$ against τ_T and $r = [(q_D/q)^2 + (1/q\xi)^2]^{1/2}$.
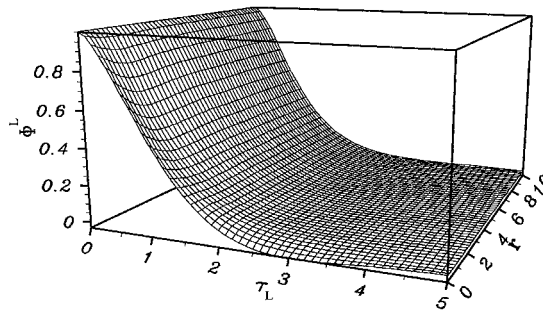

Figure 3.12.   Scaling function of the longitudinal Kubo relaxation function $\phi^L(r, \varphi, \tau_L)$ at $\varphi = 0 \cdot 97$ against τ_L and $r = [(q_D/q)^2 + (1/q\xi)^2]^{1/2}$.

the Lorentzian approximation. Roughly speaking, the overall effect of taking into account the correct line shape is approximately a shift by a constant factor. For details we refer the reader to section 4.

3.3. *Spin-wave theory in the ferromagnetic phase*

Holstein and Primakoff (1940) have investigated the dynamics of dipolar ferromagnets far below T_C using linear spin-wave theory. Upon neglecting fluctuations in the longitudinal component, $S_l^z \approx S$, they obtain the following equations of motion for the transverse spin fluctuations (see also Lovesey and Trohidou (1991)):

$$i\frac{d}{dt}S_k^+ = A_k S_k^+ + B_k^* S_{-q}^-,$$ (3.50)

$$i\frac{d}{dt}S_k^- = A_k^* S_{-q}^- + B_k S_k^+,$$ (3.51)

in terms of the raising and lowering operators $S_l^\pm = S_l^x \pm iS_l^y$. From these equations of motion the spin-wave dispersion follows (see also Keffer (1966)):

$$\varepsilon_k = (A_k + |B_k|)^{1/2}(A_k - |B_k|)^{1/2}.$$ (3.52)

The coefficients A_k and B_k are given in terms of the exchange interaction $J_k = 2S\Sigma_m J_{lm}\exp[i\mathbf{k}\cdot(\mathbf{x}_l - \mathbf{x}_m)]$ and the dipolar interaction tensor $A_k^{\alpha\beta}$ (see equation (3.3)):

$$A_k = g_L\mu_B H_0 + (J_0 - J_k) + (2E_0 + E_k),$$ (3.53)

$$E_k = SA_k^{zz},$$ (3.54)

$$B_k = -S(A_k^{xx} - A_k^{yy} - 2iA_k^{xy}) = S((A_k^{xx} - A_k^{yy})^2 + 4A_k^{xy2})^{1/2}\exp(-2i\varphi_k).$$ (3.55)

For crystals with cubic symmetry the dipolar tensor $A_k^{\alpha\beta}$ is given by $A_k^{\alpha\beta} \approx \frac{1}{2}(g_L\mu_B)^2\frac{4}{3}\pi(\delta^{\alpha\beta} - k^\alpha k^\beta/k^2)$ near the zone centre $ka \ll 1$, plus small structure-dependent terms proportional to k^2 (see section 3.1)). Note, however, that the dipolar tensor becomes severely structure dependent (requiring numerical evaluation (Cohen and Keffer 1955)) as $\mathbf{k}$ approaches the zone boundary.

Hence, for $ka \ll 1$, one finds for crystals with cubic symmetry (for more details we refer the reader to the review by Keffer (1966))

$$A_k = g_L\mu_B H_0 + (J_0 - J_\kappa) + \frac{1}{2}g_L\mu_B M_0\left[4\pi - 4\pi\left(\frac{k^z}{k}\right)^2\right],$$ (3.56)

$$B_k = \frac{1}{2}g_L\mu_B M_0\left[4\pi\frac{(k^x)^2 - i(k^y)^2}{k^2}\right] = 2\pi g_L\mu_B M_0\sin^2\Theta_k\exp(-2i\varphi_k),$$ (3.57)

where Θ_k and φ_k define the orientation of the wave-vector $\mathbf{k}$ with respect to the z axis; M_0 is the saturation magnetization. Note that the latter equations are strictly valid for long thin samples only. Otherwise, one has to take into account demagnetization effects, which amount in an additional magnetic field $H_0 \to H_0 - N^z M_0$, where N^z is a demagnetization factor (Anderson and Suhl 1955, Keffer 1966).

Using the formalism of Holstein and Primakoff (1940) the influence of the dipole–dipole interaction on the inelastic scattering of neutrons has been investigated by Elliott and Lowde (1955) (see also Lowde (1965)).

The neutron scattering cross section is proportional to the correlation function corresponding to the spin fluctuations (for example Lovesey (1984) and Collins (1989)).

If one considers N identical atoms with fixed positions, one finds for the magnetic partial differential cross-section of unpolarized neutrons in forward direction

$$\frac{d^2\sigma}{d\Omega\, dE'} = \frac{k'}{k}\frac{N}{\hbar}\, r_0^2 |F(\mathbf{Q})|^2 \frac{1}{N}\sum_{ll'} \exp\left[i\mathbf{Q}\cdot(\mathbf{x}_l - \mathbf{x}_{l'})\right] \int_{-\infty}^{+\infty} \frac{dt}{2\pi} \exp(-i\omega t)\langle S_l^{\mathrm{T}}(t)S_{l'}^{\mathrm{T}}(0)\rangle$$

$$= \frac{k'}{k}\frac{N}{\hbar}\, r_0^2 |F(\mathbf{Q})|^2 S^{\mathrm{T}}(\mathbf{Q},\omega), \tag{3.58}$$

where $S_l^{\perp}(t)$ is the component of the spin density perpendicular to the momentum transfer (scattering vector) $\mathbf{Q} = \mathbf{k} - \mathbf{k}'$, and $\hbar\omega$ is the neutron energy transfer. The length $r_0 = -5.391\,\mathrm{fm}$ is analogous to the nuclear scattering length (see also section 4), and $F(\mathbf{Q})$ the magnetic form factor. We have also defined the transverse magnetic scattering function $S^{\mathrm{T}}(\mathbf{Q},\omega)$ by

$$S^{\mathrm{T}}(\mathbf{Q},\omega) = \left(\delta^{\alpha\beta} - \frac{Q^\alpha Q^\beta}{Q^2}\right)\int_{-\infty}^{+\infty} \frac{dt}{2\pi}\exp(-i\omega t)\langle S_{-\mathbf{q}}^\alpha(t)S_{\mathbf{q}}^\beta(0)\rangle, \tag{3.59}$$

where $\mathbf{Q} = \mathbf{q} + \boldsymbol{\tau}$ with $\mathbf{q}$ the wave-vector of the magnon and $\boldsymbol{\tau}$ a reciprocal-lattice vector.

The equations of motion (equations (3.50) and (3.51)) are diagonalized in terms of the Bose operators a and $a^\dagger$ that satisfy

$$[a_{\mathbf{q}}, a_{\mathbf{q}'}^\dagger] = \delta_{\mathbf{q}\mathbf{q}'} \tag{3.60}$$

with

$$S_{\mathbf{q}}^\dagger = u_{\mathbf{q}}a_{\mathbf{q}} + v_{\mathbf{q}}a_{-\mathbf{q}}^\dagger. \tag{3.61}$$

A convenient choice for the coefficients $u_{\mathbf{q}}$ and $v_{\mathbf{q}}$ is (Keffer 1966, Lovesey and Trohidou 1991)†

$$u_{\mathbf{q}}^2 = \frac{2SN(A_{\mathbf{q}} + \varepsilon_{\mathbf{q}})}{2\varepsilon_{\mathbf{q}}} \tag{3.62}$$

$$v_{\mathbf{q}} = -\frac{u_{\mathbf{q}}B_{\mathbf{q}}^*}{(A_{\mathbf{q}} + \varepsilon_{\mathbf{q}})}. \tag{3.63}$$

The contributions from single-spin-wave events to the dynamic structure factor was calculated by Elliott and Lowde (1955) and Lowde (1965):

$$S^{\mathrm{T}}(\mathbf{Q},\omega) = \frac{S}{2}(n_{\mathbf{q}} + 1)\left[\left(1 + \frac{(Q^z)^2}{Q^2}\right)\frac{A_{\mathbf{q}}}{\varepsilon_{\mathbf{q}}} + \left(1 - \frac{(Q^z)^2}{Q^2}\right)\frac{|B_{\mathbf{q}}|}{\varepsilon_{\mathbf{q}}}\cos[2(\varphi_{\mathbf{Q}} - \varphi_{\mathbf{q}})]\right]\delta(\omega + \varepsilon_{\mathbf{q}}), \tag{3.64}$$

where $n_{\mathbf{q}}$ is the occupation number of the magnon oscillator with wave-vector $\mathbf{q}$. The second term in the dynamic structure factor is due to the dipolar interaction. For zero dipolar interaction or for wave-vectors larger than the dipolar wave-vector q_{D} the dynamic structure factor reduces to a simple angular distribution proportional to $1 + (Q^z/Q)^2$. When dipolar effects become of importance, the angular dependence of the scattered intensity becomes quite complicated.

More recently Lovesey and Trohidou (1991) and Trohidou and Lovesey (1993) have extended Lowde's analysis to scattering of polarized neutrons, and a discussion

---

† Holstein and Primakoff (1940) have ignored the phase relationship between $u_{\mathbf{q}}$ and $v_{\mathbf{q}}$, without which an incorrect expression for the scattering cross-section between spin waves and neutrons would be obtained. This error has been corrected by Elliott and Lowde (1955), Lowde (1965) and Keffer (1966).

of the longitudinal cross-section $\langle S_l^z S_{l'}^z \rangle$, which contains two-spin-wave scattering events. Furthermore, they analyse the static susceptibilities in the framework of linear spin-wave theory, correcting work by Toh and Gehring (1990) who used the incorrect expressions for the coefficients $u_{\mathbf{q}}$ and $v_{\mathbf{q}}$ from the work of Holstein and Primakoff (1940).

As a first step beyond the spin-wave theories described above, Toperverg and Yashenkin (1993) have used the perturbation approach developed by Vaks *et al.* (1967a, b) to investigate the frequency dependence of the uniform transverse and longitudinal susceptibilities.† The applicability of their results is mainly restricted to low and intermediate temperatures. Their perturbation approach for the dipolar interaction breaks down not only close to the critical temperature but also at any temperature for low frequencies. For this parameter regime a non-perturbative approach such as mode-coupling theory is needed to account for the strong fluctuations. A first attempt towards such a theory was made some time ago by Raghavan and Huber (1976). There are, however, several shortcomings in their approach. First of all, the static susceptibilities used in their analysis do not account for the coexistence anomalies and dipolar crossover properly. Instead the longitudinal susceptibility is taken to be of Ornstein–Zernike form $\chi^L \propto 1/(q^2 + \xi^{-2})$, which neglects dipolar crossover effects as well as the by now well known coexistence anomaly $\chi^L \propto 1/q$ in the limit $q \to 0$. The expression used for the transverse susceptibility is valid in certain limits only. Furthermore, in the presence of dipolar interaction, for a general angle between the wave-vector and the direction of the spontaneous magentization, there are three and not just two non-degenerate eigenvalues for the static susceptibility matrix. This fact has been neglected completely. Also, they did not evaluate the complete functional form of the relaxation functions but used instead a parametrization, which is strictly valid in the hydrodynamic regime only, and calculated the corresponding parameters. Nevertheless, the theory seems to give a quite reasonable description of the data obtained by a neutron scattering study on EuO (Passell *et al.* 1972) in the ranges $q\xi \lesssim 1$ and $q_D\xi \lesssim 1$ for not too small values of the wave-vector q. Beyond this range the approximate treatment of the dipolar interaction by Raghaven and Huber (1976) breaks down.

More recently Lovesey (1993) reported an approximate mode-coupling approach for dipolar ferromagnets below T_C. Similar to Raghavan and Huber the spin-wave dispersion relation used by Lovesey is applicable for not too small wave-vectors only. The analysis by Lovesey (1993) is restricted to the exchange region $q_D\xi \lesssim 1$. This is due to the assumption made by Lovesey (1993) that the only non-vanishing relaxation kernels are those for the spin fluctuations longitudinal and transverse to the direction of the spontaneous magnetization. Neglecting off-diagonal matrix elements excludes the applicability of the theory to the dipolar region. Note that in the dipolar region close to T_C the memory function and the relaxation functions become, similar to the situation above T_C, diagonal in terms of the spin fluctuations longitudinal and transverse with respect to the wave-vector and not to the spontaneous magnetization. Furthermore, the analysis by Lovesey (1993) is restricted to very small wave-vectors. In this limit, however, the expressions for the static susceptibility and the spin-wave dispersion relation used by Lovesey (1993) are not valid, since they do not account for the presence

---

† An excellent review on the theoretical and experimental work prior to 1984 has been given by Maleev (1987) with a particular emphasis on Green function techniques.

of the subtle combined effects of Goldstone modes and dipolar anisotropy. Also, no self-consistent solution but only a first iteration of the mode-coupling equations, based on neglecting the damping, is performed. In summary, a thorough mode-coupling analysis of the effects of the dipolar interactions in the ferromagnetic phase is still a very challenging theoretical problem and the topic of ongoing research (Schinz 1994a).

3.4. *Renormalization group theory of time-dependent Ginzburg–Landau models in the ferromagnetic phase*

The spin-wave theory, reviewed in the preceding section, is only a first step towards a more rigorous theory of the critical dynamics of dipolar ferromagnets below the Curie temperature. For a thorough understanding of the dynamics in the ferromagnetic phase a renormalization group theory or a mode-coupling approach analogous to section 3.2, which takes into account the effects of the critical fluctuations, would be necessary. A detailed analysis requires a treatment of a modified model J (Hohenberg and Halperin 1977) appropriate for the dynamics of isotropic ferromagnets, where dipolar forces are included.

Recently, the effects of the dipolar interaction on the critical dynamics of the n-component time-dependent Ginzburg–Landau models (model A (Hohenberg and Halperin 1977)) below the critical temperature have been studied within a generalized minimal subtraction scheme (Täuber and Schwabl 1993). The corresponding Langevin equation of motion reads (model A, $a = 0$; Model B, $a = 2$)

$$\frac{\partial \mathbf{S}(\mathbf{x}, t)}{\partial t} = - \lambda (i\mathbf{\nabla})^a \frac{\delta H[\{S^\alpha\}]}{\delta \mathbf{S}(\mathbf{x}, t)} + \zeta(\mathbf{x}, t), \tag{3.65}$$

where the stochastic forces are characterized by a Gaussian probability distribution function with zero mean and variance:

$$\langle \zeta^\alpha(\mathbf{x}, t) \zeta^\beta(\mathbf{x}', t') \rangle = 2\lambda k_B T (i\mathbf{\nabla})^a \delta^{(3)}(\mathbf{x} - \mathbf{x}') \delta(t - t') \delta^{\alpha\beta}. \tag{3.66}$$

The Ginzburg–Landau effective free-energy functional reads

$$H[\{S^\alpha\}] = \frac{1}{2} \int_\mathbf{q} \left(\sum_{\alpha,\beta=1}^{\min(d,n)} [(r + q^2)P_{\alpha\beta}^\mathrm{T} + (r + g + q^2)P_{\alpha\beta}^\mathrm{L}] S^\alpha(\mathbf{q}) S^\beta(-\mathbf{q}) \right.$$

$$\left. + \sum_{\alpha = \min(d,n)+1} S^\alpha(\mathbf{q}) S^\alpha(-\mathbf{q}) \right), \tag{3.67}$$

where the general situation $n \neq d$ is considered. Here $P_{\alpha\beta}^T = \delta^{\alpha\beta} - q^\alpha q^\beta / q^2$ and $P_{\alpha\beta}^L = q^\alpha q^\beta / q^2$ denote the transverse and longitudinal projection operators respectively.

Those relaxational models neglect mode-coupling terms resulting from the reversible motion of the spins in the local magnetic field. It is expected (Täuber and Schwabl 1993), however, that most of the conclusions based on the relaxational models will also hold for models with mode-coupling terms.

As a consequence of the spontaneously broken symmetry there are $n - 1$ massless Goldstone modes in the ordered phase of ideally isotropic systems. These massless modes lead to infrared singularities (coexistence singularities) in certain correlation functions for *all* temperatures below T_C. Based on the analysis of the effects of the critical and Goldstone fluctuations for the $O(n)$-symmetric time-dependent Ginzburg–Landau models (Täuber and Schwabl 1992), it has been investigated (Täuber and Schwabl 1993) how the coexistence anomalies are modified when dipolar forces or

E. Frey and F. Schwabl

Table 6. Coexistence anomalies of the isotropic relaxational models for the longitudinal dynamic susceptibility $\chi^L(\mathbf{q}, \omega)$ and correlation function $G_L(\mathbf{q}, \omega)$.

Model	a	$\chi^L(\mathbf{q}, 0)$	$\mathrm{Re}[\chi^L(0, \omega/q^a)]$	$G_L(0, \omega/q^a)$
A	0	$\propto q^{d-4}$	$\propto \omega^{(d-4)/2}$	$\propto \omega^{d/2-3}$
B	2	$\propto q^{d-4}$	$\propto (\omega/q^2)^{(d-4)/2}$	$\propto (\omega/q^2)^{d-4}$

Table 7. The influence of the dipolar interaction on the coexistence anomalies. The table summarizes the various cross-over scenarios possible if the number n of components and the dimensionality d of space is varied.

	$d=2, d=3$	$d=4$
$n=1$	Crossover to a Gaussian theory	As for $g=0$
$n=2$	Crossover to a Gaussian theory	No anomalies
$n \geqslant 3$	$u_{CD}^* = 6(4-d)/(n-2) \rightarrow$ anomalies	Logarithmic corrections

weak anisotropies are included. For latter reference the coexistence anomalies of the isotropic relaxational models are collected in table 6.

The analysis by Täuber and Schwabl (1993) shows that the influence of the dipolar interaction on the coexistence singularities is quite subtle. Although the model explicitly breaks the $O(n)$ symmetry, not all transverse modes lose their Goldstone character, and their effective number is only reduced by one. Hence, while for $n=2$ a crossover to an asymptotically uncritical theory takes place, for $n \geqslant 3$ coexistence anomalies persist, governed by a dipolar coexistence fixed point (Täuber and Schwabl 1993).

Below T_C there are two preferred axes: the axis defined by the direction of the spontaneous magnetization and the axis defined by the wave-vector $\mathbf{q}$. This leads to a complex structure of the correlation functions already on the harmonic level. It is quite remarkable, however, that a one-loop theory for the two-point cumulants becomes an exact representation in the ordered phase in the coexistence limit ($\mathbf{q} \rightarrow \mathbf{0}$ and $\omega \rightarrow 0$) (Täuber and Schwabl 1993).

For $n = d \geqslant 3$ it is found (Täuber and Schwabl 1993) that the power laws characteristic of the coexistence anomalies are *not* changed by the presence of the dipolar interaction. Hence the same power laws in table 6 apply to the dipolar case also. It is also interesting to note that there is the following exact amplitudes ratio of the longitudinal response function in the dipolar and the isotropic case:

$$\frac{\chi^L(\mathbf{q}, \omega)_{\text{dipolar}}}{\chi^L(\mathbf{q}, \omega)_{\text{isotropic}}} = \frac{n-2}{n-1}. \tag{3.68}$$

For $n = 3$ this universal amplitude ratio is $\frac{1}{2}$, in accord with the results of Pokrovsky (1979) and Toh and Gehring (1990), obtained in the framework of a spin-wave theory.

As is apparent from the value of the dipolar coexistence fixed point $u_{CD}^* = 6(4-d)/(n-2)$, the situation $n=2$ requires separate discussion. In this case there are no massless modes left, since the dipolar interaction reduces the number of Goldstone modes from $n-1$ to $n-2$. As a consequence the crossover below T_C is from a critical theory at T_C to a Gaussian theory, that is the fluctuations die out on leaving the critical region. A qualitative summary of the various crossover scenarios is given in table 7 (Täuber and Schwabl 1993).

4. Application to experiments

In this section we review the results from the numerical solution of the mode-coupling equations for dipolar ferromagnets above the transition temperature and compare them with experiments. Furthermore we give a short account of the experimental data recorded below T_C and future theoretical developments.

There are several experimental techniques such as neutron scattering, electron spin resonance, magnetic relaxation, hyperfine interaction and muon spin resonance with various complementary characteristics: different wave-vector ranges, short-range point-like probes in real space (hyperfine interaction and muon spin resonance) against probes in reciprocal space (neutron scattering, electron spin resonance and magnetic relaxation). The critical dynamics of isotropic ferromagnets such as EuO, EuS, Fe, Ni and many other materials have been studied by one or several of the above methods.

To emphasize the decisive role of the dipolar interaction we note that the experimental situation prior to the theoretical work by Frey (1986) and Frey and Schwabl (1987, 1988a, 1989a) was, however, puzzling in many ways. On the one hand, in hyperfine interaction experiments on Fe and Ni, one observed a cross-over in the dynamic critical exponent from $z = \frac{5}{2}$ to $z = 2$ (Reno and Hohenemser 1972, Gottlieb and Hohenemser 1973, Hohenemser *et al.* 1982, 1989), that is a crossover to a dynamics with a non-conserved order parameter. This was confirmed by electron spin resonance and magnetic relaxation experiments (Kötzler *et al.* 1976, 1978, Kötzler and Scheithe 1978, Kötzler and von Philipsborn 1978, Dunlap and Gottlieb 1980, Kötzler 1988), where a non-vanishing Onsager coefficient at zero wave-vector was found. These results indicated that the critical dynamics of isotropic ferromagnets cannot be explained solely on the basis of the short-range exchange interaction, which would lead to an exponent $z = \frac{5}{2}$ for the whole wave-vector range. However, on the other hand, a critical exponent $z = \frac{5}{2}$ was deduced from the wave-vector dependence of the linewidth observed in neutron scattering experiments right at the critical temperature by three different experimental groups: by Collins *et al.* (1969) and Dietrich *et al.* (1976); by Mezei (1982a, b, 1984, 1986, 1987, 1988); by Wicksted *et al.* (1984), Böni and Shirane (1986) and Böni *et al.* (1984a, b). Nevertheless and even more puzzling, the data for the linewidths above the transition temperature (Mezei 1982a, b, 1984, Böni *et al.* 1988) could not be described by the Résibois–Piette scaling function resulting from a mode-coupling theory (Résibois and Piette 1970) and a renormalization group theory (Ma and Mazenko 1975, Iro 1987), which take into account the short-range exchange interaction only (see section 2).

Those apparent experimental discrepancies could be resolved by the mode-coupling theory (Frey 1986, Frey and Schwabl 1987, 1988a, 1989a) described in section 2, which on top of the exchange interaction takes into account the dipole–dipole interaction present in all real ferromagnets. The results of this theory are reviewed in the following and compared with the experimental data.

4.1. *Neutron scattering*

Inelastic neutron scattering has been used for decades to investigate the spin dynamics of magnetic systems, providing information about the spin correlation function (Collins *et al.* 1969, Minkiewicz *et al.* 1969, Parette and Kahn 1971, Parette 1972, Dietrich *et al.* 1976, Passell *et al.* 1976). It has become one of the most important experimental techniques for studying the properties of condensed matter systems.

The cross-section for magnetic inelastic scattering of polarized neutrons (with polarization **P**) is given by (Marshall and Lovesey 1971, Lovesey 1984)
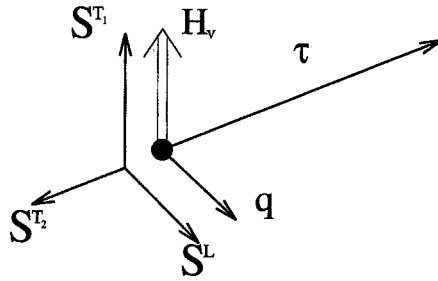
Figure 4.1.   Typical scattering geometry in neutron scattering experiments. The magnetic guide
field H_v is used to define the beam polarization P. In order to measure the longitudinal
spin fluctuations S^L, one has to go to a finite Bragg peak τ with the wave-vector q
perpendicular to the scattering vector $Q = \tau + q$. For unpolarized neutrons only transverse
fluctuations can be measured in the forward direction, $\tau = 0$.

$$\frac{d^2\sigma}{d\Omega\,dE'} = r_0^2 \frac{k'}{k} \sum_{l,d} \sum_{l',d'} \exp\left[i\mathbf{Q}\cdot(\mathbf{R}_{l,d} - \mathbf{R}_{l',d'})\right] \tfrac{1}{2}g_d F_d^*(\mathbf{Q})\tfrac{1}{2}g_{d'} F_{d'}^*(\mathbf{Q})$$

$$\times \frac{1}{2\pi\hbar} \int_{-\infty}^{\infty} dt \exp\left(-i\omega t\right)[\langle \mathbf{S}_{l,d}^{\perp}\cdot \mathbf{S}_{l',d'}^{\perp}(t)\rangle + i\mathbf{P}\cdot\langle \mathbf{S}_{l,d}^{\perp}\times \mathbf{S}_{l',d'}^{\perp}(t)\rangle], \quad (4.1)$$

where the spin fluctuations transverse to the neutron wave-vector transfer (scattering
vector) $\mathbf{Q} = \mathbf{k} - \mathbf{k}'$ are defined by $\mathbf{S}_{l,d}^{\perp} = \mathbf{Q} \times [\mathbf{S}_{l,d} \times \mathbf{Q}]/Q^2$. $\mathbf{R}_{l,d} = \mathbf{l} + \mathbf{d}$ denotes the
position vector of a nucleus in a rigid lattice, where $\mathbf{d}$ is the site of the nucleus (with
a gyromagnetic ratio g_d and a form factor $F_d(\mathbf{Q})$ within the unit cell $\mathbf{l}$). The quantity
$r_0 = -0.5391$ fm is a useful unit for the magnetic scattering length.

In neutron scattering experiments using unpolarized neutrons, one measures the
transverse scattering function $S^T(\mathbf{Q}, \omega)$

$$S^T(\mathbf{Q}, \omega) \propto \left(\delta^{\alpha\beta} - \frac{Q^\alpha Q^\beta}{Q^2}\right) \langle S_\mathbf{q}^\alpha(\omega) S_{-\mathbf{q}}^\beta(-\omega)\rangle, \quad (4.2)$$

where $\mathbf{q}$ denotes the neutron wave-vector transfer with respect to the nearest
reciprocal-lattice vector τ, that is the scattering vector is $\mathbf{Q} = \mathbf{q} + \tau$. Equation (4.2)
implies that only spin fluctuations transverse to the neutron wave-vector transfer $\mathbf{q}$ can
be measured in the forward direction, where $\tau = \mathbf{0}$. In order to measure the longitudinal
fluctuations, one has to go to a finite Bragg peak τ with $\mathbf{q}$ perpendicular to $\mathbf{Q} \approx \tau$. The
separation of the longitudinal and transverse spin fluctuations can be achieved by using
a polarized neutron beam. A typical scattering geometry is shown in figure 4.1, where
the polarization $\mathbf{P}$ is defined by a small guide field H_v. For more details on neutron
scattering using polarized neutrons we refer the reader to the books by Marshall and
Lovesey (1971), Lovesey (1984) and Williams (1988).

Recent advances in high-resolution neutron scattering techniques, such as the
neutron spin-echo technique (Mezei 1972) (see also the review articles in Mezei
(1980)), have allowed the early studies to be extended to critical fluctuations of
substantially larger wavelengths and have even made it possible to distinguish between
different line shapes (Mezei 1986).

In this subsection we compare the results of mode-coupling theory with neutron
scattering data on EuO, EuS and Fe. For a quantitative comparison we need several
material parameters (non-universal quantities) such as the magnitude of the Brillouin
zone boundary and the exchange constant (table 8).

Table 8. Material parameters for Ni, Fe, EuO and EuS. The parameters are defined in the main text. The values have been taken from the references listed below. When no reference is indicated, the parameter has been computed from a formula given in the main text with parameters given in table 4.

	a (Å)	T_C (K)	q_D (Å^{-1})	ξ_0 (Å)	$r_\mu H/4\pi$ (T=0K)	γ (Å)	A_{exp} (meV Å$^{5/2}$)	A_{Lor} (meV Å$^{5/2}$)	$\mathcal{W}_{th}$ (MHz)
Ni	3·52[a]	627[a]	0·013[b]	1·23[c]	−0·11[d]	0·00184	350[c]	241	0·358
EuO	5·12[e]	69·1[e]	0·147[b,f]	1·57[g]	0(?)	0·725	8·7[f] (8·3[h])	7·09	5·35 (5·60)
EuS	5·95[e]	16·6[e]	0·245[a,b,c]	1·81[g]	0(?)	3·16	2·1[i] (2·25[j])	2·08	6·87 (6·41)
Fe	2·87[a]	1043[a]	0·045[f] (0·033[b])	0·95[k] (0·82[l])	−0·51[d]	0·0239 (0·0129)	130[m]	90·0 (123)	2·98 (2·56)

[a] From Kittel (1971).
[b] From Kötzler (1988).
[c] From Böni et al. (1991b).
[d] From Dension et al. (1979).
[e] From Passell et al. (1972).
[f] From Mezei (1986).
[g] From Als-Nielson et al. (1976).
[h] From Böni and Shirane (1986).
[i] From Böni et al. (1987b).
[j] From Böni et al. (1988).
[k] From Wicksted et al. (1984).
[l] From Als-Nielson (1976).
[m] From Mezei (1982a, b).

4.1.1. *Shape crossover*

Owing to the recent advances in high-resolution neutron scattering techniques, it became possible to resolve not only the width but also the shape of the spin correlation functions. This progress made it possible to test the predictions for the line shape from MC theory (Wegner 1968, Hubbard 1971) and RG theory (Dohm 1976, Bhattacharjee and Ferrell 1985) which take into account solely the short-range exchange interaction. The latter theories for the critical dynamics were expected to fit the experimental data in an increasing quantitative way as one was able to measure the correlation functions at smaller and smaller wave-vectors, since the influence of additional irrelevant interactions should diminish as one moves closer to criticality. It came as quite a surprise when Mezei (1986) found a nearly exponential decay of the Kubo relaxation function by spin-echo experiments on EuO at $q = 0.024 \, \text{Å}^{-1}$ and $T = T_C$, which was in drastic disagreement with the bell-like shape predicted (Wegner 1968, Hubbard 1971, Dohm 1976, Bhattacharjee and Ferrell 1985).

In fact, in contrast with expectations, only at larger wave-vectors were the RG and MC calculations in accord with the experiment, taking into account exchange interaction only. This was shown by a comparison (Folk and Iro 1985) of the shape of the RG theory (Dohm 1976, Bhattacharjee and Ferrell 1985) with the heuristic shape found by Folk and Iro (1985). Also, a discrete version of the MC theory gives a quite reasonable agreement with experiment for large wave-vectors close to the Brillouin zone boundary (Cuccoli *et al.* 1988, 1989, 1991).

In order to explain the anomalous exponential decay found by Mezei (1986), it was asserted by Lovesey and Williams (1986) and Balucani *et al.* (1987) that neither MC nor RG theory is valid in the time regime probed by Mezei's (1986) experiments. To fit the experimental results a 'hybrid theory' (Balucani *et al.* 1987) was proposed, which is a phenomenological interpolation scheme between the short- and long-time limits. In contrast it was shown on the basis of a MC theory (Frey *et al.* 1985, 1988), which takes into account the effects of the long-range dipolar interaction between the spins, that the experimental data can be explained quite naturally without any need for a special treatment of the short-time behaviour. The results of this MC analysis will be reviewed in this section.

We have seen in section 3 that the dynamic crossover in the *linewidth* sets in at wave vectors one order of magnitude smaller than found in the static susceptibility. Here we consider the *shape* crossover, that is changes in the functional form of the spin correlation function. From the solution of the dipolar MC equations, one finds the following scenario for the shape crossover.

(1) In the immediate vicinity of the critical temperature the *transverse* relaxation function shows a nearly *exponential decay* in time for wave-vectors smaller than the dipolar wave vector q_D. Passing to wave-vectors larger than q_D there is a shape crossover to a Hubbard (1971)–Wegner (1968) shape corresponding to the isotropic Heisenberg fixed point (see section 2). This shape crossover takes place close to the dipolar wave-vector q_D in remarkable contrast with the crossover in the linewidth which sets in at wave-vectors almost one order of magnitude smaller.

(2) For wave-vectors smaller than q_D and for temperatures in the intermediate vicinity of the critical temperature the *longitudinal* Kubo relaxation function exhibits a Gaussian decay at small times and damped oscillations for larger times. This shape is quite different from the exponential decay found for the

transverse scaling function. Passing to larger wave-vectors the shapes of the transverse and longitudinal relaxation functions become identical (Hubbard–Wegner shape).

(3) For temperatures well separated from the critical temperature (i.e. for temperatures where the correlation length becomes less than the typical dipolar length scale q_D^{-1}; $q_D \xi < 1$) the shapes of the transverse and longitudinal relaxation become identical. Upon passing from small to large wave-vectors both relaxation functions show a crossover from a hydrodynamic shape, which is nearly exponential, to the bell-like Hubbard–Wegner shape.

In order to be specific and in view of spin-echo experiments on EuO above T_C (Mezei 1988, Mezei *et al.* 1989) we have displayed the Kubo relaxation function against time for a set of wave-vectors ($q = 0.018, 0.025, 0.036, 0.071$ and $0.150\,\text{Å}^{-1}$) in figures 4.2–4.5 In figures 4.2 and 4.3 these are plotted against the scaled time variables τ_α for a temperature in the immediate vicinity T_C ($T = T_C = 0.25\,\text{K}$) and in figures 4.4 and 4.5 for a temperature $T = T_C + 8\,\text{K}$ well separated from T_C. For wave-vectors $q \ll q_D = 0.147\,\text{A}^{-1}$, one can infer from figure 4.2 that the transverse scaling function decays nearly exponentially in time. This implies a Lorentzian-like shape for the frequency-dependent relaxation function for $q \ll q_D$ (solid curve in figure 4.2). For larger wave-vectors, $q \gtrsim q_D$, the curves look similar to Gaussians for small times and oscillate for larger times, $\tau_T \gtrsim 3$ (see chain curve in figure 4.2). The oscillations of the longitudinal relaxation function (figure 4.3) leads to the side peaks in figure 4.9 shown later, where the longitudinal correlation function is plotted against frequency for a fixed wave-vector.

Further away from T_C the line shape crossover of the transverse relation function is much less pronounced and the shape resembles more a Gaussian even for wave-vectors much smaller than q_D. In figures 4.4 and 4.5 the transverse and longitudinal Kubo functions are shown for the same wave-vectors as in figures 4.2 and 4.3 at $T = T_C + 8\,\text{K}$. For this temperature the shapes of the longitudinal and transverse Kubo functions are nearly the same (compare figures 4.4 and 4.5). This is precisely what one would have expected, because the influence of the dipolar forces decreases with increasing separation from the critical point and then there is no difference any longer between longitudinal and transverse modes.

To single out the line-shape crossover the appropriate time scales are τ_α of equation (3.39) used in figures 4.2–4.5. On the other hand, for comparison with experiments it may be more convenient to present the transverse Kubo relaxation function against the time scale $\tau' = \Lambda_{Lor} q^{5/2} t$. Such plots are exhibited in figure 4.6 for $T = T_C$ and the wave-vectors $q = 0.018, 0.036, 0.150$ and $0.3\,\text{Å}^{-1}$ and in figure 4.7 for $T = T_C + 0.5\,\text{K}$ and $q = 0.018, 0.025, 0.036$ and $0.071\,\text{Å}^{-1}$.

At $T = T_C$, triple-axis spectrometer scans at $q \gtrsim 0.15\,\text{Å}^{-1}$ (Mezei *et al.* 1989) show non-Lorentzian line shapes in agreement with predictions based on models with short-range exchange interaction only in agreement with the above MC result. Neutron spin-echo studies at much smaller wave-vectors (Mezei 1986, Mezei *et al.* 1989) lead to Lorentzian line shapes in agreement with the above crossover scenario for dipolar ferromagnets. In figure 4.8 data from neutron spin-echo studies (Mezei 1986) on EuO right at the critical temperature are shown for the transverse Kubo relaxation function at the wave-vector $q = 0.024\,\text{Å}^{-1}$ (solid curve) against time. We have used the theoretical value for the non-universal scale $\Lambda = 7.1/5.1326\,\text{meV}\,\text{Å}^{5/2}$ (see table 8). There is excellent agreement with the experimental data for $t \lesssim 1\,\text{ns}$. The experimental
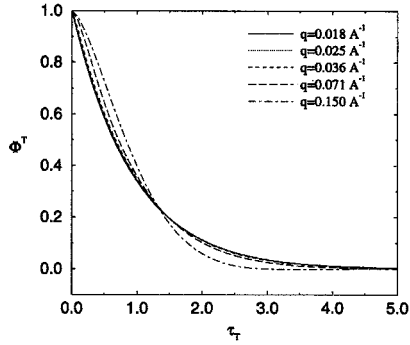
Figure 4.2.   Scaling function of the transverse Kubo relaxation function against the scaled time variable τ_T at $T = T_C + 0.25$ K for $q = 0.018\,\text{Å}^{-1}$ (——), $q = 0.025\,\text{Å}^{-1}$ (······), $q = 0.036\,\text{Å}^{-1}$ (------), $q = 0.071\,\text{Å}^{-1}$ (— — —) and $q = 0.150\,\text{Å}^{-1}$ (— · —).
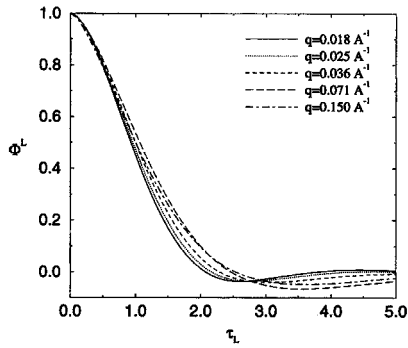

Figure 4.3.   The same as in figure 4.2 for longitudinal Kubo relaxation function.
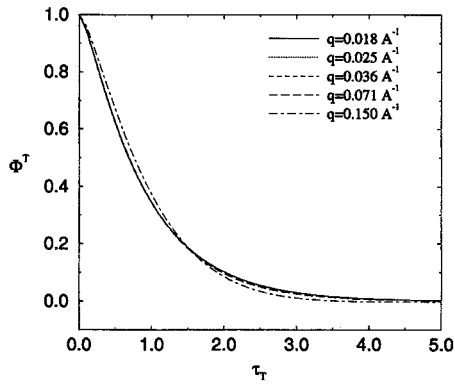

Figure 4.4.   Scaling function of the transverse Kubo relaxation function against the scaled time variable τ_T at $T = T_C + 8.0$ K for the same set of wave-vectors q as in figures 4.2 and 4.3.
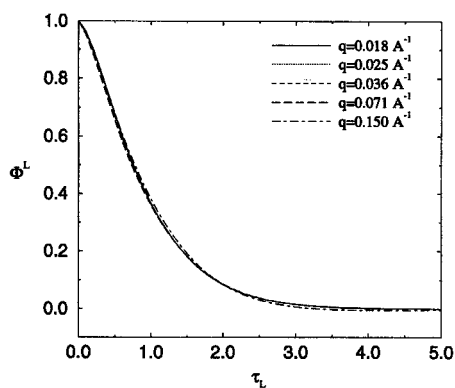
Figure 4.5. The same as in figure 4.4 for the longitudinal Kubo relaxation function.
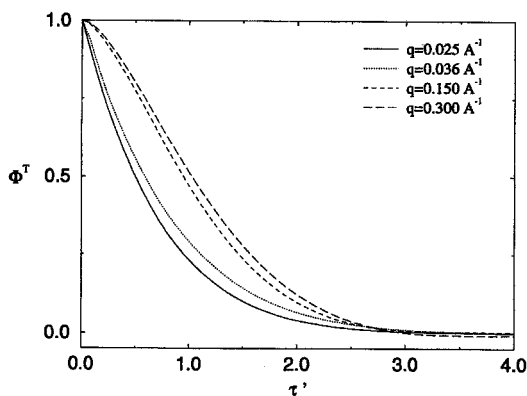

Figure 4.6. Scaling function of the transverse Kubo relaxation function against $\tau' = \Lambda_{\text{Lor}}q^z t$ at $T = T_C$ for $q = 0.025\,\text{Å}^{-1}$ (———), $q = 0.036\,\text{Å}^{-1}$ (······), $q = 0.150\,\text{Å}^{-1}$ (------) and $q = 0.300\,\text{Å}^{-1}$ (— — —).
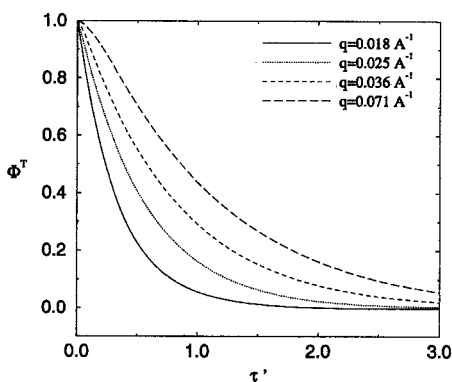

Figure 4.7. Scaling function of the transverse Kubo relaxation function against $\tau' = \Lambda_{\text{Lor}}q^z t$ at $T = T_C + 0.5\,\text{K}$ for $q = 0.018\,\text{Å}^{-1}$ (———), $q = 0.025\,\text{Å}^{-1}$ (······), $q = 0.036\,\text{Å}^{-1}$ (------) and $q = 0.071\,\text{Å}^{-1}$ (— — —).
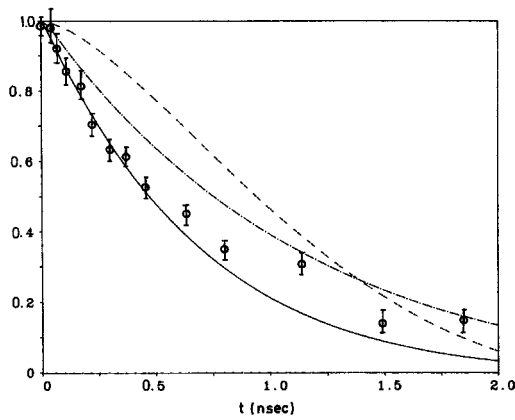
Figure 4.8.   Transverse Kubo relaxation function $\Phi^{T}(q, g, t)$ at $q = 0.024 \text{ Å}^{-1}$ (————) and $q = 0.028 \text{ Å}^{-1}$ (— · —) for dipolar ferromagnets against time: (— — — —) the Kubo relaxation function for short-range exchange interaction only at $q = 0.024 \text{ Å}^{-1}$. Data points for $q = 0.024 \text{ Å}^{-1}$ are from figure 1 of Mezei (1986).
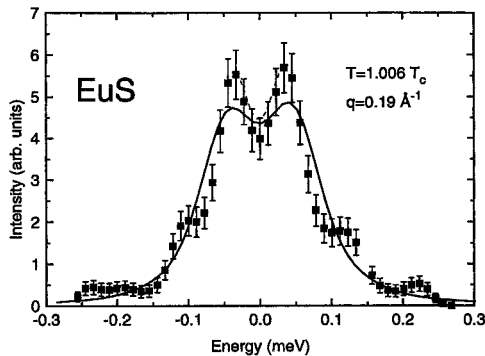

Figure 4.9.   Normalized experimental data deconvoluted by a maximum-entropy method: (————), the spectral shape function predicted by mode-coupling theory: (■, - - -), the deconvoluted data. (From Görlitz *et al.* (1992).)

data are above the theoretical curve for $t \geqslant 1$ ns. This may be due to finite collimation effects in this time domain, as noted by Mezei (1986). To substantiate this point we have also plotted in figure 4.8 the relaxation function at $q = 0.28 \text{ Å}^{-1}$ (chain curve), which is significantly higher than the curve for $q = 0.024 \text{ Å}^{-1}$ for $t \geqslant 1$ ns. The fairly large difference between the curves for $q = 0.024 \text{ Å}^{-1}$ and $q = 0.028 \text{ Å}^{-1}$ is implied by the close proximity to the crossover region.

In order to exhibit the difference from the mode-coupling theory including only short-range exchange interaction the broken curve in figure 4.8 shows the solution of equation (3.40) and (3.41) for this special case, that is $y = 0$, $x = 0$ and $\rho_{cut} = q_{BZ}/q$ with $q = 0.024 \text{ Å}^{-1}$. The result differs drastically from the actual line shape including the long-range dipolar interaction. It is important to realize that the crossover in the line shape starts nearly at q_D, whereas the linewidth still scales with the isotropic critical dynamic exponent $z = \frac{5}{2}$ in this wave-vector region.

Very recently the theoretical predictions concerning the line shape of the

longitudinal relaxation function (Frey *et al.* 1988, 1989) have been verified experimentally (Böni *et al.* 1991a, Görlitz *et al.* 1992). Figure 4.9 shows the longitudinal Kubo relaxation function for EuS at $T = 1.006T_C$ and $q = 0.19\,\text{Å}^{-1}$. The normalized experimental data deconvoluted by a maximum-entropy method agree quite well with the theoretical prediction (solid curve). In particular the double-peak structure corresponding to the overdamped oscillations in time are observed.

4.1.2. *Linewidth crossover*

From the frequency- and wave-vector-dependent Kubo relaxation function, one can define a characteristic linewidth by the HWHM:

$$\text{Re}\,[\varPhi^{\alpha}(\omega = \varGamma^{\alpha}_{\text{HW}})] = \tfrac{1}{2}\,\text{Re}\,[\varPhi(\omega = 0)], \qquad (4.3)$$

which obeys the scaling law

$$\varGamma^{\alpha}_{\text{HW}}(q) = \varLambda_{\text{HW}}q^{z}\gamma^{\alpha}_{\text{HW}}(x, y). \qquad (4.4)$$

Let us start by comparing the theoretical and experimental linewidths for Fe, EuO and EuS precisely at the critical temperature. Figure 4.10 shows the scaling functions for the transverse and longitudinal linewidth in the Lorentzian approximation, normalized such that the linewidth approaches unity for $q \gg q_D$. As already noted earlier, a remarkable result of mode-coupling theory is that the dynamic dipolar crossover of the longitudinal linewidth starts near the dipolar wave-vector $q \approx q_D$, whereas for the transverse linewidth it is shifted to a wave-vector which is about on order of magnitude smaller than q_D. This explains why no appreciable deviation from the exchange scaling prediction $\varGamma^T(q) \propto q^{5/2}$ in the wave-vector range accessible up to now was found by Collins *et al.* (1969), Dietrich *et al.* (1976), Mezei (1982, b, 1984, 1986, 1987, 1988), Wicksted *et al.* (1984), Böni and Shirane (1986) and Böni *et al.* (1987a, b) in neutron scattering experiments right at the critical temperature. The experimental data in figure 4.10 are collected from the work of Collins *et al.* (1969), Dietrich *et al.* (1976), Mezei (1982a, b, 1984, 1986, 1987, 1988), Wicksted *et al.* (1984), Böni and Shirane (1986) and Böni *et al.* (1987a, b) and are normalized with respect to the theoretical value of the non-universal frequency scale $\varLambda_{\text{Lor}} = 5.1326\varLambda$. For comparison the solid curve in figure 4.10 shows the scaling function of the transverse linewidth as obtained from the solution of the complete mode-coupling equations (Frey *et al.* 1988, 1989). Whereas the general functional form is quite similar to the scaling function obtained in the Lorentzian approximation, their asymptotic values at large values differ by a factor of approximately 1.2, which leads to even better quantitative agreement between theory and experiment. It still needs experiments at smaller momentum transfer to detect the increase in $\varGamma$ because of the crossover to the dipolar regime.

In contrast with the data on the wave-vector dependence right at the critical temperature, experiments on the scaling function above the critical temperature revealed huge derivations from the Résibois–Piette scaling function, as evident from the neutron scattering data on Fe (Mezei 1982a, b) shown in the scaling plot in figure 4.11. which become more pronounced the closer they are to T_C.

This figure also shows a comparison of the HWHM (chain curve) of the transverse Kubo functions resulting from equations (3.40) and (3.41) and the Lorentzian linewidth γ^T_{Lor} (solid curve) determined by equation (3.49). In the case of Fe, (*a*), (*b*), (*c*) and (*d*) correspond to the temperatures $T - T_C = 1.4$, 5.8, 21.0 and 51.0 K respectively. All curves are normalized with respect to their value at criticality. This implies that the non-universal frequency scale is then found to be $\varLambda_{\text{Lor}} = 5.1326\varLambda = 107.2\,\text{meV Å}^{5/2}$ in
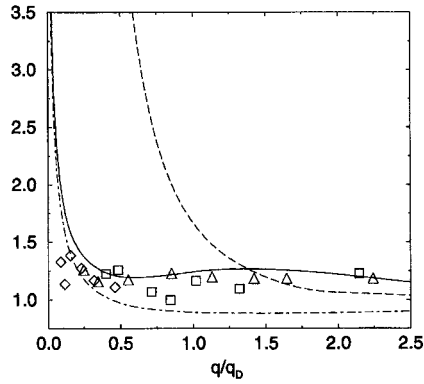
Figure 4.10. Scaling functions against $y^{-1} = q/q_D$ at T_C (in units of the theoretical non-universal A) for firstly the HWHM of the complete solution of the mode-coupling equations for the transverse Kubo relaxation function (————), secondly the transverse linewidth (—·—) and thirdly the longitudinal line width (– – –) in the Lorentzian approximation. Experimental data for the transverse linewidth for EuO ($\square$, data from Böni and Shirane (1986); $\Diamond$, data from Mezei (1984)) and Fe ($\triangle$, data from Mezei (1982a, b)) are also given.
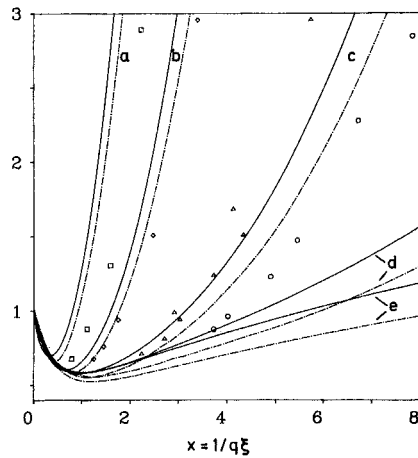
Figure 4.11. Scaling function of the transverse linewidth in Lorentzian approximation (————) and of the HWHM of the complete solution (—·—) against the scaling variable $x = (q\xi)^{-1}$ for a set of temperatures ($T - T_C = (a)$ 1·4 K, (b) 5·8 K, (c) 21 K and (d) 51 K). (e) The Résibois–Piette function (————) and the HWHM from the complete solution of the mode-coupling equations (—·—) without dipolar interaction is also plotted. Experimental results for Fe from Mezei (1982a, b, 1984) ($T - T_C = 1·4$ K ($\square$), 5·8 K ($\Diamond$), 21·0 K ($\triangle$) and 51·0 K ($\bigcirc$)) are also shown.

the Lorentzian approximation and $\Lambda_{HW} = 1\cdot 37\Lambda_{Lor} = 147\,\text{meV\,Å}^{5/2}$ for the HWHM. The latter value is in quite reasonable agreement with the experimental value $\Lambda_{exp} = 130\,\text{meV\,Å}^{5/2}$. The Lorentzian linewidth and the HWHM have nearly the same $(q\xi)^{-1}$ dependence. In particular for small wave-vectors the difference comes about only because of the different non-universal frequency scales. In summary, the linewidth is affected by the lineshape crossover only to a minor extent, since the former is only a coarse feature of the relaxation function. At small wave-vectors, only the non-universal scale is modified. This allows one to use the Lorentzian approximation for some later applications of the theory to neutron scattering, electron spin resonance, magnetic relaxation and hyperface interaction experiments.

As can be inferred from figure 4.11 the complete solution of the mode-coupling theory is in reasonable agreement with the experiment close to T_C ($T = T_C = 1\cdot 4$ and $5\cdot 8\,\text{K}$) and gives an improvement over the Lorentzian approximation. The minor differences may be due to the following reasons. Firstly, as mentioned above, the measured scaling functions of the transverse relaxation function were fitted to an exponential line, which is not the correct shape. Secondly, because the dipolar crossover temperature T_D of Fe is $8\cdot 6\,\text{K}$, static crossover effects not taken into account in the experiments may cause some changes. Furthermore the non-universal scale of the correlation length ξ_0 is affected by experimental uncertainties. A change in ξ_0 would lead to a horizontal shift of the data points in figure 4.11.

Larger differences show up for temperatures farther away from T_C ($T - T_C = 21$ and $51\,\text{K}$), which cannot be accounted for by the shape crossover or static crossover effects. Here the measured linewidths are larger than the theoretical value. In order to explain this, it is necessary to take into account the van Hove (1954) terms and further relaxation mechanisms due to irrelevant interactions. Such irrelevant interactions are unimportant as concerns the critical behaviour but nevertheless may play an important role for temperatures well separated from T_C (Frey *et al.* 1989). Pseudo-dipolar forces (van Vleck 1937) have been studied by Frey *et al.* (1989) and Aberger and Folk (1989). Those additional interactions (crystal-field interactions, and the spin–orbit interaction leading to pseudo-dipolar terms) are presumably less important in magnets with localized moments such as EuO and EuS. This can be seen from the comparison of the linewidth with the experimental data. Figure 4.12 (figure 1 from Mezei *et al.* (1989), and figure 1 from Mezei (1988)) shows a scaling plot of the transverse linewidth data for temperatures $T - T_C = 0\cdot 5$, 2 and $4\,\text{K}$ in EuO, which are in quantitative agreement with the mode-coupling theory (solid curves).

Recently the transverse and for the first time the longitudinal spin fluctuations have been measured for EuS using inelastic scattering of polarized neutrons (Böni *et al.* 1991a, Görlitz *et al.* 1992). The observed relaxation rates follow rather precisely the *transverse* and *longitudinal* linewidths calculated from the dipolar mode-coupling theory (figures 4.13 and 4.14). In particular, these measurements confirm the behaviour of the longitudinal linewidth predicted by mode-coupling theory (Frey and Schwabl 1987, 1988a, 1989a).

4.1.3. *Constant-energy scans*

In this section we return to an analysis of the line shape and review results obtained by scans at constant frequency as opposed to constant wave-vector in the previous sections. As will become clear in the following, certain features of the line shape of the correlation function can be accentuated by constant-energy scans for the scattering function $S^T(q, \omega)$. Characteristic quantities in these scans are the peak position q_0 and
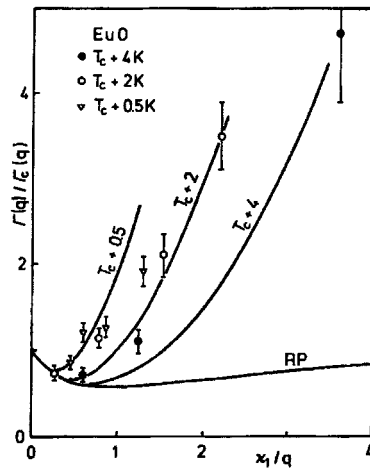
Figure 4.12. Scaling plot of the temperature dependence of the relaxation rate of critical fluctuations in EuO above the Curie temperature $T_C = 69\cdot3$ K: (———), the results from mode-coupling theory (Frey and Schwabl 1987). The data were taken between $q = 0\cdot018$ Å^{-1} and $q = 0\cdot15$ Å^{-1} ($\kappa_1 = 1/\xi$). (From Mezei (1988) and Mezei $et\,al.$ (1989).)
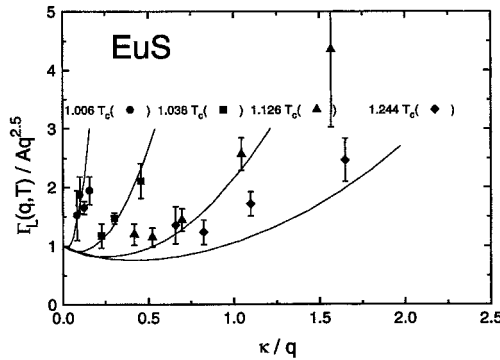
Figure 4.13. Comparison of the longitudinal linewidth of Lorenzian fits normalized to $\Lambda_{exp}q^{5/2}$ with $\Lambda_{exp} = 2\cdot1$ meV Å$^{5/2}$ to the dipolar dynamic scaling function predicted by mode-coupling theory for $q_D = 0\cdot245$ Å^{-1} for EuS ($\kappa = 1/\xi$). (From Böni $et\,al.$ (1991a).)

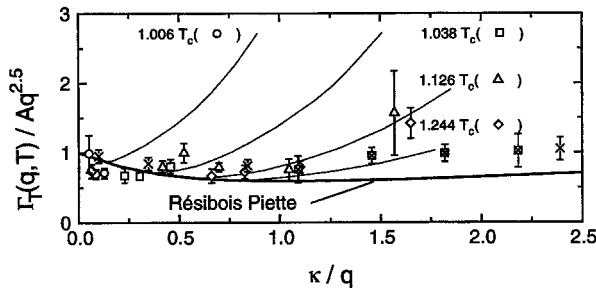Figure 4.14. The same as figure 4.13 for the transverse linewidth. (From Böni $et\,al.$ (1991a).)
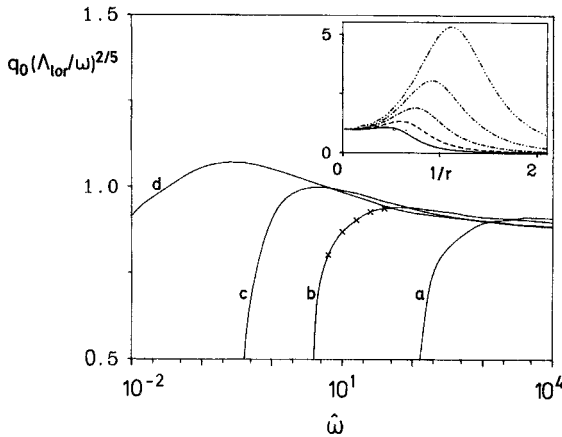
Figure 4.15. Scaled peak positions $q_0(\Lambda_{\mathrm{Lor}}/\omega)^{2/5}$ for constant-energy scans of the scattering function of the complete solution of the mode-coupling equations against the scaling variable $\hat{\omega}$ for $\varphi = (a)$ 1·490, (b) 1·294, (c) 0·970 and (d) for the isotropic case, that is $\varphi = 0$. The inset shows $S^{\mathrm{T}}(q, \omega)/S^{\mathrm{T}}(0, \omega)$ in arbitrary units against $1/r$ for $\varphi = 1·294$ for some typical values of the scaled frequency $(\hat{\omega} = 10^{L/10}$ with $L = 8$ (————), 10 (- - - - -), 12 (—·—), 14 (—··—) and 16 (—···—) indicated in the graph by crosses).

the HWHM Δq. For an isotropic Heisenberg ferromagnet, RG theory predicts a flat curve for the reduced peak positions $q_0(\Lambda/\omega)^{2/5}$ plotted against the scaled frequency $\omega\xi^{5/2}/\Lambda$ (Iro 1987, Folk and Iro 1986). This theoretical result has been confirmed experimentally in certain energy and wave-vector regions (Böni *et al.* 1987a). However, more recently Böni *et al.* (1988) have found pronounced departures from the isotropic scaling law in EuS in a region, where according to Frey and Schwabl (1987, 1988a, 1989a) the dipolar interaction should have a considerable effect on the dynamics. This is quite similar to the situation in constant-wave-vector scans, where one finds deviations from the Résibois–Piette scaling function (Mezei 1982a, 1984).

One of the most striking new features introduced by the dipolar interaction is the generalized dynamic scaling equation (3.31) with the additional scaling variable $y = q_{\mathrm{D}}/q$. In conventional constant-q scans plotted against the scaling variable $x = 1/q\xi$ the linewidths are not represented by a single scaling function but by a series of curves as exhibited in figures 3.1 and 3.2, where each curve corresponds to a fixed temperature. The failure of the isotropic scaling law in constant-energy scans can also be attributed to the influence of the dipolar forces (Aberger and Folk 1988a, b, 1989, Frey *et al.* 1988, 1989).

The generalized scaling law for the Kubo functions and characteristic frequencies leads to the following scaling law for the peak position in constant energy scans (Aberger and Folk 1989, Frey *et al.* 1989)

$$q_0 \left(\frac{\Lambda}{\omega}\right)^{2/5} = \mathcal{Q}\left(\varphi, \frac{\omega}{\Lambda(\xi^{-2} + q_{\mathrm{D}}^2)^{z/2}}\right). \tag{4.5}$$

From the above generalized scaling laws it becomes obvious that one obtains a set of curves parameterized by the scaling variable $\varphi = \tan^{-1}(q_{\mathrm{D}}\xi)$, if equation (4.5) containing the two-parameter scaling function $\mathcal{Q}$ is plotted against $\omega\xi^{5/2}/\Lambda$. In figure 4.15 the scaled peak position $q_0(\Lambda_{\mathrm{Lor}}/\omega)^{2/5}$ is plotted against $\hat{\omega} = \omega\xi^{5/2}/\Lambda_{\mathrm{Lor}}$ for the following set of scaling variables $\varphi = (a)$ 1·490, (b) 1·294, (c) 0·970 and (d) 0. Case (d) corresponds to an isotropic ferromagnet, that is $q_{\mathrm{D}} = 0$. Λ_{Lor} is related to Λ
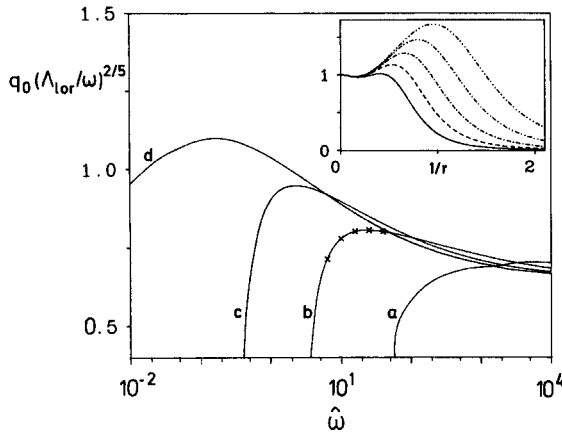
Figure 4.16.   The same as in figure 4.15 for the scattering function resulting from the Lorentzian approximation.

by $A_{Lor} = 5 \cdot 1326 A$. The above values for φ correspond in the case of EuS $(q_D = 0 \cdot 27 \text{ Å}^{-1}; \xi_0 = 1 \cdot 81 \text{ Å})$ to the temperatures $T = (a) \ 1 \cdot 01 T_C$, $(b) \ 1 \cdot 06 T_C$, and (c) $1 \cdot 21 T_C$. Owing to the generalized scaling law (4.5) the curves coincide with the isotropic theory for high frequency but deviate for low frequency. The frequency, where the deviation from the isotropic result sets in, increases upon approaching the critical temperature.

The steep decrease in the scaled peak positions at particular φ-dependent values of $\hat{\omega}$ has been explained as follows (Frey *et al.* 1989). The dipolar forces imply that the order parameter is no longer conserved and the uniform relaxation rate Γ_0 becomes finite. Hence the scattering function $S^T(q, \omega)$ remains finite for vanishing wave-vector:

$$S^T(q = 0, \omega) \propto \frac{\Gamma_0 \xi^2}{\omega^2 + \Gamma_0^2} \quad \text{for} \quad T \geqslant T_C. \tag{4.6}$$

Since Γ_0 is proportional to ξ^{-2}, equation (4.6) reduces to

$$S^T(q = 0, \omega) \propto \frac{1}{\omega^2} \quad \text{for} \quad T = T_C. \tag{4.7}$$

Therefore the maximum of the constant-energy scan at $q = 0$ increases strongly with decreasing frequency ω, whereas the local maximum at finite q is shifted to smaller q (see also the inset of figure 4.15). As a result of this competition, only the maximum at $q = 0$ survives for low frequencies. In order to substantiate this, typical constant-energy scans are shown in the inset of figure 4.15, where $S^T(q, \omega)/S^T(0, \omega)$ (in arbitrary units) is plotted against $1/r$ for $\varphi = 1 \cdot 294$ and for a set of scaled frequencies $(\hat{\omega} = 10^{L/10}$ with $L = 8, 10, 12, 14$ and 16 indicated in the graph). The corresponding scaled peak positions are indicated in the scaling plot by crosses. This behaviour explains why the scaled peak positions for dipolar ferromagnets show such a steep decrease at low frequencies.

Finally, it is important to note that the characteristic deviations from the isotropic theory exhibited in figure 4.15 result from the crossover in the time scale and not so much from the crossover in the shape function. This can be inferred from figure 4.16 where the scaled peak positions $q_0 (A/\omega)^{2/5}$ in the Lorentzian approximation is shown. Compared with figure 4.15 the maxima are overemphasized in figure 4.16, but the

portions with the steep slope are nearly identical. The differences of the exact mode-coupling theory and the Lorentzian approximation can also be seen in the insets of figures 4.15 and 4.16.

4.2. *Electron spin resonance and magnetic relaxation*

In electron spin resonance and magnetic relaxation experiments, one measures the electronic response function at zero wave-vector and finite frequency:

$$\chi^\alpha(\mathbf{q} = \mathbf{0}, \omega) = \frac{\Gamma^\alpha(\mathbf{q}, \omega)\chi^\alpha(\mathbf{q})}{i\omega + \Gamma^\alpha(\mathbf{q}, \omega)}\bigg|_{\mathbf{q}\to\mathbf{0}}, \tag{4.8}$$

where $\Gamma^\alpha(\mathbf{q}, \omega)$ is the frequency-dependent relaxation function in equation (3.19). From this, one determines the kinetic coefficient

$$L(\omega) = \Gamma^\alpha(\mathbf{q}, \omega)\chi^\alpha(\mathbf{q})|_{\mathbf{q}\to\mathbf{0}} \tag{4.9}$$

for the homogeneous magnetization dynamics. In the Lorentzian approximation, one finds for the kinetic coefficient at zero frequency

$$L_0(q_D, \xi) = \frac{g^2 J^2}{3\pi^2} k_B T \int_0^\infty dk\, k^2\, \frac{\chi^L(k, q_D)\chi^T(k, q_D)}{\Gamma^L(k, q_D) + \Gamma^T(k, q_D)}, \tag{4.10}$$

where the dependences of the Onsager coefficient on the dipolar wave-vector and the temperature are now indicated explicitly. Note that the kinetic coefficients for the homogeneous relaxation are the same for the longitudinal and transverse spin fluctuations. Using the generalized dynamic scaling and introducing polar coordinates $(r = (x^2 + y^2)^{1/2}, y/x = \tan\varphi)$ one finds that (Frey and Schwabl 1988a, 1989a)

$$L_0(q_D, \xi) = BF\left(\frac{1}{q_D\xi}\right), \tag{4.11}$$

with the universal crossover function

$$F\left(\frac{1}{q_D\xi}\right) = \left(1 + \frac{1}{q_D^2\xi^2}\right)^{-7/4} \int_0^\infty dr\, r^{5/2}\, \frac{\hat{\chi}^L(r, \varphi)\hat{\chi}^T(r, \varphi)}{\gamma^L(r, \varphi) + \gamma^T(r, \varphi)} \tag{4.12}$$

and the non-universal constant

$$B = \frac{4\pi^2}{3} A q_D^{5/2}. \tag{4.13}$$

If there were no dipolar interaction $(g = 0)$, one would simply find a vanishing Onsager coefficient owing to the factor g^2 in equation (4.10). With regard to the crossover function F of equation (4.12) it is natural to define the reduced crossover temperature by

$$\tau_D = \frac{T_D - T_C}{T_C} = (q_D^2\xi_0^2)^{1/\phi}, \tag{4.14}$$

where the crossover exponent ϕ equals the susceptibility exponent γ for a ferromagnet without dipolar interaction (Aharony 1973a, Aharony and Fisher 1973). If one neglects the dipolar crossover of the correlation length, the scaling variable $q_D^2\xi^2$ can be written as $q_D^2\xi^2 = (\tau_{cross}/\tau)^\gamma$ and the crossover temperature in terms of the dipolar wave vector is given by

$$q_D\xi_D = 1. \tag{4.15}$$

Table 9.   The dipolar wave-vector q_D, the Curie temperature T_C, the experimental non-universal
constant for the Onsager coefficient L_d, L_{bg} and for the autocorrelation time H_{exp}. The
values are taken from Kötzler (1988) and the references in table 8.

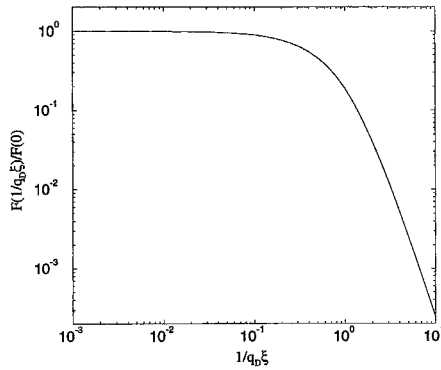|	q_D (Å^{-1})	T_C (K)	$\hbar L_d$ (μeV)	$\hbar L_{bg}$ (μeV)	H_{exp} (10^{-13}s)
EuS	0·245	16·6	38	1·8	–
EuO	0·147	69·1	24	0·64	–
$CdCr_2S_4$	0·058	84·4	5·9	0·01	–
$CdCr_2Se_4$	0·034	127·8	4·4	0·01	–
Fe	0·045 (0·033)	1043	–	–	6·0
Ni	0·013	627	3·0	–	9·2

Figure 4.17.   Universal crossover function $F(1/q_D \, \xi)/F(0)$ with $F(0) = 0\cdot1956$ for the Onsager
kinetic coefficient at zero frequency and zero wave vector against the scaling variable
$1/q_D\xi$.

The Onsager coefficient $L = \Gamma^\alpha \chi^\alpha$ does not depend on the sample shape
(Finger 1977) and is the same for the transverse and the longitudinal modes.
The universal crossover function $F(\rho)$ with $\rho = 1/q_D\xi$ is plotted in figure 4.17 in units
of its value $F(0)$ at criticality. For temperatures larger than the dipolar crossover
temperature, $F(\rho)$ shows a $\xi^{7/2}$ power-law behaviour, which was first shown by Huber
(1971) and Raghavan and Huber (1976). In the strong dipolar limit, that is very close
to the transition temperature, the Onsager coefficient approaches a constant (Finger
1977) reflecting the non-conserved nature of the order parameter due to the presence
of the dipolar interaction.

The kinetic Onsager coefficient at zero wave-vector has been measured by magnetic
relaxation experiments (Kötzler et al. 1976, 1978, De Haas and Verstelle 1977, Dunlap
and Gottlieb 1980) and electron spin resonance experiments (Kötzler et al. 1976, 1978,
Kötzler and Scheithe 1978, Kötzler and von Philipsborn 1978) for the Onsager
coefficient in EuS, EuO, $CdCr_2S_4$, $CdCr_2Se_4$ and Ni (Salamon 1967, Spörel and Biller
1975). In order to extract the contribution of the critical fluctuations one has to subtract
a non-critical background L_{bg} which in the critical region of all ferromagnets (except
Ni) is very small, $L_{bg} \ll L_{cr}$ (see table 9). The critical part of the Onsager coefficient
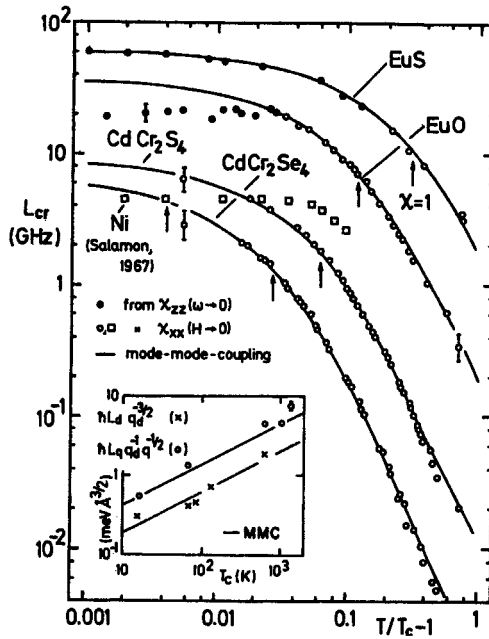
Figure 4.18. Critical part of the Onsager kinetic coefficient for the homogeneous spin dynamics above T_C of CdCr$_2$Se$_4$ (Kötzler and Van Philipsborn 1978), CdCr$_2$S$_4$ (Kötzler and Scheithe 1978), EuO (Kötzler *et al.* 1978), EuS ((●), data from Kötzler *et al.* (1976); (○), data from Kötzler (1988)), and Ni (Salamon 1967): (————) the result from mode-coupling theory (Frey and Schwabl 1988a, 1989a). The inset shows the non-universal amplitudes $\hbar L_d q_D^{-3/2}$ for the kinetic coefficient and the relaxation rate $\hbar L_d q^{-1} q_D^{-1/2} = \Gamma^T(q, T = T_C)/q^{5/2} \approx 5 \cdot 1326 A$ at the critical point for ferromagnets including Fe and Co. (From Kötzler (1988).)

$$\hbar L_0(q_D, \xi) = L_d \frac{F(\rho)}{F(0)} = BF(\rho) \qquad (4.16)$$

is compared with the crossover function F in figure 4.18 (figure 1 of Kötzler (1988)). The non-universal parameter $\hbar L_d = BF(0)$ was fixed by the data for the kinetic coefficient in the centre of the critical region. There is excellent agreement (except for Ni and EuO) of the observed crossover with the results of the mode-coupling theory. In particular, the data for EuS follow the theoretical function quite closely. The electron spin resonance data on Ni (Salamon 1967), shown in figure 4.18, deviate from the mode-coupling result. Spörel and Biller (1975), however, find an increase in the electron paramagnetic resonance linewidth of Ni near T_C, in accord with mode-coupling theory but opposite to what was found by Salamon (1967). It seems that the observation of the peak-like broadening depends critically on the quality of the sample. Recently Li *et al.* (1990, 1991) have demonstrated that it is possible to observe the critical broadening of the linewidth in ultrathin Ni films. As further possible sources for the deviations in Ni and EuO from the dipolar crossover, sample imperfections (e.g. oxygen vacancies in EuO, and internal stress in Ni) have been suggested (Kötzler 1988).

The values of the fit parameter L_d are listed in table 9, but even these values agree with the theoretical prediction as can be inferred from the inset in figure 4.18. The minor differences can be attributed to some uncertainties in the dipolar wave-vector (Kötzler *et al.* 1988).

Because electron spin resonance experiments are performed in a magnetic field B there should be an effect on the relaxation rate starting at $\gamma B = \Gamma(q = \xi^{-1})$ (Kawasaki 1976). Those data points are not given in figure 4.18. The influence of the magnetic field on the relaxation rate at zero wave-vector has recently been studied by Kötzler et al. (1991). In analysing the effect of the magnitude field in terms of the internal isothermal susceptibility $\chi_{int} = \delta M/\delta H_{int}$ (H_{int} is the internal magnetic field related to the external magnetic field by demagnetization corrections) the data were found to collapse on to a single curve. Hence, empirically, the field effect on the kinetic coefficient can be accounted for by using $q_D^2 \chi_{int}$ instead of $q_D^2 \xi^2$ as the scaling variable and the same scaling function F as for the case of zero magnetic field.

Up to now we have studied the behaviour of the uniform relaxation at zero frequency only. In fact, the kinetic coefficient is frequency dependent, which was observed first by De Haas and Verstelle (1977). Measuring the uniform dynamic susceptibility in EuO they have found a deviation from a Debye spectrum (Lorentzian form), which according to equations (4.8) and (4.9) is equivalent to a frequency-dependent kinetic coefficient. Similar deviation from a Lorentzian have been found quite recently for EuS (Grahl et al. 1991, Dombrowski et al. 1994). In order to study the frequency dependence of the kinetic coefficient, one would have to solve the full frequency-dependent mode-coupling equations and from these deduce $L(q_D, \xi, \omega)$. As a first approximation, one can use (Dombrowski et al. 1994, Kötzler et al. 1994)

$$L(q_D, \xi, \omega) = \frac{g^2 J^2}{3\pi^2} k_B T \int_0^\infty dk\, k^2 \frac{\chi^L(k, q_D)\chi^T(k, q_D)}{\Gamma^L(k, q_D) + \Gamma^T(k, q_D) + i\omega}, \qquad (4.17)$$

which is obtained as the first interaction step in a self-consistent determination of the frequency-dependent kinetic coefficient, starting with the damping coefficients $\Gamma^{L,T}(q, q_D, \xi)$ from the Lorentzian approximation. A scaling analysis of the frequency-dependent kinetic coefficient gives

$$L(q_D, \xi, \omega) = BF\left(\frac{1}{q_D\xi}, \frac{\omega\xi^z}{\Lambda}\right), \qquad (4.18)$$

with the scaling function

$$F\left(\frac{1}{q_D\xi}, \frac{\omega}{\Lambda q_D^z}\right) = \left(1 + \frac{1}{q_D^2\xi^2}\right)^{-7/4} \int_0^\infty dr\, r^{5/2} \frac{\hat{\chi}^L(r, \varphi)\hat{\chi}^T(r, \varphi)}{\gamma^L(r, \varphi) + \gamma^T(r, \varphi) + i(\omega/\Lambda q_D^z)r^z \sin^z \varphi}. \qquad (4.19)$$

The real and imaginary parts of F are shown in figures 4.19 (a) and (b) respectively against the scaled frequency $\hat{\omega} = \omega/\Lambda q_D^z$ for several values of $\varphi = \tan^{-1}(q_D\xi)$, indicated in the graphs. For small and large values of $\hat{\omega}$ the real part of the scaling function behaves asymptotically as

$$\mathrm{Re}\left[F\left(\frac{1}{q_D\xi}, \frac{\omega}{\Lambda q_D^z}\right)\right] \approx F\left(\frac{1}{q_D\xi}\right) \begin{cases} 1 - \left(\dfrac{\hat{\omega}}{\omega_{c1}(1/q_D\xi)}\right)^2, \\[2ex] \left(\dfrac{\hat{\omega}}{\omega_{c2}(1/q_D\xi)}\right)^{-1-1/z}, \end{cases} \text{ for } \begin{cases} \hat{\omega} \ll 1, \\[2ex] \hat{\omega} \gg 1. \end{cases} \qquad (4.20)$$

The corresponding scaling functions for the Onsager coefficient at zero frequency $F(1/q_D\xi)$ and the scaling functions $\omega_{c2}(1/q_D\xi)$ and $\omega_{c1}(1/q_D\xi)$ characterizing the high- and low-frequency behaviours are shown in figures 4.20 (a), (b) and (c) respectively. As can be inferred from these figures, the scaling function $\omega_{c1}(1/q_D\xi)$ is nearly constant.
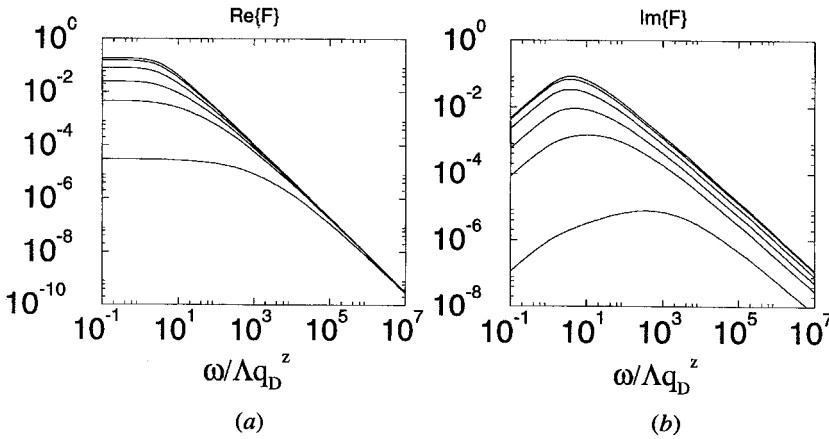
Figure 4.19. (*a*) The real and (*b*) the imaginary parts of F against the scaled frequency $\hat{\omega} = \omega/\Lambda q_D^z$ for several values of $\varphi = \tan^{-1}(q_D\xi)$: $\varphi_1 = 0.99\pi/2$ (top curve), $\varphi_2 = 0.90\pi/2$, $\varphi_3 = (\pi/2)(1 - 10^{-0.5})$, $\varphi_4 = (\pi/2)(1 - 10^{-0.25})$, $\varphi_5 = (\pi/2)(1 - 10^{-0.1})$, $\varphi_6 = (\pi/2)(1 - 10^{-0.025})$ (bottom curve).
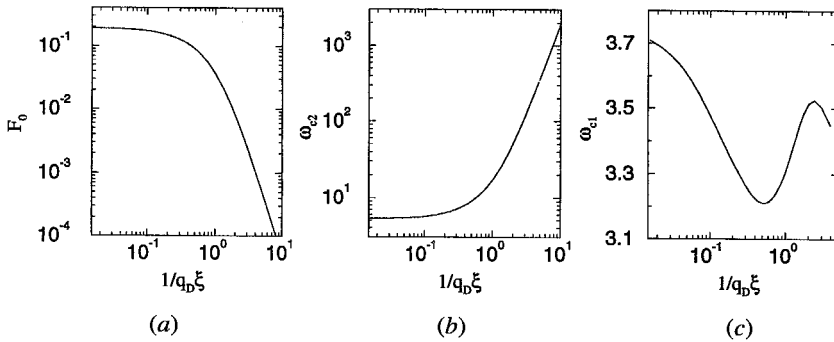
Figure 4.20. The scaling functions for the (*a*) Onsager coefficient $F(1/q_D\xi)$ at zero frequency and (*b*) the scaling function $\omega_{c2}(1/q_D\xi)$ and (*c*) the scaling function $\omega_{c1}(1/q_D\xi)$ characterizing the high- and low-frequency behaviours respectively.

This finding is in accord with experiments by Dombrowski *et al.* (1994). The experiments have been analysed assuming a Lorentzian shape for the kinetic coefficient (Dombrowski *et al.* 1994):

$$L(q_D, \xi, \omega) \approx \frac{L(q_D, \xi)}{1 + i\omega/\omega_c}. \tag{4.21}$$

This shape differs from the theoretical results presented above, especially in the high-frequency limit, that is for $\omega \gg \Lambda q_D^z$. At low frequencies the theoretical result has the same expansion as the Lorentzian approximation used in analysing the experiments. It is found experimentally that the characteristic frequency ω_c is nearly independent of temperature. This is in accord with the above theoretical result, namely that the scaling function $\omega_{c1}(1/q_D\xi)$ is nearly constant over the whole temperature range. For a more detailed comparison with the experiment, further analysis of the data on the basis of the results of the mode-coupling theory for the frequency dependence of the Onsager coefficient seems to be necessary. It would be interesting to see whether the experiment confirms the predicted high-frequency behaviour $L(\omega) \propto \omega^{-1-1/z}$.

Recently, homogeneous magnetization dynamics have also been investigated in the ferromagnetic phase (Görlitz *et al.* 1992, Dombrowski *et al.* 1994). It is found that the scaling function for the kinetic coefficient below T_C agrees exactly with that observed earlier above T_C. Since a complete theory of the critical dynamics below T_C is still lacking, these results are not explained yet. However, those experimental findings are a clear indication of the importance of the dipolar interaction below the critical temperature.

4.3. *Hyperfine interactions*

There are several nuclear, that is hyperfine interaction, methods commonly used to study critical fluctuations in magnets. These are nuclear magnetic resonance (Saham *et al.* 1980), the Mössbauer effect (Kobeissi *et al.* 1976, Kobeissi and Hohenemser 1978), perturbed angular correlations (Reno and Hohenemser 1972, Gottlieb and Hohenemser 1973, Chow *et al.* 1980, Hohenemser *et al.* 1982) of γ-rays, and muon spin relaxation (see also section 4.3). The application of nuclear techniques to study critical phenomena in magnets has recently been reviewed by Hohenemser *et al.* (1989). For recent work on the application of muon spin relaxation for the investigation of spin dynamics the reader may consult the papers by Schenk (1985), Cox (1987) and Hartmann (1989). All the hyperfine interaction methods are local probes which are related to a wave-vector integral of the spin correlation functions. As such they offer a complement of neutron scattering. Dynamic studies, using hyperfine interaction probes, utilize the process of nuclear relaxation produced by time-dependent hyperfine interaction fields, which reflect fluctuations of the surrounding electronic magnetic moments.

The hyperfine interaction stems from the magnetic interaction of the electrons with the magnetic field produced by the nucleus. The hyperfine interaction of a nucleus with spin **I**, g factor g_N and mass m_N with one of the surrounding electrons with spin **S** and orbital momentum **L** can be written in the form (Bethe and Salpeter 1957, Schwabl 1991)

$$H_{hyp} = \frac{Ze_0^2 g_N}{2m_N mc^2} \left(\frac{1}{r^3} \, \mathbf{I} \cdot \mathbf{L} + \frac{8\pi}{3} \, \delta^{(3)}(\mathbf{x}) \mathbf{I} \cdot \mathbf{S} - \frac{1}{r^3} \, \mathbf{I} \cdot \mathbf{S} + \frac{3(\mathbf{I} \cdot \mathbf{x})(\mathbf{S} \cdot \mathbf{x})}{r^5} \right). \qquad (4.22)$$

The first term represents the interaction of the orbital momentum of the electron with the nuclear magnetic moment of the nucleus. The second term is the Fermi contact interaction and the last terms represent the dipolar interaction†. The Fermi contact interaction is finite only for electrons having a finite probability density at the nucleus, that is bound s electrons or itinerant electrons.

For a substitutional nucleus the main contribution to the hyperfine field is from the bound s electrons (Goldanski and Herber 1968), which are polarized by the magnetic ions. The large (and often negative) hyperfine field for transition-element ions comes from the polarization of the core s electrons by the spin density of the unpaired 3d electrons, which then contribute to the hyperfine field through the Fermi contact interaction (Watson and Freeman 1961). The residual dipolar interaction is negligible in this case. Note also that this term is zero for cubic symmetry. The Hamiltonian in equation (4.22) can also be used for the analysis of spin resonance experiments with

---

† In fact, the Fermi contact interaction also arises from the magnetic dipole interaction. In the evaluation of the matrix elements of the (residual) dipolar interaction, represented by the last two terms, an infinitesimal sphere around the origin has to be excluded. The singular part of the dipolar interaction from the interior of the sphere is represented by the Fermi contact term.

muons. However, these do not have bound electrons; hence the Fermi contact term involves only conduction electrons and is of the same order of magnitude as the (residual) dipolar interaction (Denison *et al.* 1979, Meier 1981) (see also section 4.4). For instance in Pd, there is a dipolar contribution by the Pd f electrons which also polarize the s electrons which in turn contribute via the Fermi contact term to the hyperfine field at the muon site.

After the above general remarks, let us now return to those hyperfine interaction probes (Mössbauer effect, perturbed angular correlations and nuclear magnetic resonance), where the Fermi contact term gives the dominant contribution to the hyperfine field at the nucleus. Then the corresponding interaction Hamiltonian reduces to

$$\mathscr{H}(t) = A_{\text{contact}} \mathbf{I} \cdot \mathbf{S}(t). \tag{4.23}$$

If the spin autocorrelation time τ_c is much shorter than the Larmor period $1/\omega_L$ and the nuclear lifetime τ_N (motional narrowing regime), the nuclear relaxation rate τ_R^{-1} is directly proportional to the (averaged) spin autocorrelation time τ_c:

$$\tau_R^{-1} = C_{\text{hf}} \tau_c, \tag{4.24}$$

with a hyperfine coupling constant C_{hf} (Hohenemser *et al.* 1982). The nuclear relaxation rate equals the spin–spin relaxation ($\tau_R^{-1} = T_2^{-1}$) in the case of nuclear magnetic resonance and is proportional to the relaxation-induced excess linewidth $\Delta\Gamma$ for the Mössbauer effect; for perturbed angular correlations, τ_R is given by the relaxation time of the perturbation factor.

The (averaged) spin autocorrelation time τ_c is defined by a time integral:

$$\tau_c = \frac{1}{2} \int_{-\infty}^{+\infty} \mathrm{d}t \, \frac{1}{3} \sum_{\alpha} G^{\alpha\alpha}(\mathbf{r}=0, t) = \frac{1}{6} \sum_{\alpha} \int_{\mathbf{q}} G^{\alpha\alpha}(\mathbf{q}, \omega=0) \tag{4.25}$$

over the spin autocorrelation function $G^{\alpha\alpha}(\mathbf{r}, t) = \frac{1}{2}\langle\{S^\alpha(\mathbf{r}, t), S^\alpha(\mathbf{0}, 0)\}\rangle$. Hence hyperfine interaction methods provide an integral property of the spin–spin correlation function. Upon using the fluctuation dissipation theorem, which in the special case $\omega = 0$ reduces to

$$G^{\alpha\alpha}(q, \omega=0) = 2k_{\text{B}}T \frac{\chi^\alpha(\mathbf{q}, g)}{\Gamma^\alpha(\mathbf{q}, g)}, \tag{4.26}$$

one finds for the autocorrelation time that

$$\tau_c = \frac{k_{\text{B}}T}{V_q} \int_{\text{BZ}} \mathrm{d}^3 q \, \frac{1}{3} \sum_{\alpha} \frac{\chi^\alpha(\mathbf{q}, g)}{\Gamma^\alpha(\mathbf{q}, g)}. \tag{4.27}$$

The **q**-integration extends over the Brillouin zone, the volume of which is V_q.

Important information about the behaviour of the autocorrelation time can be gained from a scaling analysis. Upon using the static and dynamic scaling laws, equation (4.27) can be written as

$$\tau_c \propto 4\pi \int \mathrm{d}q \, q^{-z} \frac{1}{3} \sum_{\alpha} \frac{\hat{\chi}^\alpha(q\xi, q/q_{\text{D}})}{\gamma^\alpha(q\xi, q/q_{\text{D}})}. \tag{4.28}$$

If there were no dipolar interaction, one could extract the temperature dependence from the integral in equation (4.28) with the result $\tau_c \propto \xi^{z-1}$. This expression can be used to define an effective dynamical exponent $z_{\text{eff}}(\tau)$, which depends on the correlation

length by

$$\tau_c \propto \xi^{z_{eff}-1} \propto \left(\frac{T-T_C}{T_C}\right)^w. \tag{4.29}$$

In the presence of dipolar forces, one finds after introducing polar coordinates as in section 4.2 that

$$\tau_c = H\left(1 + \frac{1}{q_D^2\xi^2}\right)^{(1-z)/2} \int_{r_0}^{\infty} dr\, r^{z-2}\frac{1}{3}\sum_{\alpha}\frac{\hat{\chi}^{\alpha}(r,\varphi)}{\gamma^{\alpha}(r,\varphi)}, \tag{4.30}$$

where $z = \frac{5}{2}$ and the non-universal constant H is given by (Frey and Schwabl 1989b)

$$H = \frac{(k_B T)^2}{32\pi^6(\Lambda a^{-5/2})^3}(q_D a)^{3/2}. \tag{4.31}$$

The lower cut-off r_0 is

$$r_0 = \frac{q_D}{q_{BZ}}\left(1 + \frac{1}{q_D^2\xi^2}\right)^{1/2}, \tag{4.32}$$

where q_{BZ} is the boundary of the Brillouin zone. In the critical region it can be disregarded and replaced by r_0, since $q_{BZ} \gg q_D$ and the integrand in equation (4.30) is proportional to $r^{1/2}$ for small r. For very small ξ (outside the critical region) the cut-off reduces the autocorrelation time with respect to the critical value.

One should note that the dominant wave-vectors contributing to the relaxation time τ_c in equation (4.27) are close to the zone centre. Quantitative estimates for the wave-vector range probed by muon spin rotation experiments of Fe and Ni, which also apply for other hyperfine experiments, have been given by Dalmas de Réotier et al. (1994).

The averaged autocorrelation time is a sum of two parts:

$$\tau_c = \tfrac{1}{3}(\tau_L + 2\tau_T), \tag{4.33}$$

which we call the longitudinal and transverse relaxation times given by

$$\tau_\alpha = HI_\alpha(\varphi), \tag{4.34}$$

where we have defined

$$I_\alpha(\varphi) = \left(1 + \frac{1}{q_D^2\xi^2}\right)^{-3/4}\int_{r_0}^{\infty} dr\, r^{1/2}\frac{\hat{\chi}^{\alpha}(r,\varphi)}{\gamma^{\alpha}(r,\varphi)}, \quad \alpha = L, T. \tag{4.35}$$

These two relaxation times are shown in figure 4.21 as functions of the scaling variable $1/q_D\xi$, where we have neglected the lower cut-off r_0. Since the static longitudinal susceptibility does not diverge one finds that the longitudinal relaxation time is non-critical, whereas the transverse relaxation time diverges like $\tau_T \propto \xi$. This corresponds to an effective dynamical exponent $z_{eff} = 2$. When leaving the dipolar critical region there is a crossover to the isotropic Heisenberg region, where both curves join and the relaxation times $\tau_L = \tau_T = \tau_c$ are characterized by another power law $\tau_c \propto \xi^{3/2}$ corresponding to an effective dynamical exponent $z_{eff} = \frac{5}{2}$.

Let us now compare with hyperfine experiments on Fe and Ni. Early perturbed angular correlation (Reno and Hohenemser 1972, Gottlieb and Hohenemser 1973) and Mössbauer effect (Kobeissi et al. 1976, Kobeissi and Hohenemser 1978) experiments were performed well in the dipolar region and an effective exponent $z = 2$ was found. The crossover in the dynamic exponent from $z = 2.5$ to $z = 2$ was first observed by Chow et al. (1980) and Hohenemser et al. (1982). The autocorrelation time τ_c is shown in figure 4.22 in units of the non-universal constant H (see table 9) against the scaling
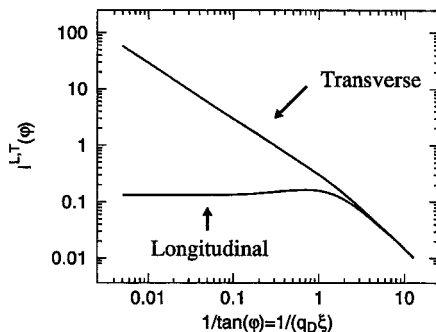
Figure 4.21. Scaling functions $I_{L,T}(\varphi)$ for the transverse and longitudinal autocorrelation time $\tau_{L,T}$ against $1/q_D\xi$.
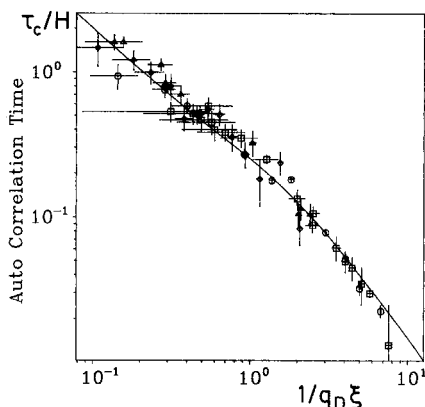

Figure 4.22. Autocorrelation time τ_c/H (in units of the non-universal constant H) against the scaling variable $1/q_D\xi$ (————). Experimental results for the autocorrelation time in units of H_{exp} for Fe (Hohenemser *et al.* 1982) (□) and Ni ((◇), data from Reno and Hohenemser (1972); (△), data from Gottlieb and Hohenemser (1973); (○), data from Hohenemser *et al.* (1982)) are also shown.

variable $1/q_D\xi$. The data points in figure 4.22 are the results of hyperfine interaction experiments on Fe and Ni (Reno and Hohenemser 1972, Gottlieb and Hohenemser 1973, Chow *et al.* 1980, Hohenemser *et al.* 1982) for the autocorrelation time τ_c (in units of their non-universal frequency scale H). As before, there is no fit parameter for the scaling variable $1/q_D\xi$. So we conclude that MC theory accounts well for the experimental data, demonstrating the universal crossover behaviour from $z_{eff} = \frac{5}{2}$ to $z_{eff} = 2$ as the critical temperature is approached.

Finally we would like to note that the Mössbauer effect (Chowdhury *et al.* 1984, 1986) and perturbed angular correlation (Collins *et al.* 1986) experiments on the dynamics of Gd show neither $z = 2.5$ nor $z = 2.0$ but $1.74 < z < 1.82$ depending on whether the system is assumed to have Heisenberg or Ising static exponents. Recent muon spin rotation experiments give similarly depressed values of the critical dynamic exponent z (Wäckelgard *et al.* 1986, 1989) (see section 4.4). Dalmos de Réotier and Yaouanc (1994) compared the muon spin rotation data (Wäckelgard *et al.* 1986, Hartmann *et al.* 1990) with the results from MC theory for isotropic dipolar ferromagnets (Frey and Schwabl 1988a, 1989a, b), and it is found that the available data

are in agreement with the MC theory. Gd is supposed to have an uniaxial exchange anisotropy along the c axis. Hence one expects that in the asymptotic region there is one critical mode along the c axis with $z_{eff} = 2$ and two uncritical modes with $z_{eff} = 0$ perpendicular to the c axis (Finger 1977b). Since for polycrystalline probes τ_c is an average over the relaxation rates of these modes, it is possible that the experimental data in the crossover region yield effective exponents less than $z = 2$. Here more experimental work with single crystals and a more detailed MC analysis beyond the scaling analysis in the paper by Finger (1977b) are needed to clarify the situation.

4.4. *Muon spin relaxation*

In muon spin relaxation experiments, one observes the muon precession in an applied magnetic field or in a local magnetic field inside the sample†. For recent work on the application of muon spin relaxation to the investigation of spin dynamics we refer the interested reader to the papers by Schenk (1985), Cox (1987) and Hartmann (1989).

In analogy with other implanted probes‡, such as those discussed in section 4.3, the muon spin will relax through interactions with fluctuating magnetic fields in its surroundings. However, in contrast the local magnetic field at the interstitial site of the muon has comparable contributions from the Fermi contact field *and* the dipolar field. In rare-earth materials the residual dipolar field is high and often the dominant field (Karlsson 1982, 1990, Hartmann *et al.* 1986). It has a reduced symmetry compared with the Fermi contact coupling. Whereas the Fermi contact coupling is isotropic in space, the residual dipolar field has an anisotropy with respect to the wave vector. In the case of a hyperfine field dominated by the residual dipolar field this implies that the spin fluctuations transverse and longitudinal with respect to the wave-vector contribute with different weights to the relaxation rate of the muon spin rotation. Hence, one has a situation quite different from for example perturbed angular correlation and Mössbauer effect measurements where the interaction of the substitutional probe with the host atoms is mainly a contact hyperfine coupling. This feature of muon spin rotation offers the possibility of designing experiments which allow one to distinguish between spin fluctuations longitudinal and transverse to the wave-vector **q** (Yaouanc *et al.* 1993a, b, Dalmas de Réotier and Yaouanc 1994).

Among the basic ferromagnets, muon relaxation has been measured in Fe (Herlach *et al.* 1986) and Ni (Nishiyama *et al.* 1984) which have a cubic crystal structure, and in Gd (Wäckelgard *et al.* 1986, 1989) which crystallizes in a hexagonal lattice. The data for the muon relaxation rate in Fe were interpreted by a dynamic exponent $z = 2\cdot0$ (Herlach *et al.* 1986) which indicate that the data are taken in the dipolar region. In fact, the data cover both the dipolar and the isotropic region (the crossover temperature for iron is $T_D - T_C = 8\cdot6$ K (see table 8)) with fairly large data error bars in the isotropic region, so that a crossover from $z = 2\cdot5$ to $z = 2\cdot0$ is not excluded by the data (M. Fähnle 1991, private communication). The observations for Ni (Nishiyama *et al.* 1984) seemed to be conflicting with perturbed angular correlation (Chow *et al.* 1980) measurements, if one assumes that in both cases the contact field is the dominant contribution to the local magnetic field at the muon site. However, one has to take into account that the interaction of the muon with the surrounding is more complicated than for the other hyperfine probes. As already pointed out by Yushankhai (1989) one has to

---

† Muon spin relaxation experiments are often performed in zero applied external field.
  ‡ The positive muon ends up in interstitial sites in solids, and in metals the actual site is in most cases identical with that preferred by hydrogen.

take into account the classical dipolar interaction between the muon magnetic moment and the lattice ion magnetic moments. This has recently been done by Yaouanc *et al.* (1993a, b), the results of which we shall review next.

A zero-field muon spin rotation measurement consists of measuring the depolarization function $P_z(t)$ (Schenk 1985):

$$P_z(t) = \tfrac{1}{2} \text{Tr} \left[\rho_m \sigma_z \sigma_z(t) \right], \tag{4.36}$$

where ρ_m is the density operator of the magnet and σ_z the projection of the Pauli spin operator of the muon spin on the z axis. $\text{Tr}[A]$ stands for the trace of A over the muon and magnet quantum states. Since the magnetic fluctuations are sufficiently rapid, the depolarization they induce can be treated in the motional narrowing limit. One finds that (Yaouanc *et al.* 1993a)

$$P_z(t) = \exp\left(-\lambda_z t \right), \tag{4.37}$$

with the damping rate

$$\lambda_z = \frac{\pi \mathscr{D}}{V} \int \frac{\mathrm{d}^3 q}{(2\pi)^3} \left\{ [\mathbf{G}(\mathbf{q})\mathbf{C}(\mathbf{q})\mathbf{G}(-\mathbf{q})]^{xx} + [\mathbf{G}(\mathbf{q})\mathbf{C}(\mathbf{q})\mathbf{G}(-\mathbf{q})]^{yy} \right\}, \tag{4.38}$$

where

$$C^{\alpha\beta}(\mathbf{q}) = \tfrac{1}{2}[\langle S_\mathbf{q}^\alpha(\omega) S_{-\mathbf{q}}^\beta(-\omega)\rangle + \langle S_\mathbf{q}^\beta(\omega) S_{-\mathbf{q}}^\alpha(-\omega)\rangle]|_{\omega=0} \tag{4.39}$$

is the symmetrized correlation function at zero frequency, and

$$\mathscr{D} = \left(\frac{\mu_0}{4\pi}\right)^2 \gamma_\mu^2 (g_L \mu_B)^2. \tag{4.40}$$

$\gamma_\mu = 851 \cdot 6 \, \text{Mrad s}^{-1} \text{T}^{-1}$ is the gyromagnetic ratio of the muon. The tensor $\mathbf{G}$ characterizes the types of interaction by which the muon spin is coupled to the magnetic moments of the material considered. It is given by

$$G^{\alpha\beta}(\mathbf{q}) = r_\mu H \delta^{\alpha\beta} + D^{\alpha\beta}(\mathbf{q}). \tag{4.41}$$

The first term describes the Fermi contact coupling, where r_μ is the number of nearest-neighbour magnetic ions to the muon localization site and H measures the strength of the hyperfine coupling (see table 8). The simple form for the contact coupling is valid only if the muon site is a centre of symmetry. The second term characterizes the dipolar coupling and can be calculated via Ewald's method (Yaouanc *et al.* 1993a). To lowest order in the wave-vector $\mathbf{q}$, one finds that

$$D^{\alpha\beta}(\mathbf{q}) = 4\pi \left(B^{\alpha\beta}(\mathbf{q}=0) - \frac{q^\alpha q^\beta}{q^2} \right). \tag{4.42}$$

The values of the tensor components $B^{\alpha\beta}(\mathbf{q}=0)$ depend on the muon site. For muons in a tetrahedral or octahedral interstitial site in a f.c.c. lattice one finds that $B^{\alpha\beta}(\mathbf{q}=0) = \tfrac{1}{3}\delta^{\alpha\beta}$ (Kronmüller *et al.* 1979). The situation is more complex for a b.c.c. lattice (Kronmüller *et al.* 1979).

For simplicity we confine ourselves to the case of a f.c.c. lattice and refer the reader to the papers by Yaouanc *et al.* (1993a, b) and Dalmas de Réotier and Yaouanc (1994) for a discussion of the more complicated cases of a b.c.c. crystal or a hexagonal lattice structure. For a f.c.c. lattice the damping rate is found to be (Yaouanc *et al.* 1993a)

$$\lambda_z = \frac{8}{3}\frac{\mu_0}{4\pi}\gamma_\mu^2 \frac{k_{\mathrm{B}}T}{v_a}\int_0^{q_{\mathrm{BZ}}} \mathrm{d}q\, q^2 \left(2p^2 \frac{\chi^{\mathrm{T}}(q)}{\Gamma^{\mathrm{T}}(q)} + (1-p)^2 \frac{\chi^{\mathrm{L}}(q)}{\Gamma^{\mathrm{L}}(q)}\right), \tag{4.43}$$

where we have defined

$$p = \frac{1}{3} + \frac{r_\mu H}{4\pi}. \tag{4.44}$$

When the Fermi contact interaction is large compared with the classical dipolar interaction, that is $|p| \gg 1$, equation 4.43 reduces to the result obtained in section 4.3, namely

$$\lambda_z^{\mathrm{contact}} = \frac{1}{6\pi^2}\frac{\mu_0}{4\pi}(\gamma_\mu r_\mu H)^2 \frac{k_{\mathrm{B}}T}{v_a}\int_0^{q_{\mathrm{BZ}}}\mathrm{d}q\, q^2\left(2\frac{\chi^{\mathrm{T}}(q)}{\Gamma^{\mathrm{T}}(q)} + \frac{\chi^{\mathrm{L}}(q)}{\Gamma^{\mathrm{L}}(q)}\right). \tag{4.45}$$

On the other hand when the Fermi interaction is negligible, that is $p \approx \frac{1}{3}$, we obtain from equation (4.43)

$$\lambda_z^{\mathrm{dipolar}} = \frac{16}{27}\frac{\mu_0}{4\pi}\gamma_\mu^2 \frac{k_{\mathrm{B}}T}{v_a}\int_0^{q_{\mathrm{BZ}}}\mathrm{d}q\, q^2\left(\frac{\chi^{\mathrm{T}}(q)}{\Gamma^{\mathrm{T}}(q)} + 2\frac{\chi^{\mathrm{L}}(q)}{\Gamma^{\mathrm{L}}(q)}\right). \tag{4.46}$$

While equation (4.45) has been derived under the hypothesis that the muon spin interacts with the lattice spins through the isotropic hyperfine interaction, equation (4.46) has been obtained supposing that the coupling is due only to the classical dipolar interaction. One should note that the relative weights of the transverse and the longitudinal modes are reversed in going from a pure contact to a pure dipolar interaction of the muon with the lattice spins. Hence in combining perturbed angular correlation with muon spin rotation measurements it should be possible to distinguish between transverse and longitudinal relaxation rates.

Upon introducing polar coordinates as in section 4.3 one can write the damping rate in scaling form:

$$\lambda_z = \mathscr{W}[2p^2 I_{\mathrm{T}}(\varphi) + (1-p)^2 I_{\mathrm{L}}(\varphi)], \tag{4.47}$$

where the non-universal constant $\mathscr{W}$ is given by

$$\mathscr{W} = \frac{8\pi^{3/2}}{3P}\left(\frac{\mu_0}{4\pi}\right)^{1/2}\frac{\gamma_\mu^2 \hbar q_{\mathrm{D}}^{3/2}}{g_{\mathrm{L}}\mu_{\mathrm{B}}}(k_{\mathrm{B}}T_{\mathrm{C}})^{1/2}. \tag{4.48}$$

The theoretical values of $\mathscr{W}$ for the four magnets considered primarily in this section are listed in table 8. The scaling functions $I^{\mathrm{L,T}}(\varphi)$ are defined in section 4.3. Figure 4.21 indicates that, while $I_{\mathrm{T}}(\varphi)$ exhibits a strong temperature dependence in the whole temperature range of the critical region, $I_{\mathrm{L}}(\varphi)$ is almost temperature independent for $q_{\mathrm{D}}\xi > 1$. Therefore the temperature dependence of the muon spin rotation damping rate λ_z depends on the relative weights of $I_{\mathrm{T}}(\varphi)$ and $I_{\mathrm{L}}(\varphi)$ which is controlled by the parameter p. As first noticed by Yushankhai (1989), the transverse fluctuations do not contribute to λ_z if $r_\mu H/4\pi = -\frac{1}{3}$. In this case, λ_z becomes temperature independent near T_{C}.

In figures 4.23 and 4.24 experimental data for Ni (Nishiyama *et al.* 1984) and Fe (Herlach *et al.* 1986) are compared with the results from mode-coupling theory. It should be noted that most of the data have been recorded in the cross-over temperature region where λ_z is not predominantly due to the transverse fluctuations. Again the mode-coupling theory gives a quantitative explanation of the observed relaxation rates.
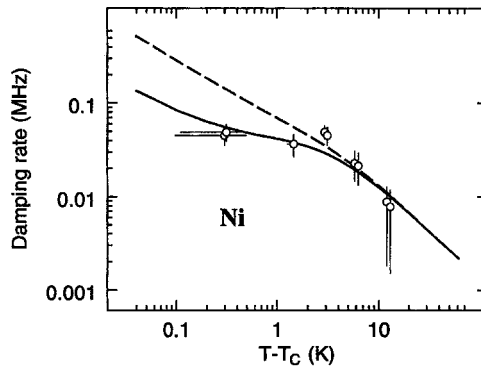
Figure 4.23. Temperature dependence of the muon spin relaxation damping rate for metallic Ni: (○), the experimental data from Nishiyama *et al.* 1984; (————) the result of the model which takes the muon dipolar interaction into account; (------), the prediction when this latter interaction is neglected.
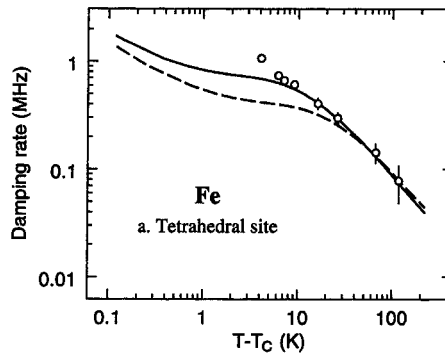
(*a*) Tetrahedral sites
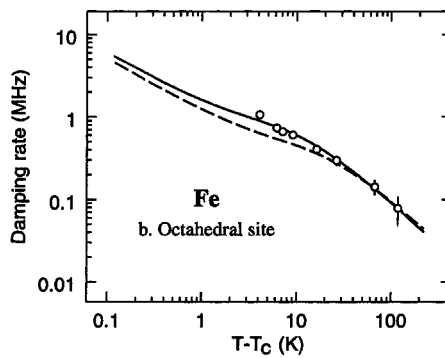
(*b*) Octahedral sites

Figure 4.24. Temperature dependence of the muon spin relaxation damping rate for metallic Fe where the muon is assumed to diffuse between (*a*) tetrahedral and (*b*) octahedral sites: (○), the experimental data of Herlach *et al.* 1986; (————), predictions of mode-coupling theory for the material parameters $q_D = 0.033 \text{ Å}^{-1}$ and $\xi = 0.82 \text{ Å}$ (see table 8); (------), predictions of mode-coupling theory for the material parameter $q_D = 0.045 \text{ Å}^{-1}$ and $\xi = 0.95 \text{ Å}$ (see table 8).

5. Other dipolar systems

Dipolar interactions are of importance not only for the critical behaviour of 3D isotropic ferromagnets, but also for other magnetic materials such as antiferromagnets, and ferromagnets with a uniaxial or planar exchange anisotropy. Furthermore, dipolar interactions play an important role in 2D systems, especially with regard to the existence of long-range order.

5.1. *Dipolar antiferromagnets*

5.1.1. *The Hamiltonian and equation of motion*

The order parameter of an antiferromagnet is the staggered magnetization, that is in the case of two sublattices the difference of the magnetization on these. Owing to the alternating nature of the order parameter, one supposes that the effect of the dipolar interaction on the long range order parameter fluctuations is averaged out and thus one expects no influence on the static critical behaviour. Indeed Aharony (1973b) showed that, in contrast with the ferromagnetic case, the main parameters characterizing the dipolar interaction become irrelevant for the critical statics of antiferromagnets. Yet there is an important effect on the dynamics, since the dipolar forces lead to new damping processes in the long-wavelength dynamics of the magnetization, because they break conservation of the total magnetization. Since the magnetization and staggered magnetization are coupled dynamically, there should be a crossover in the dynamic critical exponents and related features in the dynamical scaling functions. This effect has been studied theoretically for temperatures above and at the Néel temperature T_N by means of mode-coupling theory (Fischer 1989, Fischer *et al.* 1990, 1992).

The Hamiltonian of a dipolar antiferromagnet is

$$H = -\sum_{l \neq l'} \sum_{\alpha\beta} (J_{ll'}\delta^{\alpha\beta} + A_{ll'}^{\alpha\beta})S_l^\alpha S_{l'}^\beta, \tag{5.1}$$

with spins $\mathbf{S}_l$ at lattice sites $\mathbf{x}_l$. The first term in parentheses is the exchange interaction $J_{ll'}$ and the second the dipole–dipole interaction with the dipolar tensor given by

$$A_{ll'}^{\alpha\beta} = -\tfrac{1}{2}(g_L\mu_B)^2 \left(\frac{\delta^{\alpha\beta}}{|\mathbf{x}_l - \mathbf{x}_{l'}|^3} - \frac{3(\mathbf{x}_l - \mathbf{x}_{l'})^\alpha \cdot (\mathbf{x}_l - \mathbf{x}_{l'})^\beta}{|\mathbf{x}_l - \mathbf{x}_{l'}|^5} \right). \tag{5.2}$$

We define Fourier-transformed quantities by

$$S_l^\alpha = \frac{1}{N^{1/2}} \sum_{\mathbf{q}} \exp{(i\mathbf{q} \cdot \mathbf{x})} S_{\mathbf{q}}^\alpha, \tag{5.3}$$

$$J_{ll'} = \frac{1}{N} \sum_{\mathbf{q}} \exp{[i\mathbf{q} \cdot (\mathbf{x}_l - \mathbf{x}_{l'})]} J_{\mathbf{q}}, \tag{5.4}$$

$$A_{ll'}^{\alpha\beta} = \frac{1}{N} \sum_{\mathbf{q}} \exp{[i\mathbf{q} \cdot (\mathbf{x}_l - \mathbf{x}_{l'})]} A_{\mathbf{q}}^{\alpha\beta}, \tag{5.5}$$

and obtain

$$H = -\sum_{\mathbf{q}} (J_{\mathbf{q}}\delta^{\alpha\beta} + A_{\mathbf{q}}^{\alpha\beta})S_{\mathbf{q}}^\alpha S_{-\mathbf{q}}^\beta \tag{5.6}$$

for the Hamiltonian in terms of Fourier components. In order to study the long-wavelength behaviour of the model, one needs to know the behaviour of the dipole–dipole interaction tensor $A_{\mathbf{q}}^{\alpha\beta}$ at small wave-vectors. The result depends on

the lattice structure and the dimensionality of the system. For a 3D system the expansion has been given in section 3 (see equation (3.4)). In two dimensions the dipole-interaction tensor has been analysed by Maleev (1976). He finds for small wave-vectors that

$$A_{\mathbf{q}}^{\alpha\beta} = A^{(0)}(\tfrac{1}{3}\delta^{\alpha\beta} - \hat{z}^\alpha\hat{z}^\beta) + A^{(1)}q\left(\hat{z}^\alpha\hat{z}^\beta - \frac{q^\alpha q^\beta}{q^2}\right), \tag{5.7}$$

where $\mathbf{q} = (q_x, q_y, 0)$ is an in-plane wave vector and z denotes the direction perpendicular to the plane $\mathbf{r} = (r_x, r_y, 0)$. The constants $A^{(0)}$ and $A^{(1)}$ depend on the lattice structure

$$A^{(0)} = \tfrac{3}{4}(g_L\mu_B)^2 \sum_{\mathbf{r} \neq 0} \frac{1}{r^3}, \tag{5.8}$$

$$A^{(1)} = \frac{\pi}{v_2}(g_L\mu_B)^2, \tag{5.9}$$

where v_2 is the volume of the 2D unit cell.

With the standard commutation relation for spin operators $[S_{\mathbf{k}}^\alpha, S_{\mathbf{q}}^\beta] = i\hbar\varepsilon_{\alpha\beta\gamma}S_{\mathbf{k}+\mathbf{q}}^\gamma$ one obtains the following equations of motion (Pich 1994):

$$\begin{aligned}
\frac{d}{dt}S_{\mathbf{q}}^x = \sum_{\mathbf{k}} &[(A_{\mathbf{k}}^{yy} + J_{\mathbf{k}})(S_{\mathbf{k}+\mathbf{q}}^z S_{-\mathbf{k}}^y + S_{\mathbf{k}}^y S_{\mathbf{q}-\mathbf{k}}^z) - (A_{\mathbf{k}}^{zz} + J_{\mathbf{k}})(S_{\mathbf{k}}^z S_{\mathbf{q}-\mathbf{k}}^y + S_{\mathbf{q}+\mathbf{k}}^y S_{-\mathbf{k}}^z) \\
&+ A_{\mathbf{k}}^{xy}(S_{\mathbf{k}}^x S_{\mathbf{q}-\mathbf{k}}^z + S_{\mathbf{q}+\mathbf{k}}^z S_{-\mathbf{k}}^x) - A_{\mathbf{k}}^{xz}(S_{\mathbf{k}}^x S_{\mathbf{q}-\mathbf{k}}^y + S_{\mathbf{q}+\mathbf{k}}^y S_{-\mathbf{k}}^x) \\
&+ A_{\mathbf{k}}^{yz}(S_{\mathbf{q}+\mathbf{k}}^z S_{-\mathbf{k}}^y + S_{\mathbf{k}}^z S_{\mathbf{q}-\mathbf{k}}^z - S_{\mathbf{k}}^y S_{\mathbf{q}-\mathbf{k}}^y - S_{\mathbf{q}+\mathbf{k}}^y S_{-\mathbf{k}}^y)]. \tag{5.10}
\end{aligned}$$

5.1.2. *Critical behaviour of three-dimensional dipolar antiferromagnets*

Now we turn to the critical dynamics of dipolar antiferromagnets. Specializing to the 3D isotropic case and retaining only those terms which are dominant in the long-wavelength limit, the Hamiltonian for a s.c lattice reduces to (Fischer 1989, Fischer *et al.* 1990, 1992)

$$H = J\int_{\mathbf{q}} \left([(qa)^2 - 6]\delta^{\alpha\beta} - g\frac{q^\alpha q^\beta}{q^2}\right) M_{\mathbf{q}}^\alpha M_{-\mathbf{q}}^\beta + J\int_{\mathbf{q}} [6 - (qa)^2]\delta^{\alpha\beta} N_{\mathbf{q}}^\alpha N_{-\mathbf{q}}^\beta, \tag{5.11}$$

where $M_{\mathbf{q}}^\alpha = S_{\mathbf{q}}^\alpha$ denotes the magnetization and $N_{\mathbf{q}}^\alpha = S_{\mathbf{q}+\mathbf{q}_0}^\alpha$ the staggered magnetization, and we have introduced the abbreviation $\int_{\mathbf{q}} = \int v_a(d^3q/2\pi)^3$. The wave-vector $\mathbf{q}_0 = (\pi/a)(1, 1, 1)$ characterizes the antiferromagnetic modulation.

Starting from this Hamiltonian mode coupling equations for the correlation functions of the magnetization and staggered magnetization have been derived and analysed by Fischer (1989) and Fischer *et al.* (1990, 1992). For instance for the longitudinal magnetization mode, one finds that

$$\begin{aligned}
\Gamma_M^L(\mathbf{q}, t) = 4\Lambda_{af}^2 \int_0^{q_{BZ}} &k^2\, dk \int_{-1}^{1} d(\cos\vartheta) \left[\left(\frac{g}{12}\right)^2 \sin^2\vartheta\, \Phi_M^T(\mathbf{k}_+, \xi, t)\Phi_M^L(\mathbf{k}, t)\right. \\
&+ \frac{(2\mathbf{q}\cdot\mathbf{k} + q^2)^2}{(|\mathbf{k}|^2 + \xi^{-2})(|\mathbf{k}_+|^2 + \xi^{-2})} [\sin^2\vartheta\, \Phi_N^T(\mathbf{k}_+, t)\Phi_N^L(\mathbf{k}, t) \\
&+ \cos^2\vartheta\, \Phi_N^T(\mathbf{k}_+, t)\Phi_N^T(\mathbf{k}, t)]\bigg], \tag{5.12}
\end{aligned}$$

where we have used the abbreviations $\mathbf{k}_+ = \mathbf{k} + \mathbf{q}$, $\Lambda_{af} = a^{3/2}(Jk_BT/8\pi^2)^{1/2}$ and $q_{BZ} = (2\pi/2a)(3/4\pi)^{1/2}$.

It is found that the memory kernels obey generalized scaling laws of the form

$$\Gamma_{M,N}^{L,T}(q, g, \xi, t) = \Lambda_{\text{af}}^2 q^{2z} \gamma_{M,N}^{L,T}(x, y, \tau), \tag{5.13}$$

$$\Phi_{M,N}^{L,T}(q, g, \xi, t) = \phi_{M,N}^{L,T}(x, y, \tau), \tag{5.14}$$

where the scaling variables are defined by $x = 1/q\xi$, $y = q_A/q$, and $\tau = \Lambda_{\text{af}}q^z t$ with the dynamic critical exponent $z = \frac{3}{2}$. The characteristic wave-vector q_A is related to the dipolar wave-vector $q_D = g^{1/2}/a$ by

$$q_A = (\tfrac{1}{12})^{2/3}(q_D a)^{4/3} q_{\text{BZ}}. \tag{5.15}$$

The value $\frac{3}{2}$ is the dynamical critical exponent for isotropic antiferromagnets and any crossover to dipolar behaviour is contained in the dynamic scaling function. In evaluating the transport coefficients $\Phi_{M,N}^{L,T}$, only two-mode decay processes have been considered (see equation (5.12)). Without dipolar interaction, that is for the isotropic exchange antiferromagnet, the magnetization modes can decay into staggered modes only (Wegner 1969, Résibois and Piette 1970, Joukoff-Piette and Résibois 1973, Kawasaki 1976)

The dipolar interaction leads in addition to a decay into two magnetization modes, dominating for small wave-vectors. In the strong dipolar limit ($T \to T_N$ and $q \to 0$) the mode-coupling equations for the magnetization modes can be solved exactly with the result

$$\Gamma_M^\lambda(q, \xi, t) = \frac{\Lambda_{\text{af}}g}{12(\frac{14}{9} + \frac{1}{8}\pi^2)^{1/2}} q_{\text{BZ}}^{3/2} [\frac{16}{9}\delta^{\lambda L} + (\frac{1}{8}\pi^2 - \frac{2}{9})\delta^{\lambda T}]\delta(t), \tag{5.16}$$

corresponding to a relaxation of the magnetization modes enforced by the dipolar interaction. The phase space for this decay is the full Brillouin zone, whereas the decay into staggered modes is weighted by the critical static susceptibilities. Therefore, with separation from the critical temperature for larger wave-vectors, the decay of the magnetization mode into two staggered modes dominates the decay into two magnetization modes.

The mode-coupling equations for dipolar antiferromagnets have been solved in the Lorentzian approximation by Fischer (1989) and Fischer et al. (1990, 1992). The results for the transverse scaling function $\gamma_{M,N}^T(x, \varphi)$ for the magnetization and staggered magnetization against x for different values of $\varphi = N\pi/30$ with $N = 0, 1, \ldots, 14$ are displayed in figures 5.1 and 5.2. The corresponding plots for the longitudinal scaling functions are very similar (Fischer 1989, Fischer et al. 1990, 1992). The curves with $N = 0$ correspond to the isotropic case. It is important to note that the effect of the dipolar interaction on the scaling functions of the magnetization and staggered magnetization modes is rather different. The scaled linewidth for the magnetization modes exceeds the isotropic curve by an amount which increases with T on approaching T_C (i.e. larger values of $\varphi = \tan^{-1}(q_D\xi)$). This reflects the crossover from a diffusive behaviour $\Gamma_M \propto q^2 q_A^{-1/2}$ to a relaxational behaviour $\Gamma_M \propto q_A^{3/2}$. The linewidth of the staggered magnetization at fixed scaling variable x decreases with T approaching T_C since the magnetization modes become uncritical. However, this change is much less pronounced than for the magnetization modes and more important, the asymptotic hydrodynamic dependence on the wave-vector and correlation length is unmodified, that is the hydrodynamic behaviour is always relaxational.

In the dipolar and isotropic critical and hydrodynamic limiting regions the mode-coupling equations can be solved analytically. These regions are defined
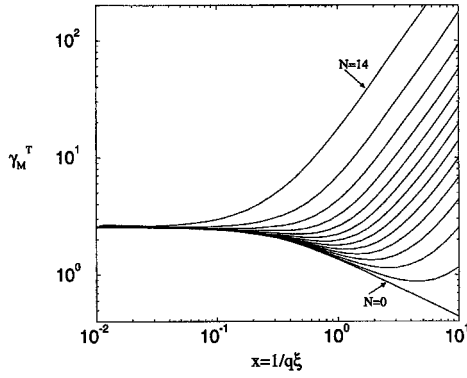
Figure 5.1. Scaling function for the linewidth of the transverse magnetization above T_N against $x = 1/q\xi$ for different values of $\varphi = N\pi/30$ ($N = 0, 1, 2, \ldots, 14$).
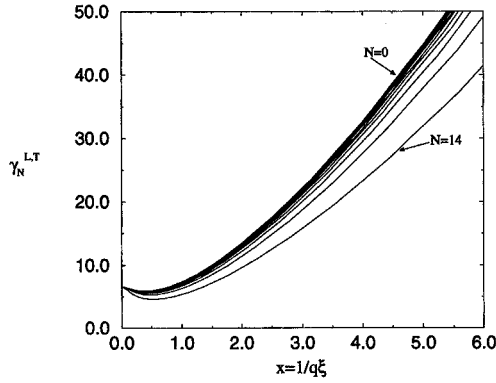
Figure 5.2. Scaling functions for the line-width of the transverse and longitudinal staggered magnetization above T_N against $x = 1/q\xi$ for different values of $\varphi = N\pi/30$ ($N = 0, 1, 2, \ldots, 14$).

Table 10. Behaviour of the scaling functions of the linewidths of an isotropic dipolar antiferromagnet in asymptotic regions.

Region	$\gamma_M^{L,T}$	$\gamma_N^{L,T}$
Dipolar critical	$y^{3/2}$	$y^{-1/2}$
Isotropic critical	1	1
Dipolar hydrodynamic	$r^{3/2}$	$r^{3/2}$
Isotropic hydrodynamic	$x^{-1/2}$	$x^{3/2}$

as follows: dipolar critical, $y \gg 1, x \ll 1$; isotropic critical, $y \ll 1, x \ll 1$; dipolar hydrodynamic, $y \gg x, x \gg 1$; isotropic hydrodynamic, $y \ll x, x \gg 1$. The results are summarized in table 10, where we note that these asymptotic power laws are the same for the longitudinal and transverse fluctuations. In the immediate vicinity of $q = q_A$ there is a dynamic crossover from $z_{eff} = \frac{3}{2}$ to $z_{eff} = 2$ for the staggered magnetization and from $z_{eff} = \frac{3}{2}$ to an uncritical value $z_{eff} = 0$ for the magnetization modes.

RbMnF$_3$ is one of the most thoroughly studied isotropic antiferromagnets (Lau *et al.* 1969, Corliss *et al.* 1970, Tucciarone *et al.* 1971). Taking the values for the exchange coupling and the static susceptibility of the magnetization from the work of Windsor and Stevenson (1966), Huber and Krüger (1970) and Tucciarone *et al.* (1971), the characteristic wave-vector q_A is about $0.02\,\text{Å}^{-1}$. Unfortunately the neutron scattering data (Lau *et al.* 1969, Corliss *et al.* 1970, Tucciarone *et al.* 1971) for the linewidth of the staggered magnetization modes are limited to the isotropic region and to our knowledge there are no data for the linewidths of the magnetization modes.

The dipolar effects could be observed more readily in EuSe and EuTe because of their smaller transition temperatures 4·8 K and 9·7 K respectively, implying larger q_A. Experiments in the appropriate wave-vector and temperature region are, however, still lacking.

5.2. Uniaxial dipolar ferromagnets

We have mainly concentrated on the influence of dipolar forces on otherwise isotropic ferromagnets. However, even in systems which are anisotropic to start with such as uniaxial ferromagnets, the dipolar interaction has a significant effect, because of its long-range nature.

The influence of the dipolar interactions on the critical statics of isotropic and uniaxial ferromagnets is quite different. Whereas for isotropic ferromagnets the dipolar interaction leads only to a slight modification of the critical exponents, Larkin and Khmelnitskii (1969) have discovered that uniaxial dipolar ferromagnets show classical behaviour with logarithmic corrections in three dimensions. This system was then studied by Aharony (1973c, d, 1976) by means of the renormalization group method. Aharony employed an isotropic elimination procedure and calculated the critical exponents to first order in $3 - d$ as well as logarithmic corrections (Aharony and Halperin 1975). Note that the dipolar interaction leads to a shift in the upper critical dimension from $d_c = 4$ to $d_c = 3$.

The existence of logarithmic corrections was verified experimentally for a number of uniaxial ferromagnetic substances (Ahlers *et al.* 1975, Frowein *et al.* 1982). However, these experiments were performed in regions of the reduced temperature where departures from the asymptotic behaviour are expected and are indeed observed. In particular, a maximum in the effective exponent of the susceptibility (Frowein *et al.* 1982) has been found. On the basis of a generalized minimal subtraction scheme the latter crossover from Ising behaviour with non-classical exponents to asymptotic uniaxial dipolar behaviour, which is characterized by classical exponents with logarithmic corrections, has been analysed by Frey and Schwabl (1988c, 1990). The theoretical results for the specific heat and susceptibility are in quantitative agreement with measurements on LiTbF$_4$, where solely the strength of the dipolar coupling constant entered as an adjustable parameter (Frey and Schwabl 1988c, 1990).

The Landau–Ginzburg free-energy functional for an *n*-component uniaxial spin system with isotropic exchange coupling and dipolar interaction is given by (Larkin and

Khmelnitskii 1969, Aharony 1973c, d)

$$\mathcal{H} = -\frac{1}{2} \int_{\mathbf{k}} \left(r + k^2 + g^2 \frac{q^2}{k^2} \right) S^{\alpha}(\mathbf{k}) S^{\alpha}(-\mathbf{k})$$

$$-\frac{u_0}{4!} \int_{\{\mathbf{k}_i\}} S^{\alpha}(\mathbf{k}_1) S^{\alpha}(\mathbf{k}_2) S^{\beta}(\mathbf{k}_3) S^{\beta}(-\mathbf{k}_1 - \mathbf{k}_2 - \mathbf{k}_3). \tag{5.17}$$

Here $S^{\alpha}(\mathbf{q})$ are the n components of the spin variables. The d-dimensional wave-vector $\mathbf{k} = (\mathbf{p}, q)$ is decomposed into q, the component along the uniaxial direction, and $\mathbf{p}$ the remaining d-1 components. The bare reduced temperature is given by $r = (T - T_C^0)/T_C^0$ and g^2 is a measure of the relative strength of the dipolar interaction. The dipolar term $g^2(q^2/k^2)$ suppresses the fluctuations in the z direction.

Folk *et al.* (1977) described the dynamics of uniaxial dipolar magnets in terms of a simple time-dependent Ginzburg–Landau model with the equation of motion

$$\frac{\partial}{\partial t} S^{\alpha}(\mathbf{k}, t) = -\Gamma_0 \frac{\delta \mathcal{H}}{\delta S^{\alpha}(-\mathbf{k}, t)} + \eta(\mathbf{k}, t). \tag{5.18}$$

Since the order parameter is a non-conserved quantity in the presence of the dipolar interaction, the kinetic coefficient Γ_0 is wave-vector independent. The random forces $\eta(\mathbf{k}, t)$ represent the uncritical degrees of freedom and are characterized by a Gaussian probability distribution. A renormalization group analysis for the above time-dependent Ginzburg–Landau model gives for the dynamic critical exponent (Folk *et al.* 1977)

$$z = 2 + c\eta, \quad \text{with} \quad c = 0.92. \tag{5.19}$$

This may be compared with the value for the time-dependent Ginzburg–Landau model for spin systems with short-range exchange interaction (Halperin *et al.* 1972, 1974, 1976), where $c = 0.73$ and the van Hove prediction $c = -1$.

Since for uniaxial dipolar magnets the fourth-order coupling is marginal at $d = 3$, there are logarithmic corrections to the classical behaviour. For the statics, one finds (Larkin and Khmelnitskii 1969, Aharony 1973c, d) for the susceptibility χ and the specific heat C:

$$\chi \propto \tau^{-1} |\ln \tau|^{1/3}, \quad C \propto |\ln \tau|^{1/3}, \tag{5.20}$$

where $\tau = (T - T_C)/T_C$ is the reduced temperature. The effect of the logarithmic corrections on the dynamics susceptibility can be approximated by (Folk *et al.* 1977)

$$\chi(\omega, \mathbf{p}, q, \tau) = \left(-\frac{i\omega}{\Gamma_0} + p^2 + g^2 \frac{q^2}{p^2} + \mu_1(0) \left| \frac{1}{2l_0} \ln\left[\mu_1(0)\right] \right|^{-1/3} \right)^{-1}, \tag{5.21}$$

where $\mu_1(0)$ is proportional to the reduced temperature τ, and l_0 is some constant. In the hydrodynamic region $q \ll p \ll \xi^{-1}$ the relaxation coefficient implied by the latter result is

$$\Gamma \propto \tau(|\ln \tau| + \text{constant})^{-1/3}. \tag{5.22}$$

This result has also been found by Maleev (1976) using mode-coupling arguments. A detailed theoretical study of the dynamics of uniaxial dipolar ferromagnets, which not only takes into account the relaxational dynamics on the basis of the time-dependent Ginzburg–Landau model but also includes nonlinear terms resulting from the Larmor precession in the local magnetic field is still lacking. A mode-coupling analysis of this problem is in progress (S. Henneberger, E. Frey and F. Schwabl 1995, unpublished).

5.3. Two-dimensional systems

2D systems are interesting, because matter behaves qualitatively different compared with its behaviour in three dimensions. We recall that the Bloch (1930) argument (Peierls 1936, Landau 1937), which is proven on a rigorous basis by the theorem of Hohenberg (1967), Mermin and Wagner (1966), excludes conventional long-range order in isotropic systems with a continuous symmetry and short-range interaction such as the Heisenberg ferromagnet, superfluid helium films and 2D crystals (Nelson 1983). Any hypothetical broken continuous magnetic or translational symmetry would be overwhelmed by long-wavelength spin or phonon excitations, since the phase space for these Goldstone-like modes is enhanced in two dimensions. Two dimensions seem to be the borderline dimension where thermal fluctuations are just strong enough to prevent the appearance of a finite order parameter.

However, since the dipolar forces reduce the fluctuations longitudinal to the wave-vector, related to the anisotropy of the dipolar interaction with respect to the separation of two spins one expects that a finite order parameter could exist in 2D isotropic systems. In fact we shall review this in the following spin-wave theories, which show that the dipolar interaction leads to the existence of long-range order in 2D ferromagnets and antiferromagnets and other systems which belong to the same universality class.

5.3.1. Ferromagnets

The possibility of a finite order parameter in 2D ferromagnets was shown first by Maleev (1976), who evaluated the low-temperature properties, and in particular the magnon excitation spectrum for Heisenberg ferromagnets in the presence of dipolar forces. Linear spin-wave theory (Maleev 1976) results in a magnon dispersion relation

$$E_{\mathbf{k}} = [(Dk^2 + \Omega_0\alpha)(Dk^2 + \Omega_0 ka \sin \varphi_{\mathbf{k}})]^{1/2}, \qquad (5.23)$$

where $Dk^2 = 2S(J_0 - J_{\mathbf{k}})$ at $ka \ll 1$, $\Omega_0 = 2\pi S(g_L\mu_B)^2/v_2 a \ll 2SJ_0$, $\alpha = SA_0/\Omega_0 \approx 1$, and $\varphi_{\mathbf{k}}$ is the angle between the wave-vector $\mathbf{k}$ and the magnetization $\mathbf{M}$. At sufficiently small k (and for $\mathbf{k}$ not parallel to the magnetization) the energy of the spin waves has the form

$$E_{\mathbf{k}} \propto \Omega_0|\sin \varphi_{\mathbf{k}}|k^{1/2}. \qquad (5.24)$$

An analysis of the relative deviations of the magnetization from saturation (in the framework of linear spin-wave theory) results in an order-of-magnitude estimate for the transition temperature (for small dipolar couplings):

$$T_C \propto \frac{2J_0 S^2}{\ln (2J_0 S/\Omega_0)}. \qquad (5.25)$$

It was also shown (Herring and Kittel 1951, Döring 1961, Bander and Mills 1988) that exchange anisotropy leads to a suppression of thermal interaction and in turn to the existence of long-range order in 2D ferromagnets.

In 2D ferromagnets, the dipolar interaction results in easy-plane anisotropy (Maleev 1976, Pokrovsky and Feigelman 1979). This is because the dipolar energy is minimized when all spins are aligned in plane. Thus the problem of the three-component Heisenberg ferromagnet with dipolar interaction is reduced to the problem of a two-component (planar) ferromagnet with renormalized values of the temperature and of the dipole–dipole interaction constant. The magnetic dipolar forces change fundamentally the nature of the low-temperature phase. This can be seen as follows. In the absence of dipolar interaction any long-range order is impossible since it becomes

destroyed by thermal fluctuations; the mean square of the spin fluctuations is given by $\langle |\delta S_{\mathbf{q}}|^2 \rangle \propto k_B T/q^2$. A planar (pure) exchange ferromagnet would undergo a Kosterlitz–Thouless (1972, 1973) transition. The Kosterlitz–Thouless phase is characterized by local but no long-range order and by bound vortex pairs. There is a divergent susceptibility throughout this phase. However, owing to the dipolar interaction the spectrum of the spin fluctuations at small wavenumbers is changed. Including the dipolar interaction (equation (5.7)), one obtains the following reduced Hamiltonian:

$$\mathscr{H} = -\frac{H}{k_B T} = -\frac{JS^2}{k_B T} v_2 a^2 \int \frac{d^2 q}{(2\pi)^2} \left[\left(q^2 - g_2 \frac{q_y^2}{|\mathbf{q}|} \right) \phi_{\mathbf{q}} \phi_{-\mathbf{q}} + O(\phi^3) \right] \quad (5.26)$$

in terms of the azimuthal angle ϕ, where we have assumed a fixed length $|\mathbf{S}|^2 = 1$ and an ordering along the $\hat{\mathbf{x}}$ direction. The relative strength of the dipolar interaction in two dimensions is characterized by the parameter $g_2 = A^{(1)}/Ja^2$. In the derivation of equation (5.26) the in plane components of the dipolar interaction tensor have been used (Pelcovits and Halperin 1979): $A_{\mathbf{q}}^{\alpha\beta} = (A^{(0)}/3)\delta^{\alpha\beta} - A^{(1)}(q^\alpha q^\beta/q) + O(q^2)$ (A^0 and $A^{(1)}$; see equations (5.8) and (5·9)). Neglecting all but the terms quadratic in $\phi_{\mathbf{q}}$, the mean square fluctuations about the local ordering are given by (Pelcovits and Halperin 1979):

$$\langle \phi^2 \rangle \propto \frac{k_B T}{J} \int \frac{d^2 q}{(2\pi)^2} \frac{1}{q^2 + g_2 |\mathbf{q}| \sin^2 \varphi_{\mathbf{q}}}, \quad (5.27)$$

where $\varphi_{\mathbf{q}}$ is the angle between $\mathbf{q}$ and the total magnetization. The above integral no longer diverges owing to the presence of the dipolar interaction. Hence the dipolar interaction stabilizes ferromagnetic long-range order in more than one dimension (Maleev 1976, Pokrovsky and Feigelman 1977). Besides stabilizing the long-range order, the dipolar forces alter the vortex behaviour (Pelcovits and Halperin 1979). Pelcovits and Halperin (1979) also carried out an analysis of the static critical behaviour. More recently the critical behaviour has been reanalysed by De'Bell and Geldart (1989). In passing we note that there are two reviews on excitations in low-dimensional systems by Pokrovsky (1979) and by Pokrovsky *et al.* (1988).

In fact the situation is more complicated in thin magnetic films. Single-layer and two-layer iron orders perpendicular to the planes for $T = 0\,\mathrm{K}$; only for layer numbers above three the expected parallel orientation is observed (see for example the review article by Allensbach (1978)). This comes from the spin–orbit interaction, which effectively leads to a perpendicular anisotropy, which overcomes the dipolar interaction for the very thinnest layers. Upon raising the temperature a reorientation phase transition (Pappas *et al.* 1990) from a perpendicular to an in-plane orientation of the magnetization has been observed experimentally. It was argued by Pescia and Pokrovsky (1990, 1993) that this transition is driven by the competition between spin–orbit and dipolar interaction. The (classical) transition temperature has been estimated (Pescia and Pokrovsky 1993, Politi *et al.* 1993) to be of the order $T_R \approx (\lambda - \Omega)4cJa^3/7(g_L\mu_B)^2$, where c is the number of nearest neighbours, $\Omega = 2\pi(g_L\mu_B S)^2/a^3$ characterizes the strength of the dipolar interaction, and λ is the single-ion anisotropy constant favouring perpendicular orientation. Since the single-ion and the dipolar anisotropy parameters scale the same under a renormalization group transformation (Pescia and Pokrovsky 1993, Politi *et al.* 1993), it depends on the relative values of the single-ion anisotropy and the dipolar parameters, whether the transition temperature for the reorientation phase transition is smaller or larger than the Curie temperature. However, since the dipolar interaction parameter increases with the number of layers, the value of T_R is reduced for thicker films, as indeed observed
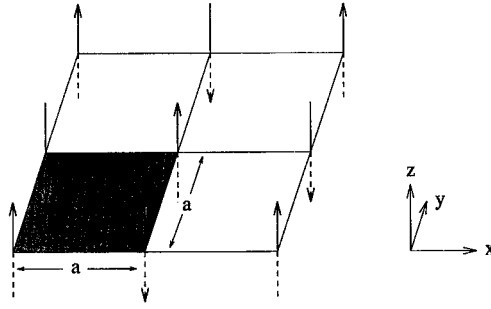
Figure 5.3.   Classical ground state of a 2D dipolar antiferromagnet with a dipolar interaction
much smaller than the exchange interaction on a quadratic lattice. (From Pich (1994).)

experimentally (Pappas *et al.* 1990). Some of the above theoretical work is still rather
controversial (Levanyuk and Garcia 1992). Owing to the combination of various
anisotropies, dipole–dipole interaction, reduced dimensionality and enhanced
importance of thermal fluctuations the phase diagram of thin magnetic films shows a
variety of new and interesting phases (Pappas *et al.* 1990, Allensbach and Bischof 1992;
Allensbach 1994) with properties still awaiting a theoretical explanation.

5.3.2. *Antiferromagnets*

Recently it has been shown (Pich and Schwabl 1993) that long-range order is also
possible in 2D antiferromagnets owing to the anisotropy of the dipolar interaction.
The existence of the long-range order is a consequence of a subtle interplay between
exchange and dipolar interaction. The classical ground state of an isotropic pure
exchange antiferromagnet has a continuous degeneracy and hence no long-range order.
The dipolar interaction lifts the continuous degeneracy of the ground state such that a
spin alignment perpendicular to the plane is energetically favoured (figure 5.3). In other
words, whereas the exchange interaction imposes antiferromagnetic order, the dipolar
interaction prevents thermal fluctuations from its destruction. This can be seen easily
by considering the equations of motion at zero wave-vector. Upon approximating the
longitudinal spin components by their equilibrium expectation value $S_l^z \approx S \exp(i\mathbf{q}_0 \cdot \mathbf{x}_l)$
the linearized form of equation (5.10) (see section 5.1) is

$$\frac{d}{dt} S_0^x = 2S (A_{\mathbf{q}_0}^{zz} - A_{\mathbf{q}_0}^{yy}) S_{\mathbf{q}_0}^y, \tag{5.28}$$

$$\frac{d}{dt} S_{\mathbf{q}_0}^y = 2S [(J_{\mathbf{q}_0} - J_0) + (A_{\mathbf{q}_0}^{zz} - A_0^{xx})] S_0^x, \tag{5.29}$$

and an analogous set of equations for S_0^y and $S_{\mathbf{q}_0}^x$. The wave-vector $\mathbf{q}_0 = (\pi/a)(1, 1, 0)$
characterizes the antiferromagnetic staggered modulation of the ground state. The
coefficient on the right hand side of equation (5.28) is non-zero owing to the anisotropy
of the dipolar interaction in two dimensions. The resulting energy gap at zero
wave-vector then is

$$E_0 = 2S(A_{\mathbf{q}_0}^{zz} - A_{\mathbf{q}_0}^{xx})^{1/2}[(J_{\mathbf{q}_0} - J_0) - (A_0^{xx} - A_{\mathbf{q}_0}^{zz})]^{1/2}. \tag{5.30}$$

More detailed information on the spin-wave spectrum can be obtained by linear
spin-wave theory (Pich and Schwabl 1993). Introducing Bose operators by a

Holstein–Primakoff transformation (Keffer 1966), given here only up to harmonic terms by

$$S_l^x = \left(\frac{S}{2}\right)^{1/2}(a_l + a_l^\dagger), \quad S_l^y = \mp i\left(\frac{S}{2}\right)^{1/2}(a_l - a_l^\dagger), \quad S_l^z = \pm(S - a_l^\dagger a_l), \quad (5.31)$$

where the upper (lower) signs refers to the first (second) sublattice, the Hamiltonian in the harmonic approximation is given by

$$H = \sum_{\mathbf{q}} [A_{\mathbf{q}} a_{\mathbf{q}}^\dagger a_{\mathbf{q}} + \tfrac{1}{2} B_{\mathbf{q}}(a_{\mathbf{q}} a_{-\mathbf{q}} + a_{\mathbf{q}}^\dagger a_{-\mathbf{q}}^\dagger)$$

$$+ C_{\mathbf{q}} a_{\mathbf{q}} a_{-\mathbf{q}-\mathbf{q}_0} + C_{\mathbf{q}}^* a_{\mathbf{q}}^\dagger a_{-\mathbf{q}-\mathbf{q}_0}^\dagger + C_{\mathbf{q}} a_{\mathbf{q}}^\dagger a_{\mathbf{q}+\mathbf{q}_0} + C_{\mathbf{q}}^* a_{\mathbf{q}+\mathbf{q}_0}^\dagger a_{\mathbf{q}}] \quad (5.32)$$

with the coefficients

$$A_{\mathbf{q}} = S(2J_{\mathbf{q}_0} - J_{\mathbf{q}} - J_{\mathbf{q}+\mathbf{q}_0}) + S(2A_{\mathbf{q}_0}^{zz} - A_{\mathbf{q}}^{xx} - A_{\mathbf{q}+\mathbf{q}_0}^{yy}), \quad (5.33\,a)$$

$$B_{\mathbf{q}} = S(J_{\mathbf{q}+\mathbf{q}_0} - J_{\mathbf{q}}) + S(A_{\mathbf{q}+\mathbf{q}_0}^{yy} - A_{\mathbf{q}}^{xx}), \quad (5.33\,b)$$

$$C_{\mathbf{q}} = iSA_{\mathbf{q}}^{xy}. \quad (5.33\,c)$$

In this description the primitive cell is the crystallographic cell, which is half the magnetic cell. Diagonalization of the Hamiltonian, achieved by a Bogoliubov transformation, results in a spin-wave spectrum with two branches:

$$E_{\mathbf{q}}^i = [\tfrac{1}{2}(\Omega_1 \pm \Omega_2)]^{1/2}, \quad (5.34)$$

where

$$\Omega_1 = A_{\mathbf{q}}^2 - B_{\mathbf{q}}^2 + A_{\mathbf{q}+\mathbf{q}_0}^2 - B_{\mathbf{q}+\mathbf{q}_0}^2 + 8C_{\mathbf{q}}C_{\mathbf{q}+\mathbf{q}_0}$$

and

$$\Omega_2^2 = (A_{\mathbf{q}}^2 - B_{\mathbf{q}}^2 - A_{\mathbf{q}+\mathbf{q}_0}^2 + B_{\mathbf{q}+\mathbf{q}_0}^2)^2 + 16[C_{\mathbf{q}+\mathbf{q}_0}(A_{\mathbf{q}+\mathbf{q}_0} - B_{\mathbf{q}+\mathbf{q}_0})$$

$$- C_{\mathbf{q}}(A_{\mathbf{q}} - B_{\mathbf{q}})][C_{\mathbf{q}}(A_{\mathbf{q}} + B_{\mathbf{q}}) - C_{\mathbf{q}+\mathbf{q}_0}(A_{\mathbf{q}} + B_{\mathbf{q}})].$$

In figure 5.4 the dispersion relation is shown for three values for the ratio of dipolar and exchange energy $\kappa = (g\mu_B)^2/4|J|a^3$ with isotropic nearest-neighbour exchange interaction $(J < 0)$. The two branches can be resolved only for large values of κ.

In particular the gap is proportional to the square root of the difference of the magnetostatic energy between the configurations of in-plane and out-of-plane magnetization. In a 3D s.c. lattice the first root in equation (5.30) vanishes because of the symmetry, but in 2D systems there is a finite gap for perpendicular antiferromagnetic order. We note that for sufficiently large exchange energy the gap is the geometric mean of dipole and exchange energy, which in turn implies that the gap is much larger than the dipolar energy for $\kappa \ll 1$.

The Néel temperature T_N has been determined via a high-temperature expansion, by employing Callen's method (Pich and Schwabl 1993, 1994, Pich 1994). If the dipolar interaction is weak in comparison with the exchange interaction, one can give an order-of-magnitude estimate for the transition temperature in the framework of linear spin-wave theory based on the Holstein–Primakoff transformation.

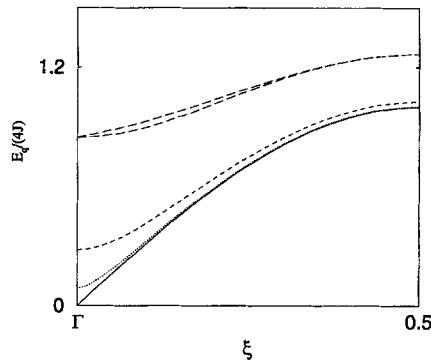$$T_N \propto \frac{|J|}{\ln(|J|/E_0)}. \quad (5.35)$$

Figure 5.4.   The spin-wave dispersion relation (equation (5.34)) of pure exchange antiferromag-
nets on a quadratic lattice with nearest-neighbour interaction (———) and with additional
dipolar interaction $(S = \frac{1}{2})$, for the ratios of dipolar energy to exchange energy
$\kappa = (g\mu_B)^2/4|J|a^3$ along the $(\pi/a)[\xi, \xi, 0]$ direction: $\kappa = 0\cdot1$ (— — —), $\kappa = 0\cdot01$ (- - - - -)
and $\kappa = 0\cdot001$ (······). The splitting of the two magnon branches is visible only for $\kappa = 0\cdot1$.

Table 11.   Exchange energy $|J|$, lattice constant a, energy gap E_0, Néel temperature T_N and
zero-temperature order parameter σ_0.

	$|J|$ (K)	a (Å)	E_0^{exp} (K)	E_0^σ (K)	E_0 (K)	T_N^{exp} (K)	T_N^{th} (K)	σ_0 r
K_2MnF_4	8·5[a]	4·17[a]	7·4[b]	7·1	7·6	42[a]	41	2·33
Rb_2MnF_4	7·4[c]	4·20[d]	7·3[b]	6·5	7·0	38[d]	36	2·33
Rb_2MnCl_4	11·2[e]	5·05[f]	7·5[e]	6·1	6·6	56[e]	48	2·32
$(CH_3NH_3)_2MnCl_4$	9·0	5·13[f]		5·3	5·7	45[e]	39	2·32

[a] From Birgeneau et al. (1973).
[b] From De Wijn et al. (1973a).
[c] From De Wijn et al. (1973b).
[d] From Birgeneau et al. (1970).
[e] From Schröder et al. (1980).
[f] From Hellwege (1976).

This, however, gives an overestimate for the transition temperature, because it uses a
temperature-independent dispersion relation. In fact, the magnon frequency softens
with increasing temperature. Those effects have been accounted for by Pich and
Schwabl (1994) by an extension of the Tyablikov decoupling scheme due to Callen
(1963). In essence this leads to a replacement of the saturation magnetization of the spins
S by the temperature-dependent order parameter σ. The resulting transition temperature
is lowered with respect to the estimate from linear spin-wave theory. E_0 has been
obtained by linear spin-wave theory, and E_0^σ and T_N^{th} by the method of Callen. The
results are summarized in table 11 and show quite satisfactory agreement with
experimental data. This theory has been extended to antiferromagnets on a honeycomb
(Pich and Schwabl 1995) and several other lattices (C. Pich and F. Schwabl 1995,
unpublished).

6. Stochastic theory

6.1. *Classical field theory and dynamical functional*

If one tries to describe the critical dynamics of ferromagnets, one is in general not interested in the complete, highly complicated microscopic time evolution. Rather, one is usually interested in the dynamics on time scales characteristic of its slowly varying dynamical quantities, such as those associated with hydrodynamic, order parameter or Goldstone modes.

A method to extract from the microscopic dynamics the equations of motion appropriate to these slowly varying quantities is the projection operator formalism of Zwanzig (1961) and Mori (1965). Since the semiphenomenological equations derived from this formalism form a common basis of mode-coupling and dynamic renormalization group theories, we briefly review the main ideas and results of this approach.

The idea is to eliminate the fast variables by introducing a projection operator $\mathscr{P}$, which projects on to the subspace of slowly varying modes. Descriptions of this formalism can be found in the papers by Kawasaki (1973) and Mori and Fujisaka (1973). A short account is given in appendix 2. After having chosen an appropriate set of slow variables (which is crucial for the validity of the dynamics), one can derive formally exact nonlinear equations of motion for these modes (here these modes are denoted by $\{S_\alpha(t)\}$):

$$\frac{\mathrm{d}}{\mathrm{d}t} S_\alpha(t) = v_\alpha(\{S(t)\})$$

$$+ \sum_\beta \int_0^t \mathrm{d}\tau \, P_{\mathrm{eq}}^{-1}(\{S(t-\tau)\}) \frac{\partial M_{\alpha\beta}(\tau; \{S(t-\tau)\}) P_{\mathrm{eq}}(\{S(t-\tau)\})}{\partial S_\beta^*(t-\tau)} + \zeta_\alpha(t), \quad (6.1)$$

where

$$P_{\mathrm{eq}}(\{S\}) = \exp\left(-\frac{1}{k_\mathrm{B}T} \mathscr{H}(\{S\})\right) \tag{6.2}$$

is the equilibrium probability function. The first term in these equations,

$$v_\alpha(\{S(t)\}) = \langle \mathrm{i}\mathscr{L}S_\alpha; \{S(t)\}\rangle, \tag{6.3}$$

is called the streaming term and describes the systematic part of the driving forces. This term can be expressed in terms of Poisson brackets. (The conditional average $\langle X; \{a\}\rangle$ is defined by $\langle X; \{a\}\rangle = \langle X\delta(S-a)\rangle/P_{\mathrm{eq}}(\{S(t)\}$ where the average is taken in the microcanonical ensemble (Kawasaki 1976)). The second term contains the memory kernel

$$M_{\alpha\beta}(t; \{S(t)\}) = \langle \zeta_\alpha(t)\zeta_\beta^*(0); \{S(t)\}\rangle \tag{6.4}$$

and characterizes the damping of this adiabatic motion by frictional effects arising from the 'random' forces. The 'random' forces are given in terms of the projection operator $\mathbb{Q} = 1 - \mathscr{P}$ and the Liouville operator $\mathscr{L}$:

$$\zeta_\alpha(t) = \exp\left[\mathrm{i}t\mathbb{Q}\mathscr{L}\right]\mathrm{i}\mathbb{Q}\mathscr{L}S. \tag{6.5}$$

Whether this force can be regarded as random or not depends crucially on the choice of the projection operator, that is whether $\mathscr{P}$ contains all the slowly varying quantities of the system under consideration.

The semiphenomenological equations of motion are obtained from the above exact equations by making the following basic and at least plausible assumptions. Firstly one

assumes that one can neglect memory effects in $M_{\alpha\beta}$ and makes the Markovian approximation

$$M_{\alpha\beta}(t; \{S(t)\}) \approx 2L_{\alpha\beta}(\{S(t)\})\delta(t). \tag{6.6}$$

Secondly one takes the kinetic coefficients to be independent of the slow variables:

$$L_{\alpha\beta}(\{a\}) \approx L_{\alpha\beta}. \tag{6.7}$$

Thirdly one assumes that all slowly varying variables are contained in the choice of the projection operator so that the forces f_α are really random and have a Gaussian probability distribution

$$w(\{\zeta\}|t_0 \leqslant t \leqslant t_1) \sim \exp\left(-\frac{1}{4}\int_{t_0}^{t_1} \mathrm{d}t\, \zeta_\alpha(t)L_{\alpha\beta}^{-1}\zeta_\beta(t)\right). \tag{6.8}$$

Then the exact equations reduce to the following semiphenomenological equations of Langevin form:

$$\frac{\mathrm{d}}{\mathrm{d}t}S_\alpha(t) = v_\alpha(\{S(t)\}) - \sum_\beta L_{\alpha\beta}^0 \frac{\delta\mathscr{H}(\{S(t)\})}{\delta S_\beta^*(t)} + \zeta_\alpha(t), \tag{6.9}$$

where the streaming term

$$v_\alpha(\{S(t)\}) = -\lambda f \sum_\beta \left[\frac{\delta}{\delta S_\beta}Q_{\alpha\beta}(\{S\}) - Q_{\alpha\beta}(\{S\})\frac{\delta\mathscr{H}(\{S\})}{\delta S_\beta(t)}\right] \tag{6.10}$$

can be expressed in terms of Poisson brackets:

$$Q_{\alpha\beta}(\{S\}) = \{S_\alpha, S_\beta\}_P = -Q_{\beta\alpha}(\{S\}). \tag{6.11}$$

The equilibrium distribution does not determine the driving force in the Langevin equations uniquely. Only the dissipative couplings which are generated by the derivative of the effective Hamiltonian $\mathscr{H}$ are related to the static properties of the system. As a direct consequence, with each static universality class are associated several dynamic universality classes depending on the structure of the Poisson brackets.

After these general preliminaries we can now start to set up a stochastic equation of motion for the dynamics of dipolar ferromagnets. If the interaction between the spins in an isotropic Heisenberg ferromagnet is solely given by the short-range exchange interaction, the dynamics are described by precession of the spins in a local magnetic field generated by the surrounding spins. The rotation invariance of the Heisenberg Hamiltonian implies that the total spin is conserved. As shown explicitly in section 3.1, this is no longer the case if one takes into account the long-range dipole–dipole interaction. Hence the spin dynamics of an isotropic dipolar ferromagnet are described by the following semiphenomenological Langevin equations:

$$\frac{\partial \mathbf{S}(\mathbf{x},t)}{\partial t} = \lambda f \mathbf{S}(\mathbf{x},t) \times \frac{\delta\mathscr{H}([S])}{\delta\mathbf{S}(\mathbf{x},t)} - \hat{L}\frac{\delta\mathscr{H}([S])}{\delta\mathbf{S}(\mathbf{x},t)} + \zeta(\mathbf{x},t), \tag{6.12}$$

where $\mathbf{S}(\mathbf{x},t)$ is the local spin density. The local magnetic field is determined by the functional derivative of the Landau–Ginzburg functional $\mathscr{H}[S]$ with respect to the spin density. For the present case the Landau–Ginzburg functional is given by

$$\mathscr{H}[S] = -\frac{1}{2}\int_\mathbf{q}\left((r+q^2)\delta^{\alpha\beta} + g\frac{q^\alpha q^\beta}{q^2}\right)S^\alpha(\mathbf{q})S^\beta(-\mathbf{q})$$

$$-\frac{u}{4!} \int_{\mathbf{q}_1} \int_{\mathbf{q}_2} \int_{\mathbf{q}_3} S^\alpha(\mathbf{q}_1) S^\alpha(\mathbf{q}_2) S^\beta(\mathbf{q}_3) S^\beta(-\mathbf{q}_1 - \mathbf{q}_2 - \mathbf{q}_3). \tag{6.13}$$

$S^\alpha(\mathbf{q})$ $(\alpha = 1, 2, \dots, n$ are the components of the bare spin variable with n equal to the space dimensionality d. We further used the abbreviation $\int_{\mathbf{q}} = \int d^d q/(2\pi)^d$, r is the reduced temperature-deviation and g denotes the relative strength of the dipolar interaction.

The dipolar interaction in equation (6.13) breaks the symmetry of the spin fluctuations transverse and longitudinal to the wave-vector $\mathbf{q}$, which is reflected in the free propagator

$$G^{\alpha\beta} = \frac{q^\alpha q^\beta}{q^2} G^L + \left(\delta^{\alpha\beta} - \frac{q^\alpha q^\beta}{q^2} \right) G^T, \tag{6.14}$$

where $G^L(r, g, q) = (r + g + q^2)^{-1}$ and $G^T(r, q) = (r + q^2)^{-1}$.

The time scale is characterized by the quantity λ. The mode-coupling coefficient f determines the strength of the coupling of the spin density to the local magnetic field. Since the order parameter is a non-conserved quantity, the leading term in the Onsager operator

$$\hat{L} = \lambda(\gamma - \nabla^2) \tag{6.15}$$

is wave-vector independent, $\lambda\gamma$, and not $-\lambda\nabla^2$ as for a conserved order parameter. The quantity γ characterizes, like g in statics, the relative strength of the dipolar interaction. The random forces $\zeta(\mathbf{x}, t)$ have a Gaussian probability distribution:

$$w_\zeta([\zeta_i(\mathbf{x}, t)]|t_0 \leqslant t \leqslant t_1) \sim \exp\left(-\frac{1}{4} \sum_i \int_{t_0}^{t_1} dt \int d^d x\, \zeta_i(\mathbf{x}, t) \hat{L}^{-1} \zeta_i(\mathbf{x}, t) \right), \tag{6.16}$$

which is uniquely determined by the lowest moments

$$\langle \zeta(\mathbf{x}, t) \rangle = 0, \tag{6.17a}$$

$$\langle \zeta_i(\mathbf{x}, t) \zeta_j(\mathbf{x}', t') \rangle = 2\hat{L}\delta(\mathbf{x} - \mathbf{x}')\delta(t - t')\delta_{ij}. \tag{6.17b}$$

Note that we have set $\beta = 1/k_B T = 1$.

In particular for the implementation of the dynamic renormalization group theory in a way analogous to static critical phenomena it is convenient to introduce a functional which generates the perturbation expansion for the frequency dependent correlation and response functions, which is equivalent to the equations of motion. We shall use the functional integral formulation (Bausch *et al.* 1976, Janssen 1976, de Dominicis and Peliti 1977, 1978), which converts the Langevin equation into a dynamic functional with one additional field (Martin *et al.* 1973). The idea is that, instead of solving the Langevin equations (6.12) for the stochastic spin fields $\mathbf{S}(\mathbf{k}, t)$ in terms of the random forces $\zeta(\mathbf{k}, t)$ and then averaging over the Gaussian weight, one can eliminate the random forces in favour of the spin variables by introducing a path probability density $W(\{s\})$ via

$$W(\{S\})\mathcal{D}[S] = w(\{\zeta\})\mathcal{D}[\zeta]. \tag{6.18}$$

Furthermore, it is convenient to perform a Gaussian transformation in order to 'linearize' the dynamic functional. This is accomplished by introducing response fields $\tilde{S}$ (Martin *et al.* 1973, Janssen 1976) by

$$W(\{S\}) = \int \mathcal{D}[i\tilde{S}] \exp\{\mathscr{J}[S, \tilde{S}]\}. \tag{6.19}$$

For more details on the general formalism we refer the reader to the papers by Martin *et al.* (1973), Bausch *et al.* (1976), de Dominicis (1976) and Janssen (1976). The generating functional for the correlation functions is

$$Z[h, \tilde{h}] = \frac{1}{\mathcal{N}} \int \mathscr{D}[S] \mathscr{D}[i\tilde{S}] \exp\left[\mathscr{J}_{t_0}^{t_1}[S, \tilde{S}] + \sum_i \int d^d x \int_{t_0}^{t_1} dt \, (h_i S_i + \tilde{h}_i \tilde{S}_i) \right], \quad (6.20)$$

where the normalization factor $\mathcal{N}$ is chosen such that $Z[h = 0, \tilde{h} = 0] = 1$. The symbols $\mathscr{D}[S]$ and $\mathscr{D}[i\tilde{S}]$ denote functional measures of the path integral. The Janssen–Dominicis functional is given by

$$\mathscr{J}_{t_0}^{t_1}[S, \tilde{S}] = \sum_i \int_{t_0}^{t_1} dt \int d^d x \left[\tilde{S}_i \hat{L} \tilde{S}_i - \tilde{S}_i \left(\frac{\partial S_i}{\partial t} - K_i[S] \right) - \frac{1}{2} \frac{\delta K_i[S]}{\delta S_i} \right], \quad (6.21)$$

where the functional of the forces is

$$\mathbf{K}[S] = \lambda f \mathbf{S}(\mathbf{x}, t) \times \frac{\delta \mathscr{H}([S])}{\delta \mathbf{S}(\mathbf{x}, t)} - \hat{L} \frac{\delta \mathscr{H}([S])}{\delta \mathbf{S}(\mathbf{x}, t)}. \quad (6.22)$$

In formulating the perturbation theory one splits the functional, equations (6.21) and (6.22), into a harmonic part

$$\mathscr{J}_{\text{harm}}[S, \tilde{S}] = \int_{\mathbf{k}} \int_\omega [\lambda(\gamma + k^2) \tilde{S}^\alpha(\mathbf{k}, \omega) \tilde{S}^\alpha(-\mathbf{k}, -\omega)$$
$$- \tilde{S}^\alpha(\mathbf{k}, \omega)[i\omega \delta^{\alpha\beta} + \lambda(\gamma + k^2) G^{\alpha\beta}(r, g, \mathbf{k})^{-1}] S^\alpha(-\mathbf{k}, -\omega)], \quad (6.23)$$

which is bilinear in the stochastic spin fields S and $\tilde{S}$ and a part $\mathscr{J}_{\text{int}}[S, \tilde{S}]$ containing the interaction terms. Here $G^{\alpha\beta}(r, g, \mathbf{k})$ denotes the static propagator, equation (6.14). Furthermore we have introduced the short-hand notations $\int_{\mathbf{k}} = \int d^d k/(2\pi)^d$, $\int_\omega = \int d\omega/2\pi$. The Fourier transform of the spin density is defined by $\mathbf{S}(\mathbf{x}, t) = \int_{\mathbf{k}} \int_\omega \mathbf{S}(\mathbf{k}, \omega) \exp[i(\mathbf{k} \cdot \mathbf{x} - \omega t)]$. Hence the generating functional can be written as

$$Z[h, \tilde{h}] = \frac{1}{\mathcal{N}} \exp\left[\mathscr{J}_{\text{int}} \left(\frac{\delta}{\delta h}, \frac{\delta}{\delta \tilde{h}} \right) \right]$$
$$\times \int \mathscr{D}[S] \mathscr{D}[i\tilde{S}] \exp\left(\mathscr{J}_{\text{harm}}[S, \tilde{S}] + \sum_i \int d^d x \int_{t_0}^{t_1} dt \, (h_i S_i + \tilde{h}_i \tilde{S}_i) \right). \quad (6.24)$$

We start with the discussion of the harmonic part, equation (6.23). It can be written in matrix notation as

$$\mathscr{J}_{\text{harm}}[S, \tilde{S}] = -\frac{1}{2} \int_{\mathbf{k}} \int_\omega (\tilde{S}^\alpha(\mathbf{k}, \omega), S^\alpha(\mathbf{k}, \omega)) \mathbf{A}^{\alpha\beta}(\mathbf{k}, \omega) (\tilde{S}^\beta(-\mathbf{k}, -\omega), S^\beta(-\mathbf{k}, -\omega))^{\mathrm{T}}.$$
$$(6.25)$$

The matrix $\mathbf{A}^{\alpha\beta}(\mathbf{k}, \omega)$ is given by

$$\mathbf{A}^{\alpha\beta}(\mathbf{k}, \omega) = \begin{pmatrix} -2L(k) & i\omega - A^{\alpha\beta}(\mathbf{k}) \\ -i\omega - A^{\alpha\beta}(\mathbf{k}) & 0 \end{pmatrix}, \quad (6.26)$$

where we have defined

$$A^{\alpha\beta}(\mathbf{k}) = -L(k)[G^{\alpha\beta}(r, g, \mathbf{k})]^{-1}, \quad (6.27)$$

$$L(k) = \lambda(\gamma + k^2). \quad (6.28)$$

The harmonic part of the partition function

$$Z_0[h, \tilde{h}] = \int \mathscr{D}[S]\mathscr{D}[i\tilde{S}] \exp\left(\mathscr{J}_{\text{harm}}[S, \tilde{S}] + \sum_i \int d^d x \int_{t_0}^{t_1} dt\,(h_i S_i + \tilde{h}_i \tilde{S}_i)\right) \qquad (6.29)$$

can be calculated explicitly with the result that

$$Z_0[h, \tilde{h}] = \exp\left[\frac{1}{2}\int_{\mathbf{k}}\int_{\omega} (\tilde{h}^{\alpha}(\mathbf{k}, \omega), h^{\alpha}(\mathbf{k}, \omega))\right.$$

$$\left. \times [\mathbf{A}^{\alpha\beta}(\mathbf{k}, \omega)]^{-1}(\tilde{h}^{\beta}(-\mathbf{k}, -\omega), h^{\beta}(-\mathbf{k}, -\omega))^{\mathrm{T}}\right]. \qquad (6.30)$$

Hence the free propagators are found to be

$$\begin{pmatrix} \langle \tilde{S}^{\alpha}(\mathbf{k}, \omega)\tilde{S}^{\beta}(\mathbf{k}', \omega')\rangle_0 & \langle \tilde{S}^{\alpha}(\mathbf{k}, \omega)S^{\beta}(\mathbf{k}', \omega')\rangle_0 \\ \langle S^{\alpha}(\mathbf{k}, \omega)\tilde{S}^{\beta}(\mathbf{k}', \omega')\rangle_0 & \langle S^{\alpha}(\mathbf{k}, \omega)S^{\beta}(\mathbf{k}', \omega')\rangle_0 \end{pmatrix} = \delta(\omega + \omega')\delta(\mathbf{k} + \mathbf{k}')$$

$$\times [\mathbf{A}^{\alpha\beta}(-\mathbf{k}, -\omega)]^{-1}, \qquad (6.31)$$

where

$$[\mathbf{A}^{\alpha\beta}(\mathbf{k}, \omega)]^{-1} = \mathbf{A}_{\mathrm{L}}^{-1}(\mathbf{k}, \omega)P_{\mathrm{L}}^{\alpha\beta}(\mathbf{k}) + \mathbf{A}_{\mathrm{T}}^{-1}(\mathbf{k}, \omega)P_{\mathrm{T}}^{\alpha\beta}(\mathbf{k}). \qquad (6.32)$$

Hence the longitudinal and transverse propagators are given by

$$\mathbf{A}_{\alpha}^{-1}(\mathbf{k}, \omega) = \begin{pmatrix} 0 & 1/[-i\omega - A_{\alpha}(k)] \\ 1/[i\omega - A_{\alpha}(k)] & 2L(k)/[\omega^2 + A_{\alpha}(k)^2] \end{pmatrix}, \qquad (6.33)$$

where

$$A_{\mathrm{L,T}}(k) = -L(k)\begin{cases} r + k^2, \\ r + g + k^2, \end{cases} \quad \text{for} \begin{cases} \alpha = \mathrm{T}, \\ \alpha = \mathrm{L}. \end{cases} \qquad (6.34)$$

In summary, one gets for the response propagators

$$R^{\alpha\beta}(\mathbf{k}, \omega) = \langle \tilde{S}^{\alpha}(\mathbf{k}, \omega)S^{\beta}(-\mathbf{k}, -\omega)\rangle_0 = R^{\mathrm{T}}(k, \omega)P_{\mathrm{T}}^{\alpha\beta}(\mathbf{k}) + R^{\mathrm{L}}(k, \omega)P_{\mathrm{L}}^{\alpha\beta}(\mathbf{k}), \qquad (6.35)$$

where the transverse and the longitudinal parts are given by

$$R^{\mathrm{L,T}}(k, \omega) \equiv \frac{1}{-i\omega - A_{\mathrm{L,T}}(k)}, \qquad (6.36)$$

and the projection operators are defined by $P_{\mathrm{T}}^{\alpha\beta} = \delta^{\alpha\beta} - q^{\alpha}q^{\beta}/q^2$ and $P_{\mathrm{L}}^{\alpha\beta} = q^{\alpha}q^{\beta}/q^2$. For the correlation propagators, one obtains

$$C^{\alpha\beta}(\mathbf{k}, \omega) = \langle S^{\alpha}(\mathbf{k}, \omega)S^{\beta}(-\mathbf{k}, -\omega)\rangle_0 = C^{\mathrm{T}}(k, \omega)P_{\mathrm{T}}^{\alpha\beta}(\mathbf{k}) + C^{\mathrm{L}}(k, \omega)P_{\mathrm{L}}^{\alpha\beta}(\mathbf{k}), \qquad (6.37)$$

where

$$C^{\mathrm{L,T}}(k, \omega) \equiv \frac{2L(k)}{\omega^2 + A_{\mathrm{L,T}}(k)^2}. \qquad (6.38)$$

The diagrammatic representations are depicted in figure 6.1 (*a*).

The interaction part of the dynamic functional

$$\mathscr{J}_{\text{int}}[S, \tilde{S}] = \mathscr{J}_{\text{MC}}[S, \tilde{S}] + \mathscr{J}_{\text{RE}}[S, \tilde{S}], \qquad (6.39)$$

consists of a mode-coupling vertex $\mathscr{J}_{\text{MC}}[S, \tilde{S}]$, originating from the Larmor term $\mathbf{S} \times \delta\mathscr{H}/\delta\mathbf{S}$ in equation (6.12), and relaxation vertices $\mathscr{J}_{\text{RE}}[S, \tilde{S}]$, originating from the

(a) ⊢⊢⊢⊢⊢⊢

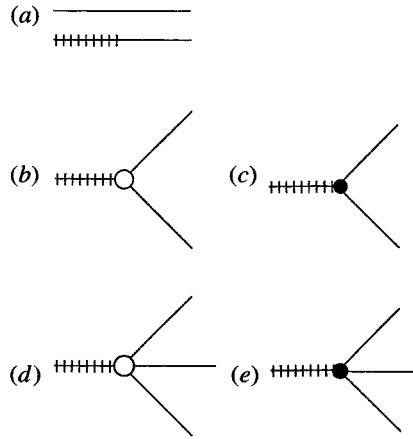(b) ⊢⊢⊢⊢⊢○   (c) ⊢⊢⊢⊢⊢●

(d) ⊢⊢⊢⊢⊢○   (e) ⊢⊢⊢⊢⊢●

Figure 6.1.   Basic elements of the dynamical perturbation theory: (a) correlation and response propagators; (b) isotropic mode-coupling vertex; (c) dipolar mode-coupling vertex; (d) isotropic relaxational vertex; (e) dipolar relaxational vertex.

nonlinear terms $\tilde{L}\delta\mathcal{H}/\delta\mathbf{S}$ of the static Hamiltonian. The mode-coupling vertex is given by

$$\mathcal{J}_{\mathrm{MC}}[S,\tilde{S}] = \lambda f \varepsilon_{\alpha\beta\gamma} \int_{\mathbf{k}} \int_{\omega} \int_{\mathbf{p}} \int_{\nu} \left(\left| \mathbf{p} + \frac{\mathbf{k}}{2} \right|^2 \delta^{\gamma\mu} + g \frac{(p^{\mu} + k^{\mu}/2)(p^{\gamma} + k^{\gamma}/2)}{|\mathbf{p} + \mathbf{k}/2|^2} \right)$$

$$\times \tilde{S}^{\alpha}(\mathbf{k},\omega) S^{\beta}\left(\mathbf{p} - \frac{\mathbf{k}}{2}, \nu - \frac{\omega}{2}\right) S^{\mu}\left(-\mathbf{p} - \frac{\mathbf{k}}{2}, -\nu - \frac{\omega}{2}\right). \quad (6.40)$$

It consists of an isotropic part

$$\mathcal{J}_{\mathrm{MCI}}[S,\tilde{S}] = \lambda f \varepsilon_{\alpha\beta\gamma} \int_{\mathbf{k}} \int_{\omega} \int_{\mathbf{p}} \int_{\nu} (\mathbf{p} \cdot \mathbf{k}) \tilde{S}^{\alpha}(\mathbf{k},\omega) S^{\beta}(\mathbf{p}_-, \nu_-) S^{\gamma}(\mathbf{p}_+, \nu_+) \quad (6.41)$$

and a dipolar part

$$\mathcal{J}_{\mathrm{MCD}}[S,\tilde{S}] = \lambda f g \varepsilon_{\alpha\beta\gamma} \int_{\mathbf{k}} \int_{\omega} \int_{\mathbf{p}} \int_{\nu} \frac{p_+^{\mu} p_+^{\gamma}}{p_+^2} \tilde{S}^{\alpha}(\mathbf{k},\omega) S^{\beta}(\mathbf{p}_-, \nu_-) S^{\mu}(\mathbf{p}_+, \nu_+) \quad (6.42)$$

whose graphical representations are shown in figures 6.1 (b) and (c). We have used the short-hand notations $\mathbf{p}_{\pm} = \mp(\mathbf{p} \pm \mathbf{k}/2)$ and $\nu_{\pm} = \mp(\nu \pm \omega/2)$.

The dipolar mode-coupling vertex can be symmetrized by the substitution $\mathbf{p} \to -\mathbf{p}$ in equation (6.41) leading to

$$\mathcal{J}_{\mathrm{MCD}}[S,\tilde{S}] = \tfrac{1}{2}\lambda f g \varepsilon_{\alpha\beta\gamma} \int_{\mathbf{k}} \int_{\omega} \int_{\mathbf{p}} \int_{\nu} \left(\frac{p_+^{\mu} p_+^{\gamma}}{p_+^2} \tilde{S}^{\alpha}(\mathbf{k},\omega) S^{\beta}(\mathbf{p}_-, \nu_-) S^{\mu}(\mathbf{p}_+, \nu_+) \right.$$

$$\left. - \frac{p_-^{\mu} p_-^{\beta}}{p_-^2} \tilde{S}^{\alpha}(\mathbf{k},\omega) S^{\mu}(\mathbf{p}_-, \nu_-) S^{\gamma}(\mathbf{p}_+, \nu_+) \right). \quad (6.43)$$

The relaxation vertex is given by

$$\mathcal{J}_{\mathrm{RE}}[S,\tilde{S}] = -\frac{u}{3!} F^{\alpha\beta\gamma\delta} \int_{\mathbf{k}_1} \int_{\mathbf{k}_2} \int_{\mathbf{k}_3} \int_{\omega_1} \int_{\omega_2} \int_{\omega_3} \lambda \left(\gamma + \left(\sum_i \mathbf{k}_i \right)^2 \right)$$

$$\times \tilde{S}^{\alpha}\left(\sum_i \mathbf{k}_i, \sum_i \omega_i \right) S^{\beta}(-\mathbf{k}_1, -\omega_1) S^{\gamma}(-\mathbf{k}_2, -\omega_2) S^{\delta}(-\mathbf{k}_3, -\omega_3). \quad (6.44)$$

It contains a diffusive part

$$\mathscr{J}_{\text{diff}}[S, \tilde{S}] = -\frac{u}{3!} \lambda F^{\alpha\beta\gamma\delta} \int_{\mathbf{k}_1} \int_{\mathbf{k}_2} \int_{\mathbf{k}_3} \int_{\omega_1} \int_{\omega_2} \int_{\omega_3} \left(\sum_i \mathbf{k}_i\right)^2 \tilde{S}^\alpha \left(\sum_i \mathbf{k}_i, \sum_i \omega_i\right)$$

$$\times S^\beta(-\mathbf{k}_1, -\omega_1) S^\gamma(-\mathbf{k}_2, -\omega_2) S^\delta(-\mathbf{k}_3, -\omega_3) \qquad (6.45)$$

and a relaxational part

$$\mathscr{J}_{\text{rel}}[S, \tilde{S}] = -\frac{u}{3!} \lambda F^{\alpha\beta\gamma\delta} \int_{\mathbf{k}_1} \int_{\mathbf{k}_2} \int_{\mathbf{k}_3} \int_{\omega_1} \int_{\omega_2} \int_{\omega_3} \gamma \tilde{S}^\alpha \left(\sum_i \mathbf{k}_i, \sum_i \omega_i\right)$$

$$\times S^\beta(-\mathbf{k}_1, -\omega_1) S^\gamma(-\mathbf{k}_2, -\omega_2) S^\delta(-\mathbf{k}_3, -\omega_3), \qquad (6.46)$$

whose diagrammatic representations are given in figures 6.1 (*d*) and (*e*). This decomposition is not important from a technical point of view, since both terms have the same tensorial structure. However, it emphasizes that the relaxational vertices due to the exchange interaction and dipolar interaction are diffusive and relaxational respectively.

With the above perturbation theory at hand, we can now calculate the Green's functions defined by

$$G_{N,\tilde{N}}^{\alpha_1, \dots, \alpha_N, \beta_1, \dots, \beta_{\tilde{N}}}(\mathbf{k}_1, \omega_1; \dots; \mathbf{k}_N, \omega_N; \mathbf{k}_{N+1}, \omega_{N+1}; \dots; \mathbf{k}_{N+\tilde{N}}, \omega_{N+\tilde{N}})$$

$$= \langle S^{\alpha_1}(\mathbf{k}_1, \omega_1) \dots S^{\alpha_N}(\mathbf{k}_N, \omega_N) \tilde{S}^{\beta_1}(\mathbf{k}_{N+1}, \omega_{N+1}) \dots \tilde{S}^{\beta_{\tilde{N}}}(\mathbf{k}_{N+\tilde{N}}, \omega_{N+\tilde{N}}) \rangle$$

$$= \frac{\delta^{N+\tilde{N}}}{\delta h^{\alpha_1}(\mathbf{k}_1, \omega_1) \dots \delta \tilde{h}^{\beta_{\tilde{N}}}(\mathbf{k}_{N+\tilde{N}}, \omega_{N+\tilde{N}})} Z[h, \tilde{h}]\big|_{h, \tilde{h} = 0}. \qquad (6.47)$$

It is convenient to consider the vertex functions

$$\Gamma_{N,\tilde{N}}^{\alpha_1, \dots, \alpha_N, \beta_1, \dots, \beta_{\tilde{N}}}(\mathbf{k}_1, \omega_1; \dots; \mathbf{k}_N, \omega_N; \mathbf{k}_{N+1}, \omega_{N+1}; \dots; \mathbf{k}_{N+\tilde{N}}, \omega_{N+\tilde{N}}), \qquad (6.48)$$

which can be obtained from the cumulants by a Legendre transformation (Bausch *et al.* 1976).

6.2. *Self-consistent one-loop theory*

In the preceding sections we have derived a path integral representation of the dynamics starting from semiphenomenological Langevin equations. Within this method a perturbation theory for the correlation and response functions could be formulated which is similar to the usual field theoretical procedure for static critical phenomena. In each finite order of perturbation theory, infrared divergences arise reflecting the infrared divergences in the second derivatives of the free energy close to a critical point. In order to remove these divergences (which appear combined with the ultraviolet divergences at the upper critical dimension of the model) and to have a perturbation theory with a small parameter, one can use the concepts of renormalized field theories, that is upon introducing renormalization factors and expanding around the upper critical dimension.

Instead we follow here an alternative route, which consists in the resummation of certain classes of diagrams to infinite order in perturbation theory. Such methods are frequently used in condensed-matter physics quite successfully. These methods are characterized by the fact that they lead to self-consistent equations for the correlation functions.
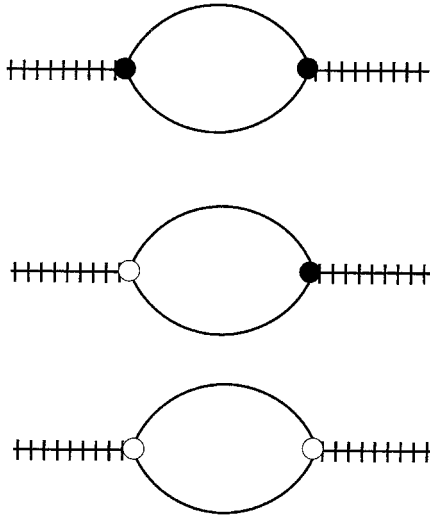
Figure 6.2.   One-loop diagrams for the vertex function $\Gamma_{02}^{\alpha\beta}(\mathbf{q}, \omega)$.

In this section we formulate such a self-consistent procedure for critical dynamics. It will turn out that the resulting equations are equivalent to mode-coupling theory.

6.2.1. *Self-consistent determination of the linewidth in the Lorentzian approximation*

As we have already seen in the discussion of the mode-coupling theory, one can obtain quite reasonable results for the linewidth by assuming that the line shape is given by a Lorentzian. In the above formulation in terms of a dynamical functional the linewidth is given by (Bausch *et al.* 1976)

$$\Gamma_{\text{Lor}}^{\alpha} = -2 \frac{[\Gamma_{11}^{\alpha}(q,0)]^2}{\Gamma_2^{\alpha}(q)\Gamma_{02}^{\alpha}(q,0)}, \tag{6.49}$$

where $\Gamma_2^{\alpha}(q)$ is the inverse static susceptibility ($\alpha = $ L,T). Upon using the fluctuation dissipation theorem

$$\Gamma_{11}^{\alpha}(q,0) = [\lambda(\gamma + q^2) + \lambda f \Gamma_{X,10}^{\alpha}(q,0)]\Gamma_2^{\alpha}(q), \tag{6.50}$$

one obtains to one-loop order $-2\Gamma_{11}^{\alpha}(q,0) = \Gamma_2^{\alpha}(q)\Gamma_{02}^{\alpha}(q,0)$ and consequently $\Gamma_{\text{Lor}}^{\alpha} = \Gamma_{11}^{\alpha}(q,0) = \frac{1}{2}\Gamma_2^{\alpha}(q)\Gamma_{02}^{\alpha}(q,0)$. To zeroth order we have $\Gamma_{02}^{\alpha}(q,0) = -2\lambda(\gamma + q^2)$. The one-loop contributions to $\Gamma_{02}^{\alpha\beta}(q,0)$ are shown in figure 6.2. The transverse and longitudinal Lorentzian linewidths are found to be

$$\Gamma_{\text{Lor}}^{\text{T}}(q)\chi^{\text{T}}(q) = \lambda(\gamma + q^2) + 2(\lambda f)^2 \int_p \int_\omega [v_{\text{TT}}^{\text{T}}(g,\mathbf{p},\mathbf{q})C^{\text{T}}(\mathbf{p}_-,\omega)C^{\text{T}}(\mathbf{p}_+,\omega)$$

$$+ v_{\text{TL}}^{\text{T}}(g,\mathbf{p},\mathbf{q})C^{\text{T}}(\mathbf{p}_-,\omega)C^{\text{L}}(\mathbf{p}_+,\omega)$$

$$+ v_{\text{LL}}^{\text{T}}(g,\mathbf{p},\mathbf{q})C^{\text{L}}(\mathbf{p}_-,\omega)C^{\text{L}}(\mathbf{p}_+,\omega)] \tag{6.51}$$
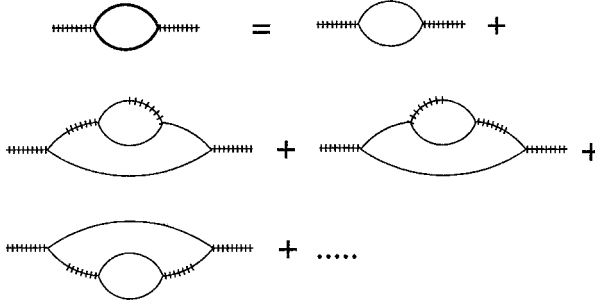
Figure 6.3. Partial summation of the perturbation theory for $\Gamma_{02}^{\alpha\beta}(\mathbf{q}, \omega)$, where vertex corrections are neglected. This resummation leads to the mode-coupling equations.

and

$$\Gamma_{\mathrm{Lor}}^{\mathrm{L}}(q)\chi^{\mathrm{L}}(q) = \lambda(\gamma + q^2) + 2(\lambda f)^2 \int_p \int_\omega [v_{\mathrm{TT}}^{\mathrm{L}}(g, \mathbf{p}, \mathbf{q})C^{\mathrm{T}}(\mathbf{p}_-, \omega)C^{\mathrm{T}}(\mathbf{p}_+, \omega)$$
$$+ v_{\mathrm{TL}}^{\mathrm{L}}(g, \mathbf{p}, \mathbf{q})C^{\mathrm{T}}(\mathbf{p}_-, \omega)C^{\mathrm{L}}(\mathbf{p}_+, \omega)], \tag{6.52}$$

where we have introduced the notation $\mathbf{p}_\pm = \mathbf{p} \pm \mathbf{q}/2$. The vertex functions $v_{\alpha\beta}^\sigma(g, \mathbf{p}, \mathbf{q})$ are given by

$$v_{\mathrm{TT}}^{\mathrm{T}}(g, \mathbf{p}, \mathbf{q}) = \frac{1}{d-1}\left(d^2 - 4d + 6 - \frac{(\mathbf{p}_+ \cdot \mathbf{p}_-)^2}{p_+^2 p_-^2} - 2\frac{(\mathbf{p}_+ \cdot \mathbf{q})^2}{p_+^2 q^2}\right)(\mathbf{p}\cdot\mathbf{q})^2, \tag{6.53 a}$$

$$v_{\mathrm{TL}}^{\mathrm{T}}(g, \mathbf{p}, \mathbf{q}) = \frac{4}{d-1}\left(d - 3 + \frac{(\mathbf{p}_+ \cdot \mathbf{p}_-)^2}{p_+^2 p_-^2} + \frac{(\mathbf{p}_+ \cdot \mathbf{q})^2}{p_+^2 q^2}\right)\left(\mathbf{p}\cdot\mathbf{q} + \frac{g}{2}\right)^2, \tag{6.53 b}$$

$$v_{\mathrm{LL}}^{\mathrm{T}}(g, \mathbf{p}, \mathbf{q}) = \frac{1}{d-1}\left(1 - \frac{(\mathbf{p}_+ \cdot \mathbf{p}_-)^2}{p_+^2 p_-^2}\right)(\mathbf{p}\cdot\mathbf{q})^2, \tag{6.53 c}$$

$$v_{\mathrm{TT}}^{\mathrm{T}}(g, \mathbf{p}, \mathbf{q}) = \left(d - 3 + 2\frac{(\mathbf{p}_+ \cdot \mathbf{q})^2}{p_+^2 q^2}\right)(\mathbf{p}\cdot\mathbf{q})^2, \tag{6.53 d}$$

$$v_{\mathrm{TL}}^{\mathrm{L}}(g, \mathbf{p}, \mathbf{q}) = 4\left(1 - \frac{(\mathbf{p}_+ \cdot \mathbf{q})^2}{p_+^2 q^2}\right)\left(\mathbf{p}\cdot\mathbf{q} + \frac{g}{2}\right)^2. \tag{6.53 e}$$

Upon substituting in the integrals (6.51) and (6.52) and substituting $\mathbf{p}_+ = \mathbf{p} + \mathbf{q}/2 \to \mathbf{p}$ the above vertex functions are identical with the vertex functions in section 3, equations (3.20)–(3.24). The frequency integration can readily be done, leading to

$$\int_\omega C^\alpha(\mathbf{p}_-, \omega)C^\beta(\mathbf{p}_+, \omega) = \frac{\chi^\alpha(\mathbf{p}_-)\chi^\beta(\mathbf{p}_+)}{\lambda[(\gamma + p_-^2)/\chi^\alpha(\mathbf{p}_-) + (\gamma + p_+^2)/\chi^\beta(\mathbf{p}_+)]}, \tag{6.54}$$

that is the product of the static susceptibilities divided by the sum of the linewidth to zeroth order. This structure corresponds to the first step in an iteration procedure and suggests defining a self-consistent approximation by replacing the bare linewidth by the full linewidth:

$$\frac{\chi^\alpha(\mathbf{p}_-)\chi^\beta(\mathbf{p}_+)}{\lambda[(\gamma + p_-^2)/\chi^\alpha(\mathbf{p}_-) + (\gamma + p_+^2)/\chi^\beta(\mathbf{p}_+)]} \to \frac{\chi^\alpha(\mathbf{p}_-)\chi^\beta(\mathbf{p}_+)}{[\Gamma_{\mathrm{Lor}}^\alpha(\mathbf{p}_-) + \Gamma_{\mathrm{Lor}}^\beta(\mathbf{p}_+)]}. \tag{6.55}$$

This self-consistent approach corresponds to a partial resummation of the perturbation series as shown in figure 6.3. The resulting equations are identical with the mode-coupling equations in Lorentzian approximation found by the conventional

derivation in section 3. The factorization approximation (two-mode approximation) in the conventional derivation corresponds to the structure of the one-loop diagrams here.

6.2.2. *Self-consistent equation for the Kubo relaxation function*

In the preceding section we derived for simplicity the mode-coupling equations in the so-called Lorentzian approximation for the line shape. Here we go beyond this approximation and derive a self-consistent theory for the full wave-vector- and frequency-dependent relaxation functions. The dynamic susceptibility can be written as (Bausch *et al.* 1976) ($\alpha = $ L,T)

$$\chi^\alpha(q, \omega) = \frac{\lambda(\gamma + q^2) + \lambda f \Gamma^\alpha_{X,10}(q, \omega)}{\Gamma^\alpha_{11}(-q, -\omega)}. \tag{6.56}$$

The X insertion is defined by (Bausch *et al.* 1976)

$$X^\alpha(\mathbf{q}, \omega) = \varepsilon_{\alpha\beta\gamma} \int_k \int_v \tilde{S}^\beta\left(\mathbf{k} - \frac{\mathbf{q}}{2}, v - \frac{\omega}{2}\right) S^\gamma\left(-\mathbf{k} - \frac{\mathbf{q}}{2}, -v - \frac{\omega}{2}\right). \tag{6.57}$$

Upon using the (explicit) structure of the dynamic propagators $C^\alpha(q, t)\Theta(t) = \chi^\alpha(q)R^\alpha(q, t)$, one can show that the relation

$$\Gamma^\alpha_{11}(-q, -\omega) = -i\omega + [\lambda(\gamma + q^2) + \lambda f \Gamma^\alpha_{X,10}(q, \omega)]\Gamma^\alpha_2(q) \tag{6.58}$$

holds to one-loop order. This implies for the Kubo relaxation function $\Phi^\alpha(q, \omega)$, which is related to the dynamic susceptibility by

$$\Phi^\alpha(q, \omega) = \frac{1}{i\omega}[\chi^\alpha(q, \omega) - \chi(q)], \tag{6.59}$$

a structure analogous to equation (3.25):

$$\Phi^\alpha(q, \omega) = \frac{\chi^\alpha(q)}{\Gamma^\alpha_{11}(-q, -\omega)} = \frac{\chi^\alpha(q)}{-i\omega + [\lambda(\gamma + q^2) + \lambda f \Gamma^\alpha_{X,10}(q, \omega)]\Gamma^\alpha_2(q)}. \tag{6.60}$$

To one-loop order, one obtains for $\Gamma^\alpha_{X,10}(q, t)$

$$\Gamma^T_{X,10}(q, t) = 2\lambda f \int_p \Theta(t)[v^T_{TT}(g, \mathbf{p}, \mathbf{q})C^T(\mathbf{p}_-, t)C^T(\mathbf{p}_+, t)$$

$$+ v^T_{TL}(g, \mathbf{p}, \mathbf{q})C^T(\mathbf{p}_-, t)C^L(\mathbf{p}_+, t)$$

$$+ v^T_{LL}(g, \mathbf{p}, \mathbf{q})C^L(\mathbf{p}_-, t)C^L(\mathbf{p}_+, t)] \tag{6.61 a}$$

and

$$\Gamma^L_{X,10}(q, t) = 2\lambda f \int_p \Theta(t)[v^L_{TT}(g, \mathbf{p}, \mathbf{q})C^T(\mathbf{p}_-, t)C^T(\mathbf{p}_+, t)$$

$$+ v^L_{TL}(g, \mathbf{p}, \mathbf{q})C^T(\mathbf{p}_-, t)C^L(\mathbf{p}_+, t)], \tag{6.61 b}$$

where the vertex functions are identical with equations (6.53 a)–(6.53 e). We have $C^\alpha(q, t)\Theta(t) = \chi^\alpha(q)R^\alpha(q, t)$. Equations (6.60)–(6.61 b) can be written in a self-consistent form by replacing the propagator $C^\alpha(q, t)$ by the full Kubo relaxation function $\Phi^\alpha(q, t)$ on the right-hand side of equations (6.61 a)–(6.61 b). This corresponds, as in the preceding section, to a partial resummation of the perturbation series. The resulting equations are identical with the mode-coupling equations (3.19)–(3.25) in section 3. Hence we have shown that mode-coupling theory is equivalent to a self-consistent

one-loop theory. The factorization approximation in the conventional derivation of mode-coupling theories is here a direct consequence of the structure of the one-loop theory. Furthermore the present procedure has the advantage that it can be extended to a self-consistent formulation of higher loop order. In order to justify the validity of the mode-coupling approach, one has to ask in what sense higher-order terms are small compared with the self-consistent one-loop theory. This question will be addressed in appendix 3, where we restrict ourselves to the isotropic case (in order to simplify the discussion).

7. Conclusions and outlook

The past decade has witnessed substantial progress in understanding the critical dynamics of real ferromagnets, on both the experimental and the theoretical side. In this review we have concentrated on the interplay between exchange and dipole–dipole interaction. We have presented theoretical and experimental evidence that many aspects of the critical dynamics of ferromagnets such as Fe, Ni, EuO, EuS and many other magnetic materials are now fairly well understood on the basis of a mode-coupling theory which takes into account exchange as well as the dipole–dipole interaction. In this final section we conclude our overview by summarizing some of the main theoretical and experimental achievements and by briefly discussing a number of open problems in the field of critical dynamics of magnets.

One of the most important theoretical advances towards our understanding of the critical dynamics of real ferromagnets was the realization that additional interactions such as the dipole–dipole interaction can lead to a qualitatively new behaviour of the frequency and wave-vector dependences of the spin–spin correlation functions (Frey 1986, Frey and Schwabl 1987). A description of a mode-coupling theory, which on top of the exchange interaction takes into account the dipole–dipole interaction, has been given in section 3. The main results of this mode-coupling analysis can be summarized as follows. The dipolar interaction leads to an anisotropy of the spin fluctuations with respect to the direction of the wave-vector and introduces a second length scale q_D^{-1} besides the correlation length ξ. The presence of a second length scale leads to generalized dynamic scaling laws, containing two scaling variables $x = 1/q\xi$ and $y = q_D/q$ for the length scale, and one scaling variable $\tau_\alpha = Aq^z\Omega^\alpha(x, y)t$ for the time scale. Because of the dipolar anisotropy the characteristic time scales $1/Aq^z\Omega^\alpha(x, y)$ are different for the longitudinal and transverse modes ($\alpha = $ L,T). This is mainly due to the non-critical longitudinal static susceptibility, implying that the longitudinal characteristic frequency $Aq^z\Omega^L(x, y)$ shows no critical slowing down asymptotically. Furthermore, the dipolar interaction leads to a quite interesting crossover in the linewidth and line shape of the spin–spin correlation functions.

Precisely at the critical temperature the dynamic critical exponent for the transverse linewidth undergoes a crossover from $z = \frac{5}{2}$ to $z = 2$, which is displaced with respect to the static crossover to wave-vectors smaller by almost one order of magnitude. This explains why up to now this crossover has escaped detection by neutron scattering experiments right at T_C. For the longitudinal linewidth the crossover is predicted to be from $z = \frac{5}{2}$ to an uncritical behaviour $z = 0$ and, in contrast with the transverse width, it occurs in the immediate vicinity of the static crossover, characterized by q_D. If the line shapes are approximated by Lorentzians the concomitant Lorentzian linewidths obey the scaling law $\Gamma^\alpha(q, \xi, g) = Aq^z\gamma^\alpha(x, y)$. For vanishing dipolar coupling g, the scaling functions coincide with the Résibois–Piette scaling function. If the strength g of the dipolar interaction is finite, the curves approach the Résibois–Piette scaling

function for small values of the scaling variable x and deviate therefrom with increasing x. Since the dipolar interaction leads to a non-conserved order parameter, the linewidth in the hydrodynamic limit is given by $\Gamma \propto q^0$ instead of $\Gamma \propto q^2$ as for an isotropic exchange ferromagnet.

Close to T_C the line shapes of the longitudinal and transverse relaxation functions coincide in the isotropic Heisenberg limit, that is for large values of the wave-vector q ($q \gg q_D$). In this limit the dipolar interaction becomes negligible and the shape is of the Hubbard–Wegner type as discussed in section 2. Upon increasing the value of the scaling variable $r = [(1/q\xi)^2 + (q_D/q)^2]^{1/2}$, the line shapes of the transverse and longitudinal relaxation functions become drastically different. Whereas the transverse relaxation function shows a nearly exponential temporal decay, overdamped oscillations show up for a longitudinal relaxation function. The line-shape crossover starts in the vicinity of the dipolar wave-vector q_D in contrast with the linewidth crossover, which starts at a wave-vector almost one order of magnitude smaller. The situation is quite different for temperatures well separated from the critical temperature. Then, the difference between the shape crossovers of the longitudinal and transverse relaxation functions diminishes with decreasing $q_D\xi$. For $q_D\xi \ll 1$ the shape crossover as a function of r corresponds to the crossover from the critical (Hubbard–Wegner) shape to the hydrodynamic shape as discussed in section 2.

On the experimental side, an important development began with the observation that the data for the linewidths above the transition temperature (Mezei 1982a, b, 1984, Böni *et al.* 1988) in magnetic materials such as EuO and Fe could not be described by the Résibois–Piette (1970) scaling function resulting from mode-coupling theory as well as renormalization group theory (Ma and Mazenko 1975, Iro 1987), which take into account the short-range exchange interaction only. Furthermore, the data could not be collapsed on to any other single scaling function. Those experimental results were explained quantitatively on the basis of the mode-coupling theory (Frey 1986, Frey and Schwabl 1987, 1988a, 1989a) described in section 3. Clear indications of the importance of the dipolar interaction have also been observed in hyperfine interaction experiments on Fe and Ni, where one found a crossover in the dynamical critical exponent from $z = \frac{5}{2}$ to $z = 2$ (Reno and Hohenemser 1972, Gottlieb and Hohenemser 1973, Hohenemser *et al.* 1982, 1989), and with electron spin resonance and magnetic relaxation experiments (Kötzler *et al.* 1976, 1978, Kötzler and Scheithe 1978, Kötzler and von Philipsborn 1978, Dunlap and Gottlieb 1980, Kötzler 1988), where a non-vanishing Onsager coefficient at zero wave-vector was found. For all these data now there exists a quantitative theoretical description (see section 4).

With advances in the neutron scattering technique, subsequent experiments investigated the line shape of the spin–spin correlation function. This progress made it possible to test the predictions for the line shape from mode-coupling theory (Wegner 1968, Hubbard 1971a) and renormalization group theory (Dohm 1976, Bhattacharjee and Ferrell 1985), which take into account solely the short-range exchange interaction. Originally those theories for the critical dynamics were expected to fit the experimental data in an increasingly quantitative way as one was able to measure the correlation functions at smaller and smaller wave vectors, since the influence of additional irrelevant interactions should diminish as one moves closer to criticality. It came as quite a surprise when Mezei found a nearly exponential decay of the Kubo relaxation function by spin-echo experiments on EuO at $q = 0.024$ Å^{-1} and $T = T_C$ (Mezei 1986), which was in drastic disagreement with the bell-like shape predicted (Wegner 1968, Hubbard 1971a, Dohm 1976, Bhattacharjee and Ferrell 1985). The anomalous

exponential decay found by Mezei (1986) was shown again to be a dipolar effect (Frey and Schwabl 1988, 1989). Recently, significant experiments have been performed using polarized neutrons (Böni *et al.* 1991a, Görlitz *et al.* 1992), which allowed for the first time measurement of the longitudinal and transverse spin–spin correlation functions separately. The results confirmed the theoretical predictions concerning the linewidth (Frey and Schwabl 1987) as well as the line shape of the longitudinal relaxation function (Frey *et al.* 1988, 1989). The experimental data, deconvoluted by a maximum-entropy method, agree quite well with the theoretical predictions, especially the double-peak structure corresponding to the overdamped oscillations in time which have been observed. This can be regarded as a success of the mode-coupling theory.

For the critical dynamics below T_C, experimental investigations are scarce. In contrast with the very satisfactory situation above T_C, where quantitative agreement between experiment and theory has been achieved, the situation in the ferromagnetic phase is far less clear. Theoretical investigations so far have concentrated on the dynamics of isotropic exchange ferromagnets, neglecting dipolar effects (Frey and Schwabl 1988a, 1989a, Schinz and Schwabl 1994). In this context it has been shown within the framework of mode-coupling theory that the amplitude of the scaling function for the spin–wave frequency of the isotropic Heisenberg Hamiltonian is universal (Schinz and Schwabl 1994). A comparison of the theory (Frey and Schwabl 1988a, 1989a), taking into account the so-determined universal amplitude (Schinz and Schwabl 1994), with recent measurements of the longitudinal linewidth on Ni (Böni *et al.* 1991b) below and not too close to the critical point gives quantitative agreement.

However, also in the ferromagnetic phase, profound effects of the dipolar interaction on the spin dynamics have been revealed in recent experiments. Using polarized neutron scattering the spin excitations in EuS and Pd_2MNSn have been investigated below T_C by Böni (1993) and Böni *et al.* (1994). These investigations indicate that there are deviations from the theoretical correlation functions of isotropic exchange ferromagnets. In particular, anisotropy of the spin fluctuations with respect to the polarization relative to the wave-vector **q** has been observed. Still further experimental and theoretical progress in needed in order to reach a thorough understanding of the spin dynamics in the ferromagnetic phase. The most convincing experimental indication for the importance of the dipolar interaction below T_C has been obtained recently in a measurement of the homogeneous magnetization dynamics (Dombrowski *et al.* 1994). It is found that the scaling function for the kinetic coefficient below T_C coincides with that observed earlier above T_C. Up to now, there is no theoretical explanation for these interesting experimental findings, but work in the framework of mode-coupling theory is in progress (Schinz 1994a).

Besides 3D ferromagnetic materials with isotropic exchange interaction there are other magnetic systems, where the dipole–dipole interaction influences the critical behaviour, such as antiferromagnets or ferromagnets with uniaxial or planar exchange anisotropy. The critical dynamics of isotropic dipolar antiferromagnets are affected by the dipolar interaction featuring a crossover from diffusive to relaxational dynamics of the magnetization and a crossover in the dynamic exponent (Aharony 1973b). The effect on the staggered magnetization is much less pronounced than for the corresponding order parameter modes in the ferromagnetic case. For ferromagnets with a uniaxial exchange anisotropy the dipolar interaction leads first of all to a reduction in the upper critical dimension from $d_c = 4$ to $d_c = 3$. As a consequence the critical statics is described by mean-field theory with logarithmic corrections (Larkin and Khmelnitskii

1969). A time-dependent Ginzburg–Landau model (Folk *et al.* 1977) for the dynamics results in logarithmic corrections to the convolutional van Hove theory of critical dynamics.

We conclude with some comments on 2D magnetic systems. These are interesting because the theorem of Hohenberg (1967) and Mermim and Wagner (1966) excludes conventional long-range order in isotropic systems with a continuous symmetry and short-range interaction. Two dimensions seem to be the borderline dimension where the thermal fluctuations are just strong enough to prevent the appearance of a finite order parameter. However, the anisotropy of the dipolar interaction with respect to the separation of two spins leads to a suppression of the longitudinal fluctuations and thus a finite order parameter may exist in two dimension (see section 5). The dipolar interaction is responsible for the existence of long-range order in both ferromagnetic (Maleev 1976) and antiferromagnetic thin films (Pich and Schwabl 1993, 1994). There is quite an interesting phase diagram with various spin-flop and intermediate phases for 2D ferromagnets in a finite external magnetic field (Pich 1994).

2D ferromagnets are interesting for practical reasons as magnetic storage devices as well as from a fundamental point of view. With the recent advances in thin film technology it becomes possible to study the critical behaviour of 2D magnetic systems (Allensbach 1994). Owing to the combined effect of anisotropy, dipole–dipole interaction and increased importance of thermal fluctuations in two dimensions, the phase diagram of ferromagnetic thin films shows a variety of new phases (Pappas *et al.* 1990, Allensbach and Bischof 1972, Allensbach 1994). The theoretical predictions in this field are still rather controversial (Pescia and Pokrovsky 1990, 1993, Kashuba and Pokrovsky 1993a b, Levanyuk and Garcia 1993). A still open and very interesting question is the critical dynamics of all those phases.

Acknowledgements

Appendix 1: Fluctuation–dissipation relations
In this appendix we collect several fluctuation dissipation theorems, which are of importance for the dynamics of systems described by nonlinear Langevin equations.

Let $\mathcal{T}$ be the time reversal operation $t \to t$. Then detailed balance (time reversal symmetry) implies (Janssen 1979) that

$$\mathcal{T} \exp(\mathcal{J}_{t_1}^{t_2} - \mathcal{H}_{t_1}) = \exp(\mathcal{J}_{-t_2}^{-t_1} - \mathcal{H}_{-t_2}),   \tag{A 1.1}$$

where $\mathcal{H}_t = \mathcal{H}(S(t))$ is the stationary probability distribution function and $\mathcal{J}_{t_1}^{t_2}[S, \tilde{S}]$ the dynamic functional. For simplicity we have assumed a one-component field S. Without loss of generality, one can assume that the field $S(x, t)$ is even or odd under time reversal, that is

$$\mathcal{T}S = \varepsilon S, \quad \varepsilon = \pm 1.   \tag{A 1.2}$$

In the case of spins, S is odd under time reversal. The stationary distribution $P_{st}[S] = \exp(-\mathcal{H}[S])$ is characterized by the 'free energy' $\mathcal{H}[S]$. The time reversal

symmetry implies that

$$\mathcal{T}\tilde{S}(t) = -\varepsilon\left(\tilde{S}(-t) - \frac{\delta\mathcal{H}[S(-t)]}{\delta S(-t)}\right). \tag{A1.3}$$

Now one uses the causality property of the response functions

$$\langle S(t_1)S(t_2)\dots S(t_k)\tilde{S}(\tilde{t}_1)\tilde{S}(\tilde{t}_2)\dots\tilde{S}(\tilde{t}_k)\rangle = 0, \quad \text{if one } \tilde{t}_j > \text{all } t_i. \tag{A1.4}$$

Then for example

$$\langle S(t)\tilde{S}(0)\rangle = 0 \text{ for } t < 0. \tag{A1.5}$$

With the time reversal operation and equation (A 1.3) it then follows from equation (A 1.5) for $t < 0$ that

$$\left\langle S(-t)\left(\tilde{S}(0) - \frac{\delta\mathcal{H}[S(0)]}{\delta S(0)}\right)\right\rangle = 0. \tag{A1.6}$$

Upon redefining $t = -t$, one obtains for $t > 0$

$$\langle S(t)\tilde{S}(0)\rangle = \Theta(t)\left\langle S(t)\frac{\delta\mathcal{H}[S(0)]}{\delta S(0)}\right\rangle \tag{A1.7}$$

The same arguments can be repeated for $\langle S(t_1)S(t_2)\dots S(t_k)\tilde{S}(\tilde{t}_1)\rangle$ with $\tilde{t}_1 > $ all t_j. The result is

$$\langle S(t_1)S(t_2)\dots S(t_k)\tilde{S}(\tilde{t}_1)\rangle = \Theta(\tilde{t}_1, \{t_j\})\left\langle S(t_1)S(t_2)\dots S(t_k)\frac{\delta\mathcal{H}[S(\tilde{t}_1)]}{\delta S(\tilde{t}_1)}\right\rangle \tag{A1.8}$$

where $\Theta(\tilde{t}_1, \{t_j\})$ is an obvious generalization of the Θ function. Note that these generalized fluctuation dissipation theorems hold for the cumulants and not for the vertex functions. In particular we get

$$G_{11}(k, t) = \Theta(t)\chi^{-1}(k)G_{02}(k, t). \tag{A1.9}$$

In a completely analogous way one can derive the following identities (Bausch *et al.* 1976, Janssen 1979):

$$\chi_{\alpha\beta}(x - x', t - t') = -\Theta(t - t')\frac{d}{dt}\langle S^\alpha(x, t)S^\beta(x', t')\rangle, \tag{A1.10a}$$

$$C_{\alpha\beta}(k, \omega) = \frac{2k_BT}{\omega}\text{Im}[\chi_{\alpha\beta}(k, \omega)], \tag{A1.10b}$$

$$-\Theta(t - t')\frac{d}{dt}\langle S^\alpha(x, t)S^\beta(x', t')\rangle = L_{\gamma\beta}\langle S^\alpha(x, t)\tilde{S}^\gamma(x', t')\rangle - \lambda f\langle S^\alpha(x, t)X^\beta(x', t')\rangle, \tag{A1.10c}$$

with $X^\beta = \varepsilon_{\beta\mu\nu}\tilde{S}^\mu S^\nu$. From this, one can deduce the following identities for the vertex functions:

$$\Gamma_{11}^{\alpha\beta}(q, \omega = 0) = [\lambda q^a\delta^{\alpha\gamma} + \lambda f\Gamma_{X,10}^{\alpha\gamma}(q, \omega = 0)]\Gamma_2^{\gamma\beta}(q), \tag{A1.11a}$$

$$-i\omega\Gamma_{20}^{\alpha\beta}(q, \omega) = \lambda q^a[\Gamma_{11}^{\alpha\beta}(q, \omega) - \Gamma_{11}^{\alpha\beta}(-q, -\omega)] + \lambda f[\Gamma_{11}^{\alpha\gamma}(q, \omega)\Gamma_{X,10}^{\gamma\beta}(q, \omega)$$
$$-\Gamma_{11}^{\alpha\gamma}(-q, -\omega)\Gamma_{X,10}^{\gamma\beta}(-q, -\omega)], \tag{A1.11b}$$

where $\Gamma_2^{\alpha\beta}(q) = \langle S^\alpha(-q)S^\beta(q)\rangle^{-1}$ is the static two-point vertex function, and $\Gamma_{X,\tilde{N}N}^{\alpha\beta}$ denotes a vertex function with one X insertion. If the Hamiltonian is quadratic in the

fields $\{S\}$, that is $\mathcal{H} = \frac{1}{2}\int d^d x\, c_{\alpha\beta} S^\alpha S^\beta$, then one has a further identity

$$\langle S^\alpha(t) \tilde{S}^\beta(t') \rangle = \Theta(t - t') c_{\alpha\beta} \langle S^\alpha(t) S^\beta(t') \rangle. \tag{A1.12}$$

Appendix 2: Derivation of the nonlinear Langevin equations

In this appendix we give a short deviation of nonlinear Langevin equations based on the projector formalism of Mori (1965) and Zwanzig (1961). In our presentation we follow closely the papers by Kawasaki (1973), Mori and Fujisaka (1973) and Mori *et al.* (1974).

As a first step in deriving nonlinear Langevin equations for a particular physical system, one has to choose the relevant slow variables. This choice is in general dictated by the conversation laws and spontaneously broken symmetries in the system under consideration. Let us assume that we have found an appropriate set of slowly varying variables $\{S\} = (S_1, S_2, \ldots S_n)$. Then, the next step consists in separating an arbitrary dynamical variables X into a part that is associated with the slow variables $\{S\}$ and the rest. This is accomplished by introducing a projector operator by

$$\mathcal{P} X(t) = \sum_j (X, \Psi_j) \Phi_j(\{S\}), \tag{A2.1}$$

where one defines the inner product as the value of the Kubo relaxation function at $t = 0$:

$$(A, B) = \Phi_{AB}(t = 0) = i \lim_{\varepsilon \to 0} \int_t^\infty d\tau \exp(-\varepsilon\tau) \langle [A, B^\dagger] \rangle|_{t=0}, \tag{A2.2}$$

which is identical with the static susceptibility. The functions $\Phi_j(\{S\})$ and $\Psi_j(\{S\})$ are two suitable sets of functions which are orthonormal with respect to the inner product defined in equation (A2.2):

$$(\Phi_i, \Psi_j) = \delta_{ij}. \tag{A2.3}$$

The microscopic dynamics of an arbitrary dynamic variable X following from the Heisenberg equations of motion can formally be presented by the Liouville equation

$$\frac{d}{dt} X(t) = i\mathcal{L} X(t). \tag{A2.4}$$

It was shown by Kawasaki (1973) that with the aid of the operator identity

$$\frac{d}{dt} \exp(it\mathcal{L}) = \exp(it\mathcal{L}) i\mathcal{L}0 + \int_0^t ds \exp[i(t-s)\mathcal{L}] i\mathcal{L}_0 \exp[it(\mathcal{L} - \mathcal{L}_0)] i(\mathcal{L} - \mathcal{L}_0)$$

$$+ \exp[it(\mathcal{L} - \mathcal{L}_0)] i(\mathcal{L} - \mathcal{L}_0), \tag{A2.5}$$

one can derive a formally exact nonlinear Langevin equation

$$\frac{d}{dt} X(t) = \sum_\beta (i\mathcal{L}X, \Psi_\beta) \Phi_\beta(\{S(t)\})$$

$$- \sum_\beta \int_0^t d\tau (f_X(\tau), \tilde{f}_\beta) \Phi_\beta(\{S(t-\tau)\}) + f_X(t), \tag{A2.6}$$

with the 'random' forces

$$f_x(t) = \exp(it\mathcal{QL}) i\,\mathcal{QL}X, \tag{A2.7a}$$

$$\tilde{f}_\alpha = \tilde{\mathcal{Q}} i\mathcal{L} \Psi_\alpha(\{S(t)\}), \tag{A2.7b}$$

where $\mathcal{Q} = 1 - \mathcal{P}$. Note that the adjoint operators $\mathcal{L}$ and $\mathcal{P}$ are denoted by $\tilde{\mathcal{L}}$ and $\tilde{\mathcal{P}}$.

The first term in equation (A 2.6) is the so-called 'adiabatic' term, and it describes the time variation in the dynamic variable X which follows adiabatically the changes in the slow variables $\{S(t)\}$. The second term represents the damping of this adiabatic motion. The last term is the stochastic force acting upon the dynamical variable X. Note, however, that this interpretation depends on the appropriate choice of the slow variables and the sets of functions $\Phi_\alpha(\{S(t)\})$ and $\Psi_\alpha(\{S(t)\})$. Upon choosing (we assume that the statics is diagonal in the variables S^α)

$$\Phi_\alpha(\{S(t)\}) = \chi_\alpha^{-1/2} S_\alpha, \qquad (A\,2.8\,a)$$

$$\Psi_\alpha(\{S(t)\}) = \chi_\alpha^{-1/2} S_\alpha, \qquad (A\,2.8\,b)$$

with $(S_\alpha, S_\beta) = \delta_{\alpha\beta}\chi_\alpha$, one obtains Mori's (1965) generalized Langevin equations

$$\frac{d}{dt} S_\alpha(t) = \sum_\beta i\omega_{\alpha\beta} S_\beta(t) - \sum_\beta \int_0^t d\tau\, (f_\alpha(\tau), f_\beta) S_\beta(t-\tau) + f_\alpha(t), \qquad (A\,2.9)$$

where

$$i\omega_{\alpha\beta} = (i\mathscr{L} S_\alpha, S_\beta)\chi_\alpha^{-1}, \qquad (A\,2.10\,a)$$

$$f_\alpha(t) = \exp(it\mathcal{Q}\mathscr{L})\,\mathcal{Q}i\mathscr{L} S_\alpha. \qquad (A\,2.10\,b)$$

The latter equations are the basis for the mode-coupling theory discussed in sections 2 and 3. However, with the above choice of a linear projection operator the 'random' forces are orthogonal with respect to the slow variables S_α only. It has been shown by Kawasaki (1970, 1976) and Zwanzig (1972) that the 'random' forces may not be really random since they contain products of the slow variables S_α. Another choice for the projection operator is to include all the suitable symmetrized polynomials of $\{S\}$ among the sets of functions $\{\Psi\}$ and $\{\Phi\}$. Now we restrict ourselves to the case of classical mechanics, where one has $\{\Psi\} = \{\Phi\}$. This choice corresponds to the projection operator introduced by Zwanzig (1960, 1961). The completeness relation for the Zwanzig projection operator reads

$$\sum_\alpha \Phi_\alpha(\{S\})\Phi_\alpha^*(\{S'\}) = \frac{\delta(S - S')}{P_{\text{eq}}(\{S\})} \qquad (A\,2.11)$$

with the equilibrium probability distribution function

$$P_{\text{eq}}(\{S\}) = \exp\left(-\frac{1}{k_B T}\mathscr{H}(\{S\})\right). \qquad (A\,2.12)$$

The resulting generalized Langevin equation takes the form

$$\frac{d}{dt} S_\alpha(t) = v_\alpha(\{S(t)\})$$

$$+ \sum_\beta \int_0^t d\tau\, P_{\text{eq}}^{-1}(\{S(t-\tau)\})\, \frac{\partial M_{\alpha\beta}(\tau; \{S(t-\tau)\})P_{\text{eq}}(\{S(t-\tau)\})}{\partial S_\beta^*(t-\tau)} + \zeta_\alpha(t),$$

$$(A\,2.13)$$

with the so-called mode-coupling term

$$v_\alpha(\{S(t)\}) = \langle i\mathscr{L} S_\alpha; \{a\}\rangle \qquad (A\,2.14\,a)$$

and the memory kernel

$$M_{\alpha\beta}(t; \{a\}) = \langle f_\alpha(t) f_\beta^*(0); \{a\}\rangle, \qquad (A\,2.14\,b)$$

where we have introduced the notation $\langle X; \{a\} \rangle = \langle X\delta(S-a) \rangle / P_{eq}(\{a\})$ for the conditional average.

The semiphenomenological equations of motion are obtained from the above exact equations by making three basic plausible assumptions. Firstly one makes a Markovian approximation for the kinetic coefficients. This is justified by the fact that one has included all suitable symmetrized polynomials of the slow variables in the projection operator:

$$M_{\alpha\beta}(t; \{a\}) \approx 2L_{\alpha\beta}(\{a\})\delta(t). \tag{A 2.15 a}$$

Secondly one assumes that all kinetic coefficients are independent of the slow variables

$$L_{\alpha\beta}(\{a\}) \approx L_{\alpha\beta}. \tag{A 2.15 b}$$

Thirdly one takes the random forces ζ as Gaussian white noise:

$$w(\{\zeta\}|t_0 \leqslant t \leqslant t_1) \sim \exp\left(-\frac{1}{4}\int_{t_0}^{t_1} dt\, \zeta_\alpha(t) L_{\alpha\beta}^{-1} \zeta_\beta(t)\right). \tag{A 2.15 c}$$

Then the generalized Langevin equations reduce to

$$\frac{d}{dt} S_\alpha(t) = v_\alpha(\{S(t)\}) - \sum_\beta L_{\alpha\beta}^0 \frac{\delta \mathscr{H}(\{S(t)\})}{\delta S_\beta^*(t)} + \zeta_\alpha(t), \tag{A 2.16}$$

where

$$\mathscr{H}(\{S\}) = -k_B T \ln(P_{eq}(\{S\})), \tag{A 2.17 a}$$

$$v_\alpha(\{S(t)\}) = -\lambda f \sum_\beta \left(\frac{\delta}{\delta S_\beta} Q_{\alpha\beta}(\{S\}) - Q_{\alpha\beta}(\{S\}) \frac{\delta \mathscr{H}(\{S\})}{\delta S_\beta(t)}\right). \tag{A 2.17 b}$$

The Poisson brackets are defined by

$$Q_{\alpha\beta}(\{S\}) = \{S_\alpha, S_\beta\}_P = -Q_{\beta\alpha}(\{S\}). \tag{A 2.18}$$

We close this appendix by presenting the generalized Langevin equation for the example of an isotropic ferromagnet:

$$\mathscr{H} = \frac{1}{2}\int d^d x\, \{rS^2(\mathbf{x}, t) + [\nabla S(\mathbf{x}, t)]^2\} + \frac{u}{4!}\int d^d x\, [S^2(\mathbf{x}, t)]^2. \tag{A 2.19}$$

The Poisson brackets are given by

$$Q_{\alpha\beta}(\mathbf{k}, \mathbf{k}') = \varepsilon_{\alpha\beta\gamma} S^\gamma(\mathbf{k} + \mathbf{k}'). \tag{A 2.20}$$

Since the order parameter is conserved, the kinetic coefficient is

$$L(\mathbf{k}) = \lambda k^2 \tag{A 2.21}$$

(in general $L(\mathbf{k}) = \lambda k^a$). Hence one obtains the following generalized Langevin equation for isotropic ferromagnets:

$$\frac{d}{dt} \mathbf{S}(\mathbf{x}, t) = \lambda f \mathbf{S} \times \frac{\delta \mathscr{H}}{\delta \mathbf{S}(\mathbf{x}, t)} - \lambda (i\nabla)^a \frac{\delta \mathscr{H}}{\delta \mathbf{S}(\mathbf{x}, t)} + \zeta(\mathbf{x}, t). \tag{A 2.22}$$

Note that the conventional (van Hove) theory of critical dynamics is obtained by making the following additional assumptions. Firstly the Onsager coefficient L remains finite at the critical point. Secondly the mode-coupling term is ignored: $f = 0$.

Thirdly a quadratic approximation is made for the free-energy functional $\mathscr{H} = \frac{1}{2}\int_{\mathbf{k}}\chi^{-1}(\mathbf{k})\mathbf{S}(\mathbf{k},t)\mathbf{S}(-\mathbf{k},t)$, where $\chi(\mathbf{k})$ is the static susceptibility.

One should also note that, in mode-coupling theory, solely the latter approximation is made (and further additional approximations such as two-mode approximation and neglecting the vertex corrections).

Appendix 3: Validity of mode-coupling theory; higher orders in perturbation theory

In this section we analyse how higher orders in perturbation theory can be incorporated in the self-consistent approach. For simplicity and clarity we restrict ourselves to the case of isotropic ferromagnets with exchange interaction only. The extension to dipolar ferromagnets is straightforward.

First we consider the corrections from two-loop contributions to the vertex functions Γ_{02} and Γ_{11} shown in figures A 1 and A 2. Owing to the tensorial structure of the relaxation and mode-coupling vertices they cannot be contracted ($F^{\alpha\beta\gamma\delta}\varepsilon_{\alpha'\gamma\delta} = 0$).
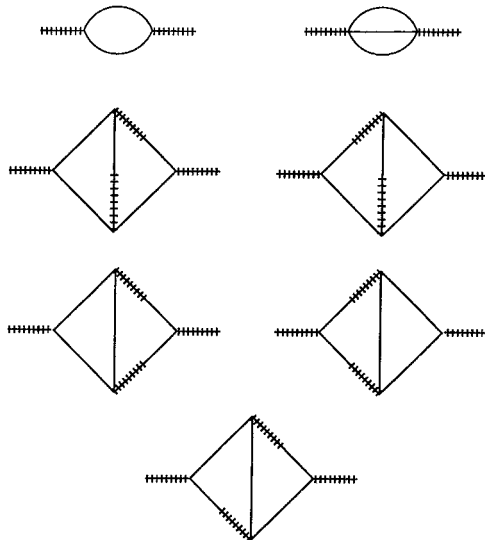

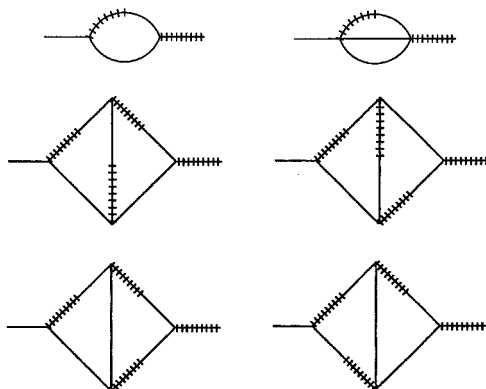Figure A 1. One-loop and two-loop diagrams contributing to the vertex function Γ_{02}.

Figure A 2. One-loop and two-loop diagrams contributing to the vertex function Γ_{11} (the self energy).
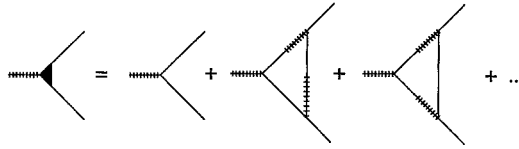
Figure A 3.   Diagrams contributing to the one-loop vertex correction.

Figure A 4.   One-loop and two-loop diagrams contributing to the vertex function Γ_{11} drawn in terms of the renormalized vertex.

Figure A 5.   One-loop and two-loop diagrams contributing to the vertex function Γ_{02}, drawn in terms of the renormalized vertex.

The two-loop diagrams of Γ_{11} and Γ_{02} can be divided into two categories. The first category consists of 'true' two-loop diagrams connecting two relaxation vertices. The second type consists of diagrams whose structure is, up to vertex corrections, identical with the one-loop diagrams. Upon defining a renormalized mode-coupling vertex, as shown in figure A 3, the two-loop contributions to the vertex functions Γ_{11} and Γ_{02} are given by the diagrams in figure A 4 and A 5.

The modifications of the self-consistent equations resulting from these types of two-loop diagrams are now discussed separately.

(I) The vertex corrections in figure A 3 correspond to the vertex function $\Gamma_{12}(q, p\, v = 0, \omega)$. Since all diagrams have a bare mode-coupling vertex with an external response line (for example Deker and Haake (1974)), the one-loop contribution to $\Gamma_{12}(q, p, v = 0, \omega)$ is proportional to $\mathbf{p} \cdot \mathbf{q}$, that is it has the same wave-vector dependence as the original bare mode-coupling vertex. The remaining frequency integral is a function $f(\omega)$ of the external frequency ω. Because only the long-time behaviour is of importance for the critical dynamics the limit $\omega \to 0$ merely leads to a renormalization of the amplitude λf of the mode-coupling vertex and not to a change in its wave-vector dependence. (However, see the discussion of higher-order vertex corrections later.)

(II) The two-loop diagram connecting two relaxation vertices Γ_{02}^{RR} is proportional to

$$\Gamma_{02}^{RR} \propto \lambda^2 q^4 \int_p \int_k \int_\omega C(\mathbf{p}, \omega) C(\mathbf{k}, \omega) C(\mathbf{q} - \mathbf{p} - \mathbf{k}, \omega). \qquad (A\,3.1)$$

Upon introducing the dimensionless wave-vector variables $\hat{\mathbf{p}} = \mathbf{p}/q$ and $\hat{\mathbf{k}} = \mathbf{k}/q$, carrying out the frequency integrals, and replacing the correlation propagators according to equations (6.55) one finds that

$$\Gamma_{02}^{RR} \propto q^{4-z}. \qquad (A\,3.2)$$

In comparing this result with the wave-vector dependence q^{3-z} of the one-loop diagram connecting two mode-coupling vertices, one recognizes that the contribution of Γ_{02}^{RR} can be neglected in the long-wavelength limit. Hence this two-loop diagram does not change the self-consistent equations as well.

The above discussion shows that in a self-consistent theory the two-loop diagrams are small compared with the one-loop diagrams in the long-time and long-wavelength limit.

Now we discuss higher-order vertex corrections, where an internal line of a one-loop vertex correction is decorated with a static insertion. It can be shown that the renormalization of the mode-coupling vertex is of purely static origin (Frey 1989). This is due to an exact relation between the renormalization factor of the mode-coupling vertex and the time scale and field renormalization. To lowest order the mode-coupling vertex is given by

$$\Gamma_{12}^{(0)}(\mathbf{p}, \mathbf{q}) = v_3(\mathbf{p}, \mathbf{q}) = \lambda_0 f_0 \varepsilon_{\alpha\beta\gamma} \mathbf{p} \cdot \mathbf{q}. \tag{A3.3}$$

This expression can also be written in terms of the bare static susceptibilities as

$$v_3(\mathbf{p}, \mathbf{q}) = \frac{\lambda_0 f_0}{2} \varepsilon_{\alpha\beta\gamma} \left[\chi_{\text{B}}^{-1}\left(\mathbf{p} + \frac{\mathbf{q}}{2}\right) - \chi_{\text{B}}^{-1}\left(\mathbf{p} - \frac{\mathbf{q}}{2}\right) \right], \tag{A3.4}$$

showing that the wave-vector dependence of the mode-coupling vertex is determined by the static susceptibilities. In order to take into account the static infrared divergences correctly, one way to proceed is to replace the bare static susceptibilities by the fully renormalized static susceptibilities

$$\lambda_0 f_0 \mathbf{p} \cdot \mathbf{q} \to \frac{\lambda f}{2} \left[\chi^{-1}\left(\mathbf{p} + \frac{\mathbf{q}}{2}\right) - \chi^{-1}\left(\mathbf{p} - \frac{\mathbf{q}}{2}\right) \right] \tag{A3.5}$$

in the mode-coupling vertex. This replacement is suggested by the exact relation between the renormalization factors. It is also equivalent to replacing the nonlinear Landau–Ginzburg functional by

$$\mathcal{H}_{\text{eff}} = \int_{\mathbf{k}} \chi^{-1}(\mathbf{k}) \mathbf{S}(\mathbf{k}) \cdot \mathbf{S}(-\mathbf{k}), \tag{A3.6}$$

where $\chi(\mathbf{k})$ is the fully renormalized static susceptibility. This approximation is often used in mode-coupling theories without any justification. Here it is a consequence of the exact relation between the renormalization factors.

Besides these static vertex renormalizations (due to the nonlinearity in the Landau–Ginzburg functional) there could also be dynamic vertex renormalizations, but this is not the case here as we shall show next. This can be seen from the diagrammatic representation of the dynamic vertex renormalization (see figure A3). Any diagram contributing to the vertex corrections starts with a bare mode-coupling vertex. Therefore to leading order in the wavenumber one can replace the remaining wave vectors (in the integrals of the corresponding diagrams) by their values at $\mathbf{p} = \mathbf{q} = 0$. this leads then only to changes in the amplitude. Hence we have

$$v_3(\mathbf{p}, \mathbf{q}) = \frac{\lambda f}{2} \left[\chi^{-1}\left(\mathbf{p} + \frac{\mathbf{q}}{2}\right) - \chi^{-1}\left(\mathbf{p} - \frac{\mathbf{q}}{2}\right) \right] + O(\omega, p). \tag{A3.7}$$

This gives a precise specification of the approximations involved by neglecting the vertex corrections.

E. Frey and F. Schwabl

As we have seen above, the effects of the four-point coupling can be taken into account by a static renormalization of the mode-coupling vertex (equation (A 3.7)). Then one is left with a dynamic theory with a harmonic (effective) Landau–Ginzburg functional and a mode-coupling vertex. In this case the fluctuation dissipation relation (A 1.12) applies (see appendix 1), which in the case of a purely quadratic Landau–Ginzburg functional reduces to

$$G_{11}(\mathbf{k}, t) = \Theta(t)\chi^{-1}(\mathbf{k})G_{02}(\mathbf{k}, t).$$ \hfill (A 3.8)

This implies for the Fourier transform $G_{11}(\omega) + G_{11}(-\omega) = \chi^{-1}G_{02}(\omega)$ and consequently

$$2\,\mathrm{Re}\,[G_{11}(\omega)] = \chi^{-1}G_{02}(\omega).$$ \hfill (A 3.9)

By using the generalized fluctuation dissipation theorems in appendix 1 we find

$$\Phi(\mathbf{q}, \omega) = \frac{1}{i\omega}\,[\chi(\mathbf{q}, \omega) - \chi(\mathbf{q})] = \frac{\chi(\mathbf{q})}{-i\omega + [\lambda q^2 + \lambda f\Gamma_{X,10}(\mathbf{q}, \omega)]/\chi(\mathbf{q})}.$$ \hfill (A 3.10)

This is exactly the same structure as the nonlinear Langevin equations (with the linear projection operator) (see section 3) with the memory kernel

$$M(\mathbf{q}, \omega) = \frac{\lambda q^2 + \lambda f\Gamma_{X,10}(\mathbf{q}, \omega)}{\chi(\mathbf{q})}.$$ \hfill (A 3.11)

Neglecting the mode-coupling contribution ($f = 0$) leads immediately to the conventional theory (van Hove theory) of critical dynamics. The mode-coupling contribution to the memory function is given by

$$\Gamma_{X,10}(\mathbf{q}, t) = \lambda f \int_{\mathbf{k}} \left[\frac{1}{\chi(\mathbf{q} + \mathbf{k}/2)} - \frac{1}{\chi(\mathbf{q} - \mathbf{k}/2)} \right] \frac{1}{\chi(\mathbf{q} + \mathbf{k}/2)}\, \Phi\left(\mathbf{q} + \frac{\mathbf{k}}{2}, t\right)\Phi\left(\mathbf{q} - \frac{\mathbf{k}}{2}, t\right).$$ \hfill (A 3.12)

In the strong-coupling limit, where the van Howe term λq^2 (in general there will be a crossover from van Hove to strong coupling) can be neglected, a scaling analysis of the above self-consistent equations shows that the dynamic exponent is given by

$$z = \tfrac{1}{2}(d + 2 - \eta),$$ \hfill (A 3.13)

that is with this generalized mode-coupling theory we find the correct dynamic exponent. This resolves a long-standing problem with the conventional derivation of the mode-coupling theory, which gives a dynamic exponent with the wrong sign of η. The correct expression, equation (A 3.13), is a consequence of the fact that we have correctly taken into account the vertex renormalizations of the mode-coupling vertex by static decorations of internal lines.

    The above analysis is not a rigorous derivation of a self-consistent theory. It shows, however, that the neglected terms are small in the long-term and long-wavelength limit. Furthermore, taking into account static corrections of the mode-coupling vertex (suggested by an exact relation between the renormalization factors of the mode-coupling vertex and the static field renormalization) we could show that the self-consistent theory (generalized mode-coupling theory) is capable of giving the exact result for the dynamic critical exponent with the correct sign of η.

References

ABERGER, C., and FOLK, R., 1988a, *Phys. Rev.* B, **38**, 6693; 1988b, *Ibid.*, **38**, 7207; 1989, *Physica* B, **156–157**, 229.

AHARONY, A., and FISHER, M. E., 1973, *Phys. Rev.* B, **8**, 3323.

AHARONY, A., 1973a, *Phys. Rev.* B, **8**, 3342; 1973b, *Ibid.*, **8**, 3349; 1973c, *Ibid.*, **8**, 3363; 1973d, *Phys. Lett.* A, **44**, 313; 1976, *Phase Transitions and Critical Phenomena*, Vol. 6, edited by C. Domb and M. S. Green (New York: Academic Press), pp. 358–424.

AHARONY, A., and HALPERIN, B. I., 1975, *Phys. Rev. Lett.*, **35**, 1308.

AHLERS, G., KORNBLIT, A., and GUGGENHEIM, H. J., 1975, *Phys. Rev. Lett.*, **34**, 1227.

ALLENSPACH, R., 1994, *J. Magn. Mater.*, **129**, 160, and references cited therein.

ALLENSPACH, R., and BISCHOF, A., 1992, *Phys. Rev. Lett.*, **69**, 3385.

ALS-NIELSON, J., 1976, *Phase Transitions and Critical Phenomena*, Vol. 5a, edited by C. Domb and M. S. Green (New York: Academic Press), pp. 87–164 and references therein.

ALS-NIELSON, DIETRICH, O. W., and PASSELL, L., 1976, *Phys. Rev.* B, **14**, 4908.

AMIT, D. J., 1984, *Field Theory, the Renormalization Group, and Critical Phenomena* (Singapore: World Scientific).

ANDERSON, P. W., and SUHL, H., 1955, *Phys. Rev.*, **100**, 1788.

ARTS, A. F. M., and DE WIJN, H. W., 1990, *Magnetic Properties of Layered Transition Metal Compounds*, edited by L. J. De Jongh (Deventer: Kluwer), pp. 191ff.

BALUCANI, U., PINI, M. G., CARRA, P., LOVESEY, S. W., and TOGNETTI, V., 1987, *J. Phys.* C, **20**, 3953.

BANDER, M., and MILLS, D. L., 1988, *Phys. Rev.* B, **38**, 12015.

BAUSCH, R., JANSSEN, H. K., and WAGNER, H., 1976, *Z. Phys.* B, **24**, 113.

BENNETT, H. S., and MARTIN, P. C., 1965, *Phys. Rev.*, **138**, A608.

BETHE, H. A., and SALPETER, E. E., 1957, *Quantum Mechanics of One- and Two-Electron Atoms* (Berlin: Springer).

BHATTACHARJEE, J. K., and FERRELL, R. A., 1981, *Phys. Rev.* B, **24**, 6480; 1985, *J. statist. Phys.*, **41**, 899.

BIRGENEAU, J. R., GUGGENHEIM, H. J., and SHIRANE, G., 1970, *Phys. Rev.* B, **1**, 2211; 1973, *Ibid.*, **8**, 304.

BLOCH, F., 1930, *Z. Phys.*, **61**, 206.

BOHN, H. G., KOLLMANN, A., and ZINN, W., 1984, *Phys. Rev.* B, **30**, 6504.

BORCKMANS, P., WALGRAEF, D., and DEWEL, G., 1977, *Physica* A, **91**, 411.

BÖNI, P., 1993, *Physica* B, **192**, 94.

BÖNI, P., CHEN, M. E., and SHIRANE, G., 1987a, *Phys. Rev.* B, **35**, 8449.

BÖNI, P., ENDOH, Y., GRAF, H. A., HENNION, M., MARTÍNEZ, J. L., and SHIRANE, G., 1994, Preprint.

BÖNI, P., GÖRLITZ, D., KÖTZLER, J., and MARTINEZ, J. L., 1991a, *Phys. Rev.* B, **43**, 8755.

BÖNI, P., MARTINEZ, J. L., and TRANQUADA, J. M., 1991b, *Phys. Rev.* B, **43**, 575.

BÖNI, P., and SHIRANE, G., 1986, *Phys. Rev.* B, **33**, 3012.

BÖNI, P., SHIRANE, G., BOHN, H. G., and ZINN, W., 1987b, *J. appl. Phys.*, **61**, 3397; 1988, *Ibid.*, **63**, 3089.

BORCKMANS, P., WALGRAEF, D., and DEWEL, G., 1978, *Physica* A, **91**, 411.

BREZIN, E., and DE DOMINICIS, C., 1975, *Phys. Rev.* B, **12**, 4954.

BRUCE, A. D., 1977, *J. Phys.* C, **10**, 419.

BRUCE, A. D., KOSTERLITZ, J. M., and NELSON, D. R., 1976, *J. Phys.* C, **9**, 825.

CALLEN, H. B., 1963, *Phys. Rev.*, **130**, 890.

CHOW, L., HOHENEMSER, C., and SUTER, R. M., 1980, *Phys. Rev. Lett.*, **45**, 908.

CHOWDHURY, A. R., COLLINS, G. S., and HOHENEMSER, C., 1984, *Phys. Rev.* B, **30**, 6277; 1986, *Ibid.*, **33**, 5070, 6231.

COHEN, M. H., and KEFFER, F., 1955, *Phys. Rev.*, **99**, 1135.

COLLINS, G. S., CHOWDHURY, A. R., and HOHENEMSER, C., 1986, *Phys. Rev.* B, **33**, 4747.

COLLINS, M. F., 1989, *Magnetic Critical Scattering* (Oxford University Press).

COLLINS, M. F., MINKIEWICZ, V. J., NATHANS, R., PASSELL, L., and SHIRANE, G., 1969, *Phys. Rev.*, **179**, 417.

CORLISS, L. M., DELAPALME, A., HASTINGS, J. M., NATHANS, R., and TUCCIARONE, A., 1970, *J. appl. Phys.*, **41**, 1384.

COX, S. F., 1982, *J. Phys.* C, **20**, 3187.

CUCCOLI, A., TOGNETTI, V., and LOVESEY, S. W., 1989, *Phys. Rev.* B, **39**, 2619.

CUCCOLI, A., TOGNETTI, V., LOVESEY, S. W., and VAIA, R., 1988, *Phys. Lett.* A, **131,** 57; 1991, *J. Phys.: condens. Mater.*, **2,** 3339.

DALMAS DE RÉOTIER, P., and YAOUANC, A., 1994, *Phys. Rev. Lett.*, **72,** 290.

DALMAS DE RÉOTIER, P., YAOUANC, A., and FREY, E., 1994, *Phys. Rev.* B, **50,** 3033.

DE'BELL, K., and GELDART, D. J. W., 1989, *Phys. Rev.* B, **39,** 743.

DE DOMINICIS, C., 1975, *Nuovo Cim. Lett.*, **12,** 567; 1976, *J. Phys., Paris*, **37,** C–247.

DE DOMINICIS, C., BREZIN, E., and ZINN-JUSTIN, J., 1975, *Phys. Rev.* B, **12,** 4945.

DE DOMINICIS, C., and PELITI, L., 1977, *Phys. Rev. Lett.*, **38,** 505; 1978, *Phys. Rev.* B, **18,** 353.

DE HAAS, L. J., and VERSTELLE, J. C., 1977, *Physica* B, **86–88,** 1291.

DEKER, U., and HAAKE, F., 1974, *Phys. Rev.* A, **11,** 2043.

DENISON, A. B., GRAF. H., KÜNDIG, W., and MEIER, P. F., 1979, *Helv. Phys. Acta*, **52,** 460.

DE WIJN, H. W., WALKER, L. R., GESCHWIND, S., and GUGGENHEIM, H. J., 1973a, *Phys. Rev.*, **8,** 299.

DE WIJN, H. W., WALKER, L. R., and WALSTEDT, R. E., 1973b, *Phys. Rev.*, **8,** 285.

DIETRICH, O. W., ALS-NIELSON, J., and PASSELL, L., 1976, *Phys. Rev.* B, **14,** 4923.

DOHM, V., 1976, *Solid St. Commun.*, **20,** 659.

DOMBROWSKI, R., GÖRLITZ, D., KÖTZLER, J., and MARX, CHR., 1994, *J. appl. Phys.*, **75,** 6054.

DÖRING, W., 1961, *Z. Naturforsch.* a, **16,** 1008, 1146.

DUNLAP, R. A., and GOTTLIEB, A. M., 1980, *Phys. Rev.* B, **22,** 3422.

DYSON., F. J., 1956a, *Phys. Rev.*, **102,** 1217; 1956b, *Ibid.*, **102,** 1230.

ELLIOTT, R. J., and LOWDE, R. D., 1955, *Proc. R. Soc.* A, **230,** 46.

EWALD, P. P., 1917a, *Ann. Phys.*, **54,** 57; 1917b, *Ibid.*, **54,** 519; 1921, *Ibid.*, **64,** 253.

FERRELL, R. A., MENYHÁRD, N., SCHMIDT, H., SCHWABL, F., and SZÉPFALUSY, P., 1971a, *Phys. Rev. Lett.*, **18,** 891; 1967b, *Phys. Rev. Lett.* A, **24,** 493; 1968, *Ann. Phys.* (N.Y.), **47,** 565.

FINGER, W., 1977a, *Physica* B, **90,** 251; 1977b, *Phys. Lett.* A, **60,** 165.

FISCHER, T. M., 1989, Diploma Thesis, Technische Universität Munchen.

FISCHER, T. M., FREY, E., and SCHWABL, F., 1990, *Phys. Lett.* A, **146,** 457; 1992, *J. Magn. magn. Mater.*, **104–107,** 201.

FISHER, M. E., and AHARONY, A., 1973, *Phys. Rev. Lett.*, **30,** 559.

FIXMAN, M. J., *J. chem. Phys.*, **33,** 1363; 1962, *Ibid.*, **36,** 1961.

FOLK, R., and IRO, H., 1985, *Phys. Rev.* B, **32,** 1880; 1986, *Ibid.*, **34,** 6571.

FOLK, R., IRO, H., and SCHWABL, F., 1977, *Z. Phys.* B, **27,** 169.

FREY, E., 1986, Diploma Thesis, Technische Universität München; FREY, E, 1989, Doctoral Thesis, Technische Universität München.

FREY, E., and SCHWABL, F., 1987, *Phys. Lett.* A, **123,** 49; 1988a, *Z. Phys.* B, **71,** 355; 1988b, *J. Phys., Paris* C8–1531; 1988c, *Ibid.*, C8–1569; 1989a, *Z. Phys.* B, **76,** 139; 1989b, *Hyper. Interalt.*, **50,** 767; 1990, *Phys. Rev.* B, **42,** 8261; 1991, *Ibid.*, **43,** 833.

FREY, E., SCHWABL, F., and THOMA, S., 1988, *Phys. Lett.* A, **129,** 343; 1989, *Phys. Rev.* B, **40,** 7199.

FROWEIN, R., KÖTZLER, J., SCHAUB, B., and SCHUSTER, H. G., 1982, *Phys. Rev.* B, **25,** 4905.

GOLDANSKI, V. I., and HERBER, R. H. (editors), 1968, *Chemical Applications of Mössbauer Spectroscopy* (New York: Academic Press).

GOLDSTONE, J., 1961, 1961, *Nuovo Cim.*, **19,** 154.

GÖRLITZ, D., KÖTZLER, J., BERMEJO, F. J., BÖNI, P., and MARTINEZ, J. L., 1992, *Physica* B, **180,** 214.

GÖRLITZ, D., KÖTZLER, J., and LANGE, T., 1992, *J. Magn. magn. Mater.*, **104,** 339.

GOTTLIEB, A. M., and HOHENEMSER, C., 1973, *Phys. Rev. Lett.*, **31,** 1222.

GRAHL, M., GÖRLITZ, D., KÖTZLER, J., LANGE, T., and SESSLER, I., 1991, *J. appl. Phys.*, **69,** 6179.

HALPERIN, B. I., and HOHENBERG, P. C., 1967, *Phys. Rev. Lett.*, **19,** 700; 1969, *Phys. Rev.*, **177,** 952.

HALPERIN, B. I., HOHENBERG, P. C., and MA, S., 1972, *Phys. Rev. Lett.*, **29,** 1548; 1974, *Phys. Rev.* B, **10,** 139; 1976, *Ibid.*, **13,** 4119.

HARRIS, A. B., 1968, *Phys. Rev.*, **175,** 674.

HARTMANN, O., 1989, *Hyp. Interact.*, **49,** 61.

HARTMANN, O., KARLSSON, E., WÄPPLING, R., CHAPPERT, J., YAOUANC, A., ASCH, L., and KALVIUS, G. M., 1986, *J. Phys.* F, **16,** 1593.

HARTMANN, O., WÄPPLING, R., KARLSON, E., KALVIUS, G. M., ASCH, L., LITTERST, F. J., AGGARWAL, K., MÜNCH, K. H., GYGAX, F. N., and SCHENK, A., 1990, *Hyper. Interact.*, **64,** 369.

HEISENBERG, W., 1928, *Z. Phys.*, **49**, 619.
HELLWEGE, K.-H (editor), 1978, *Landolt–Börnstein, New Series, Vol. 12 Numerical Data and Functional Relationship in Science and Technology* (Berlin: Springer).
HERLACH, D., FÜRDERER, K., FÄHNLE, M., and SHIMMELE, L., 1986, *Hyper. Interact.*, **31**, 287.
HERRING, C., and KITTEL, C., 1951, *Phys. Rev.*, **81**, 869.
HERTZ, J. A., 1971, *Int. J. Magn.*, **1**, 253, 307, 313.
HOHENBERG, P. C., 1987, *Phys. Rev.*, **158**, 383.
HOHENBERG, P. C., and HALPERIN, B. I., 1977, *Rev. mod. Phys.*, **49**, 435.
HOHENEMSER, C., CHOW, L., and SUTER, R. M., 1982, *Phys. Rev. B*, **26**, 5056.
HOHENEMSER, C., ROSOV, N., and KLEINHAMMES, A., 1989, *Hyper. Interact.*, **49**, 267, and references therein.
HOLSTEIN, T., and PRIMAKOFF, H., 1940, *Phys. Rev.*, **58**, 1098.
HUBBARD, J., 1971a, *J. Phys. C*, **4**, 53; 1971b, *J. appl. Phys.*, **42**, 1390; 1979a, *Phys. Rev. B*, **19**, 2626; 1979b, *Ibid.*, **20**, 4584.
HUBER, D. L., 1971, *J. Phys. Chem. Solids*, **32**, 2145.
HUBER, D. L., and KRÜGER, D. A., 1970, *Phys. Rev. Lett.*, **24**, 111.
IRO, H., 1987, *Z. Phys. B*, **68**, 485; 1988, *J. Magn. magn. mater.*, **73**, 175; 1989, *Physica B*, **156–157**, 232.
ISING, E., 1925, *Z. Phys.*, **31**, 253.
JANSSEN, H. K., 1976, *Z. Phys. B*, **23**, 377; 1979, *Dynamic Critical Phenomena and Related Topics*, Lecture Notes in Physics, Vol. 104, edited by C. P. Enz (Berlin: Springer), pp. 25–47.
JOUKOFF-PIETTE, C., and RÉSIBOIS, P., 1973, *Phys. Lett.*, **42**, 531.
KADANOFF, L. P., and SWIFT, J., 1968, *Phys. Rev.*, **166**, 89.
KALASHNIKOV, V. P., and TRET'JAKOV, S. V., 1990a, *Phys. Lett. A*, **146**, 463; 1900b, *Physica B*, **162**, 265; 1991, *Phys. Lett. A*, **156**, 239.
KASHCHEEV, V. N., and KRIVOGLAZ, M. A., 1961, *Fiz. tverd. Tela*, **3**, 1541 (Engl. Transl., 1961, *Soviet Phys. Solid St.*, **3**, 1117).
KASHUBA, A., and POKROVSKY, V. L., 1993a, *Phys. Rev. Lett.*, **70**, 3155; 1993b, *Phys. Rev. B*, **48**, 10335.
KARLSSON, E. B., 1982, *Phys. Rep.*, **82**, 272; 1990, *Hyper. Interact.*, **64**, 331.
KAWASAKI, K., 1967, *J. Chem. Solids*, **28**, 1277; 1970, *Ann. Phys.*, (*N.Y.*), **61**, 1; 1973, *J. Phys. A*, **6**, 1289; *Phase Transitions and Critical Phenomena*, Vol. 5a, edited by C. Domb and M. S. Green (New York: Academic Press), pp. 165–403, and references therein.
KEFFER, F., 1966, *Encyclopedia of Physics*, Vol. XVIII/2, edited by S. Flügge (Berlin: Springer), pp. 37ff.
KITTEL, C., 1971, *Introduction to Solid State Physics*, fourth edition (New York: Wiley).
KOBEISSI, M. A., and HOHENEMSER, C., 1978, *Hyper. Interact.*, **4**, 480.
KOBEISSI, M. A., SUTER, R., GOTTLIEB, A. M., and HOHENEMSER, C., 1976, *Phys. Rev. B*, **11**, 2455.
KOSTERLITZ, J. M., and THOULESS, D. J., 1972, *J. Phys. C*, L124; 1973, *J. Phys. C*, **6**, 1181.
KÖTZLER, J., 1986, *J. Magn. magn. Mater.*, **54**, 649.
KÖTZLER, J., GÖRLITZ, D., HARTL, M., and MAR, CHR., 1994, *IEEE Trans. Magn.*, **30**, 828.
KÖTZLER, J., GÖRLITZ, D., MEZEI, F., and FARAGO, B., 1986, *Europhys. Lett.*, **1**, 675.
KÖTZLER, J., KAMLEITER, G., and WEBER, G., 1976, *J. Phys. C*, **9**, L361.
KÖTZLER, J., KALDIS, E., KAMLEITER, G., and WEBER, G., 1991, *Phys. Rev. B*, **43**, 11280.
KÖTZLER, J., and SCHEITHE, W., 1978, *J. Magn. magn. Mater.*, **9**, 4.
KÖTZLER, J., SCHEITHE, W., BLICKHAN, R., and KALIDS, E., 1978, *Solid St. Commun.*, **26**, 641.
KÖTZLER, J., and VON PHILIPSBORN, H., 1978, *Phys. Rev. Lett.*, **40**, 790.
KRONMÜLLER, H., HILZINGER, H.-R., MONACHESI, P., and SEEGER, A., 1979, *Appl. Phys.*, **18**, 183.
KUBO, R., 1957, *J. phys. Soc. Japan*, **12**, 570.
LANDAU, L. D., 1937, *Zh. eksp. teor. Fiz.*, **7**, 627.
LANDAU, L. D., and KHALATNIKOV, I. M., 1954, *Dokl. Akad. Nauk SSSR*, **96**, 469.
LARKIN, A. I., and KHMELNITSKII, D. E., 1969, *Soviet Phys. JETP*, **29**, 1123.
LAU, H. Y., CORLISS, L. M., DELAPALME, A., HASTINGS, J. M., NATHANS, R., and TUCCIARONE, A., 1969, *Phys. Rev. Lett.*, **23**, 1225.
LEVANYUK, A. P., and GARCIA, N., 1992, *J. Phys.: condens. Matter*, **4**, 10277; 1993, *Phys. Rev. Lett.*, **70**, 1184.
LI, Y., BABERSCHKE, K., and FARLE, M., 1991, *J. appl. Phys.*, **69**, 4992.
LI, Y., FARLE, M., and BABERSCHKE, K., 1990, *Phys. Rev. B*, **41**, 9596.

LOVESEY, S. W., 1984, *Theory of Neutron Scattering from Condensed Matter*, Vols I and II (Oxford: Clarendon); 1993, *J. Phys.: condens. Matter*, **5**, L251.

LOVESEY, S. W., and WILLIAMS, R. D., 1986, *J. Phys.* C, **19**, L253.

LOVESEY, S. W., and TROHIDOU, K. N., 1991, *J. Phys.: condens. Matter*, **3**, 1827 (Erratum, 1991, *J. Phys.: condens. Matter*, **3**, 5255.

LOWDE, R. D., 1965, *J. appl. Phys.*, **36**, 884.

LYNN, J. W., 1975, *Phys. Rev.* B, **11**, 2624; 1983, *Ibid.*, **28**, 6550; 1984, *Phys. Rev. Lett.*, **52**, 775.

MA, S.-K., 1976, *Modern Theory of Critical Phenomena* (New York: Benjamin–Cummings).

MA, S., and MAZENKO, G. F., 1975, *Phys. Rev.* B, **11**, 4077.

MALEEV, S. V., 1974, *Zh. eskp. teor. Fiz.*, **66**, 1809 (Engl. Transl., 1974, *Soviet. Phys. JETP*, **39**, 889; 1975, *Ibid.*, **69**, 1398 (Engl. Transl., 1976, *Ibid.*, **42**, 713; 1976, *Ibid.*, **70**, 2374 (Engl. Transl., 1976, *Ibid.*, **43**, 1240; 1987, *Soc. Sci. Rev.* A, *Phys.*, **8**, 323.

MÅNSON, M., 1974, *J. Phys.* C, **7**, 4073.

MARSHALL, W., and LOVESEY, S. W., 1971, *Theory of Thermal Neutron Scattering* (Oxford: Clarendon).

MARTIN, P. C., SIGGIA, E. D., and ROSE, H. A., 1973, *Phys. Rev.* A, **8**, 423.

MARTINEZ, J. L., BÖNI, P., and SHIRANE, G., 1985, *Phys. Rev.* B, **32**, 7037.

MAZENKO, G. F., 1976, *Phys. Rev.* B, **14**, 3933.

MEIER, P. F., 1981, *Hyper. Interact.*, **8**, 591.

MERMIN, N. D., and WAGNER, H., 1966, *Phys. Rev. Lett.*, **17**, 1133.

MEZEI, F., 1972, *Z. Phys.*, **255**, 146 (editor), 1980, *Neutron Spin Echo*, Lecture Notes in Physics, Vol. 128 (Berlin: Springer); 1982a, *Phys. Rev. Lett.*, **49**, 1096; 1982b, *Ibid.*, **49**, 1537; 1984, *J. Magn. magn. Mater.*, **45**, 67; 1986, *Physica* B, **136**, 417; 1987, *Magnetic Excitations and Fluctuations II*, edited by U. Balucani, S. W. Lovesey, M. Rasetti and V. Tognetti, Springer Proceedings in Physics, Vol. 54 (Berlin: Springer); 1988, *J. Phys.*, *Paris*, C8–1537.

MEZEI, F., FARAGO, B., HAYDEN, S. M., and STIRLING, W. G., 1989, *Physica* B, **156–157**, 266.

MINIKIEWICZ, V. J., COLLINS, M. F., NATHANS, R., and SHIRANE, G., 1969, *Phys. Rev.*, **182**, 624.

MITCHELL, P. W., COWLEY, R. A., and PYNN, R., 1984, *J. Phys.* C, **17**, L875.

MOOK, H. A., LYNN, J. W., and NICKLOW, R. M., 1973, *Phys. Rev. Lett.*, **30**, 556.

MORI, H., 1965, *Progr. theor. Phys.*, *Osaka*, **33**, 423.

MORI, H., and FUJISAKA, H., 1973, *Progr. theor. Phys.*, *Osaka*, **49**, 764.

MORI, H., FUJISAKA, H., and SHIGEMATSU, H., 1974, *Progr. theor. Phys.*, *Osaka*, **51**, 109.

MORRISH, A. H., 1965, *The Physical Principles of Magnetism* (New York: Wiley).

NATTERMANN, T., and TRIMPER, S., 1976, *J. Phys.* C, **9**, 825.

NELSON, D. R., 1983, *Phase Transitions and Critical Phenomena*, Vol. 7, edited by C. Domb and J. L. Lebowitz (New York: Academic Press).

NISHIYAMA, K., YAGI, E., ISHIDA, K., MATSUZAKI, T., NAGAMINE, K., and YAMAZAKI, T., 1984, *Hyper. Interact.*, **17–19**, 473.

PAPPAS, D. P., KAMPER, K. P., and HOPSTER, H., 1990, *Phys. Rev. Lett.*, **64**, 3179.

PASSELL, L., ALS-NIELSON, J., and DIETRICH, O. W., 1972, *Proceedings of the Fifth Symposium on Neutron Inelastic Scattering* (Vienna: International Atomic Energy Agency), p. 619.

PARETTE, G., 1972, *Ann. Phys. (N.Y.)*, **7**, 313.

PARETTE, G., and KAHN, R., 1971, *J. Phys.*, *Paris*, **32**, 447.

PASSELL, L., DIETRICH, O. W., and ALS-NIELSEN, J., 1976, *Phys. Rev.* B, **14**, 4897, 4908, 4923, and references therein.

PEIERLS, R., 1936, *Helv. Phys. Acta*, **7**, Suppl. 2, 81.

PESCIA, D., and POKROVSKY, V. L., 1990, *Phys. Rev. Lett.*, **65**, 2599; 1993, *Phys. Rev. Lett.*, **70**, 1185.

PELCOVITS, R. A., and HALPERIN, B. I., 1979, *Phys. Rev.* B, **19**, 4614.

PICH, C., 1994, Doctoral Thesis, Technische Universität München.

PICH, C., and SCHWABL, F., 1993, *Phys. Rev.* B, **47**, 7957; 1994, *Ibid.*, **49**, 413; 1995, *J. Magn. magn. Mater.*, **140–144**, 1709.

PIEPER, M. W., KÖTZLER, J., and NEHRKE, K., 1993, *Phys. Rev.* B, **47**, 11962.

POKROVSKY, V. L., 1979, *Adv. Phys.*, **28**, 595.

POKROVSKY, V. L., and FEIGELMAN, M. V., 1977, *Zh. eksp. teor. Fiz.*, **72**, 557 (Engl. Transl., 1971, Soviet Phys. JETP, **45**, 291); 1979, *Ibid.*, **76**, 784 (Engl. Transl., 1979, *Ibid.*, **49**, 395).

POKROVSKY, V. L., FEIGELMAN, M. V., and TSVELIK, A. M., 1988, *Spin Waves and Excitations II*, edited by A. S. Borovik-Roamov and S. K. Sinha (Amsterdam: Elsevier).

POLITI, P., RETTORI, A., and PINI, M. G., 1993, *Phys. Rev. Lett.*, **70**, 1183.

PRIVMAN, V., HOHENBERG, P. C., and AHARONY, A., 1991, *Phase Transitions and Critical Phenomena*, Vol. 14, edited by C. Domb and J. L. Lebowitz (New York: Academic Press).

RAGHAVAN, R., and HUBER, D. L., 1976, *Phys. Rev. B*, **14**, 1185.

RENO, R. C., and HOHENEMSER, C., 1972, *Proceedings of the Seventh Annual Conference on Magnetism and Magnetic Materials*, edited by D. C. Graham and J. J. Rhyne (New York: American Institute of Physics).

RÉSIBOIS, P., and PIETTE, C., 1970, *Phys. Rev. Lett.*, **24**, 514.

RÉSIBOIS, P., and DE LEENER, M., 1967, *Phys. Rev. Lett. A*, **25**, 65; 1969, *Phys. Rev.*, **178**, 806, 819.

SAHAM, M., BARAK, J., EL-HANANY, U., and WARREN, W. W., 1980, *Phys. Rev. B*, **22**, 5400.

SALAMON, M. B., 1967, *Phys. Rev.*, **155**, 24.

SASVÁRI, L., 1977, *J. Phys. C*, **10**, L633.

SPÖREL, F., and BILLER, E., 1975, *Solid St. Commun.*, **17**, 833.

SCHENK, A., 1985, *Muon Spin Rotation Spectroscopy, Principles and Applications in Solid State Physics* (Bristol: Adam Hilger).

SCHINZ, H., 1994a, Doctoral Thesis, Technische Universität München; 1994b, private communication.

SCHINZ, H., and SCHWABL, F., 1994, *J. Magn. magn. Mater.*, **140–144**, 1527.

SCHRÖDER, B., WAGNER, V., LEHNER, N., KESHARWANI, K. M., and GEICK, R., 1980, *Phys. Stat. sol. (b)*, **97**, 501.

SCHWABL, F., 1971, *Z. Phys.*, **246**, 13; 1988, *J. appl. Phys.*, **64**, 5867; 1991, *Quantum Mechanics* (Berlin: Springer).

SCHWABL, F., and MICHEL, K. H., 1970, *Phys. Rev. B*, **2**, 89.

STEINSVOLL, O., MAJKRZAK, C. F., SHIRANE, G., and WICKSTED, J. P., 1983, *Phys. Rev. Lett.*, **51**, 300; 1984, *Phys. Rev. B*, **30**, 2377.

TÄUBER, U. C., and SCHWABL, F., 1992, *Phys. Rev. B*, **46**, 3337; 1993, *Ibid.*, **48**, 186.

TOH, H. S., and GEHRING, G. A., 1990, *J. Phys.: condens. Matter.*, **2**, 7511.

TOPERVERG, B. P., and YASHENKIN, A. G., 1993, *Phys. Rev. B*, **48**, 16505.

TROHIDOU, K. N., and LOVESEY, S. W., 1993, *J. Phys.: condens. Matter*, **5**, 1109.

TUCCIARONE, A., LAU, H. Y., CORLISS, L. M., DELAPALME, A., and HASTINGS, A., 1971, *Phys. Rev. B*, **4**, 3206.

TUROV, E. A., 1965, *Physical Properties of Magnetically Ordered Crystals* (New York: Academic Press).

VAKS, V. G., LARKIN, A. I., and PIKIN, S. A., 1967a, *Zh. eksp. theor. Fiz.*, **53**, 281 (Engl. Transl., 1968, *Soviet Phys. JETP* **26**, 188); 1967b, *Ibid.*, **53**, 1089 (Engl. Transl., 1968, *Ibid.*, **26**, 647).

VAN HOVE, L., 1954, *Phys. Rev.*, **93**, 1374.

VAN VLECK, J. H., 1937, *Phys. Rev.*, **52**, 1137.

WÄCKELGARD, E., HARTMANN, O., KARLSSON, E., WÄPPLING, R., ASCH, L., KALVIUS, G. M., CHAPPERT, J., and YAOUANC, A., 1986, *Hyper. Interact.*, **31**, 325; 1989, *Ibid.*, **50**, 781.

WATSON, R. E., and FREEMAN, A. J., *Phys. Rev.*, **123**, 2027.

WEGNER, F., 1968, *Z. Phys.*, **216**, 433; 1969, *Ibid.*, **218**, 260.

WICKSTED, J. P., BÖNI, P., and SHIRANE, G., 1984, *Phys. Rev. B*, **30**, 3655.

WILLIAMS, W. G., 1988, *Polarized Neutrons* (Oxford: Clarendon Press).

WILSON, K. G., and KOGUT, J., 1974, *Phys. Rep. C*, **12**, 76.

WINDSOR, C. G., and STEVENSON, R. W. H., 1966, *Proc. phys. Soc.*, **87**, 501.

YAOUANC, A., DALMAS, DE RÉOTIER, P., and FREY, E., 1993a, *Phys. Rev. B*, **47**, 796; 1993b, *Europhys. Lett.*, **21**, 93.

YUSHANKHAI, V. YU., 1989, *Hyper. Interact.*, **50**, 775.

ZOBEL, M., 1991, Diploma Thesis, Technische Universität München.

ZWANZIG, R., 1960, *J. chem. Phys.*, **33**, 1388; 1961, *Phys. Rev.*, **124**, 983; 1972, *Statistical Mechanics*, edited by S. Rice, K. Freed and J. Light (University of Chicago Press).